Earth Oriented Space Research

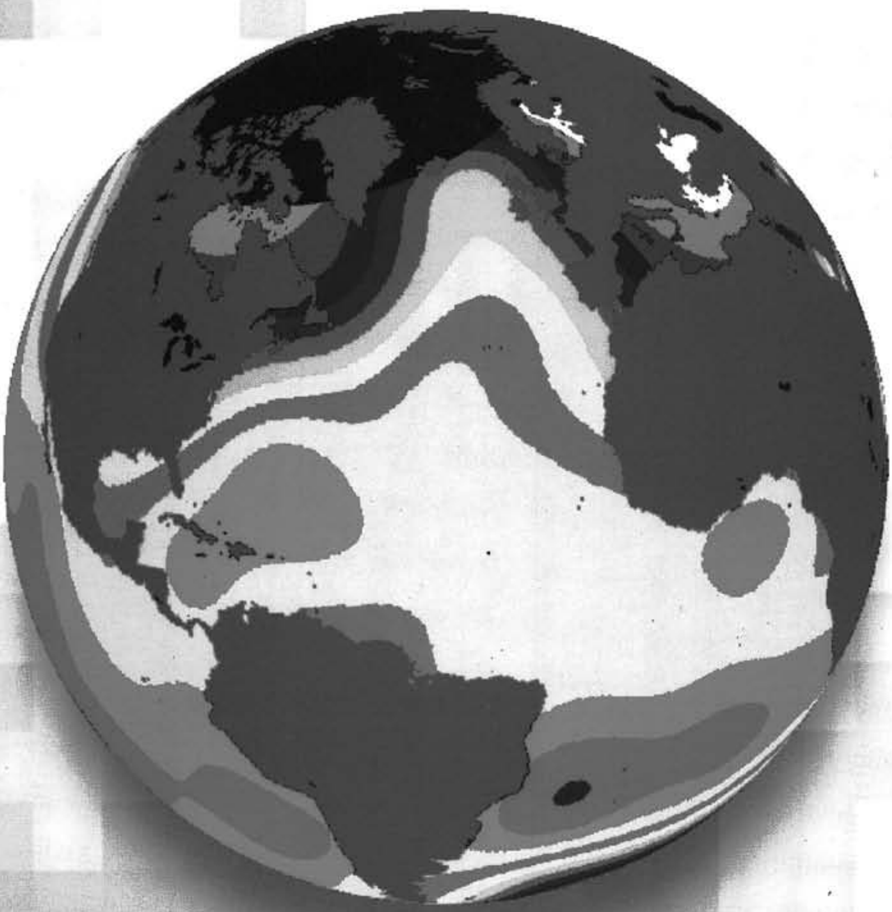

at

Delft University of Technology

Faculty of Geodetic Engineering
Faculty of Aerospace Engineering

Cug 112

EARTH ORIENTED SPACE RESEARCH
AT
DELFT UNIVERSITY OF TECHNOLOGY

1990-1993

Faculty of Geodetic Engineering
Thijsseweg 11
2629 JA Delft
The Netherlands

Faculty of Aerospace Engineering
Kluyverweg 1
2629 HS Delft
The Netherlands

EARTH ORIENTED SPACE RESEARCH
AT
DELFT UNIVERSITY OF TECHNOLOGY

1990-1993

B.A.C. Ambrosius, R.H.N. Haagmans, E. Vermaat
(Editors)

Delft University Press, 1994

The project "Earth Oriented Space Research" is carried out at the Faculties of Geodetic and Aerospace Engineering of Delft University of Technology (DUT). During the period 1990 to 1993, which is covered in this report, the principal investigators of this project were:

Prof. dr. ing. R. Rummel (Geodetic Engineering)
Prof. ir. K.F. Wakker (Aerospace Engineering)
Ir. E. Vermaat (Geodetic Engineering)

Prof. Rummel left DUT in June 1993 to accept a position at the Institut für Astronomische und Physikalische Geodäsie of the Technische Universität München.
Prof. Wakker temporarily vacated his chair at the Faculty of Aerospace Engineering to take the position of Rector Magnificus of DUT on September 1, 1993.

Published and distributed by:

Delft University Press
Stevinweg 1
2628 CN Delft
The Netherlands

Telephone +31 15 783254
Fax +31 15 781661

CIP-DATA KONINKLIJKE BIBLIOTHEEK, DEN HAAG

Ambrosius, B.A.C., Haagmans, R.H.N., Vermaat, E.

Earth Oriented Space Research at Delft University of Technology : 1990 - 1993 / B.A.C. Ambrosius, R.H.N. Haagmans, E. Vermaat. -
Delft: Delftse Universitaire Pers. - I11.
With summary in English.
ISBN 90-407-1021-X
NUGI 816
Subject headings: instrumentation and tracking, orbit determination, crustal dynamics, Earth rotation, ocean currents, gravity field, altimetry, etc

Printed in The Netherlands

Acknowledgement

The work described in this report was carried out under the auspices of the Space Research Organization Netherlands (SRON), who provided major financial support. Also, we would like to acknowledge the contributions from the Delft University research fund, the Netherlands Remote Sensing Board (BCRS) and the European Space Agency (ESA), who provided additional support.

The investigations were performed by a large number of researchers, technicians and students, several of whom have also written large sections of this document. The editors would like to thank them all for their efforts. A special word of gratitude is passed to Dirk Kuijper. He has coordinated the integration of all the individual contributions and was responsible for the formatting of the complete text and all the figures in WordPerfect 5.2, including the styling of this report. Also, we would like to express our appreciation for the design of the cover by Axel Smit and for his assistence in the field of computer graphics.

List of investigators, students, and technicians during the period 1990-1993

Faculty of Geodetic Engineering

Investigators

Bakker, G.
Bax, A.
Belikov, M.
Butkiewicz, E.
Gelder, B.H.W. van
Gelderen, M. van
Haagmans, R.H.N.
Koop, R.J.J.
Min, E.J. de[*]
Offierski, J.W.
Oskam, D.
Rummel, R.
Schrama, E.J.O.
Sneeuw, N.J.
Strang van Hees, G.L.
Verheijen, A.J.M.
Vermaat, E.
Xu, P.
Zarinjsh, A.

Students

Bollweg, A.
Bouman, J.
Bun, R.
Burger, M.G.
Coevorden, R.G. van
Elema, I.A.
Everts, R.
Hamed, M.
Hanssen, R.
Kap, A.P.
Kester, J.
Khafid, K.
Kuis, E.
Nohlmans, R.A.M.
Onselen, K.I. van
Ree, R.E. van
Robers, M.
Roemer, S. v.d.
Stelpstra, D.
Valten, B.
Verheijen, A.J.M.
Weesie, E.
Welting, J.H.M.
Zuidweg, K.

Technicians

Beek, W
Es, C van
Hoeneveld, M.
Loon, D.L.F. van
Otten, K.H.
Plugers, P.
Vukotić, D.

Faculty of Aerospace Engineering

Investigators

Ambrosius, B.A.C.
Hesper, E.T.
Gaalen, W.J. van[*]
Kooij, M.W.A. van der
Kuijper, D.C.
Leenman, H.
Mets, G.J.
Noomen, R.
Naeije, M.C.
Ourensma, G.J.
Overgaauw, B.[*]
Piersma, H.J.D.
Scharroo, R.
Smith, A.J.E.[*]
Springer, T.A.[*]
Visser, P.N.A.M.
Wakker, K.F.
Wisse, E.[*]
Zandbergen, R.C.A.

Students

Boekhout, H.A.
Boomkamp, H.J.
Kruizinga, G.L.H.
Palm, D.J.G. de
Spruijt, M.R.F.
Stoel, W.F.
Verstraeten, L.M.E.

Technicians

Geldorp, G.H.M. van

[*] also contributed as students

Summary

This report describes the work that has been carried out during the period 1990 - 1993 in the framework of the research project "Earth Oriented Space Research at Delft University of Technology". This project is a cooperative effort of the Section Space Research and Technology (SSR&T) of the Faculty of Aerospace Engineering and the Section Physical, Geometric and Space Geodesy (FMR) of the Faculty of Geodetic Engineering, the latter including the Kootwijk Observatory for Satellite Geodesy (KOSG). It forms an integral part of the basic research activities of both groups, funded by the University. In the four-year period described here, the project also received major financial support from the Space Research Organization in The Netherlands (SRON), which is the primary motivation for the compilation of this report. Additional support was obtained from a special Delft University research fund. Furthermore, several smaller scale projects were carried out, which were sponsored by various national and international scientific and industrial organizations such as the Netherlands Remote Sensing Board (BCRS) and the European Space Agency (ESA).

The major theme of the project has been the use of artificial earth satellites for geodetic and geophysical applications. This involves the acquisition and analysis of many types of satellite tracking observations, which yields information on such diverse subjects as tectonic plate motions, earth rotation, marine geoid, ocean currents and the earth's gravity field. A common denominator in the analyses is the need to accurately determine the orbits of the satellites, which serve as a target or the platform for the measurements. The latter consist of Satellite Laser Range (SLR) observations, and radio-frequency range and/or velocity measurements obtained by various techniques such as GPS, DORIS, PRARE and Radar Altimetry.

By virtue of its nature the research described in this report is of international character. Therefore, the majority of the work was carried out in the framework of international agreements and projects. This enabled the participation in international observation campaigns, and access to international databases. In this regard, a major contribution was provided by the quite unique Modular Transportable Laser Ranging System (MTLRS-2), which is one of the few mobile SLR systems in the world. During the past 4 years, it has been deployed at various remote sites in Southern Europe and in Scandinavia, and its operational capabilities were further improved. In another development on the operational side, the joint groups acquired and installed a high-precision GPS receiver at KOSG. The continuous operation of this receiver represents a new important step in the strengthening of our position in this international research field.

From a scientific point of view, important milestones have been achieved in the time-frame covered by this report. In 1992, the fourth major mobile SLR campaign was

carried out in the Eastern Mediterranean area. The analysis of the data acquired during this campaign confirmed the results for the station motions, derived from the data of the previous campaigns since 1986. It also made it possible to generate an improved overall solution, showing clear indications of contemporary plate motions in that area with rates of up to 3.5 cm/yr with an uncertainty of less than 1.0 cm/yr. The quality of the results is now at a level where they warrant a thorough geophysical interpretation. Further evidence of the tectonic motions is provided by our analysis of a dedicated GPS campaign in the same area, also in 1992. The results line-up perfectly with the SLR solutions, demonstrating the maturity of the GPS technique for this type of application. Global SLR network analyses now provide a reference frame with a 1.0 cm accuracy and earth rotation time-series of similar quality.

In another area, significant progress has been made in the study of the marine geoid and ocean currents. This is mainly the result of the analysis of radar altimeter data of the new ERS-1 and TOPEX/Poseidon satellites. Due to recent advances in the quality of gravity field models for the earth, the orbits of those satellites can now be computed with unprecedented accuracies of 5 cm rms for TOPEX/Poseidon to 16.0 cm rms for ERS-1. This, in turn, has made it possible to derive accurate models of the dynamic sea surface topography from the altimeter data, which give information about the main ocean currents. Of crucial importance for the further advancement of this science field, and for space geodesy applications in general, is the development of more detailed gravity field models. This requires a dedicated satellite mission, that would preferably use both gradiometry and GPS. An example is ARISTOTELES, which has been extensively studied and promoted. In addition, theoretical studies have been performed to define a unified system, relating all different measurement types to the present day description of the earth's gravity field.

Technology continues to be an important driver for advancing the field of Earth Oriented Space Research. This holds in particular for the applications of GPS, which seems to be the focus of the developments for the coming years. Among other things, it has the capability to provide a major step forward in gravity field research, at relatively low cost. Since it is unlikely that an ARISTOTELES-type mission will be launched soon, it may be an interesting option to fly a high-precision GPS receiver as unique payload onboard a cheap small satellite in low earth orbit. Although the science return would be somewhat less than from a full-fledged ARISTOTELES mission, it would still provide extremely useful data.

Finally, it is strived for to strengthen the geophysical interpretation of the results, which will further increase the scientific value of our research. An important step towards this goal is a planned intensification of our cooperation with the Faculty of Earth Sciences of the University of Utrecht.

1 Introduction

In May 1987, the project "Earth Oriented Space Research at Delft University of Technology" started as a cooperative effort of the Section Space Research and Technology (SSR&T) of the Faculty of Aerospace Engineering and the Section Physical, Geometric and Space Geodesy (FMR) of the Faculty of Geodetic Engineering, the latter including the Kootwijk Observatory for Satellite Geodesy (KOSG). These groups, who have been working together since 1976, have a long experience in Satellite Laser Ranging (SLR), satellite orbit mechanics, physical and space geodesy and satellite radar altimetry. The decision to join the research efforts was taken to combine relevant expertise of each of the individual groups and to create a larger team that could more effectively cover the large field of research topics.

This team has successfully participated in many international research projects, e.g. the NASA LAGEOS Project and the NASA Crustal Dynamics Project. Such international cooperation has become a strong tradition and presently the team is involved in a variety of international programs and projects; e.g. WEGENER-2 project, which is embedded in the NASA Dynamics Of the Solid Earth (DOSE) Project, LAGEOS-2 project (NASA/ASI), ERS-1 project (ESA), TOPEX/POSEIDON project (NASA/CNES), International Earth Rotation Service (IERS) and phase A and B studies for the ARISTOTELES and STEP missions. In a relatively new development, the team is actively exploring the use of the NAVSTAR Global Positioning System (GPS) for geodetic and geophysical research, which has resulted in active participation in the International GPS Geodynamics Service (IGS).

Also at national level, cooperation has been established with various research groups, in particular in the areas of geophysics and oceanography, e.g. the Faculty for Earth Sciences and the Institute for Marine and Atmospheric Sciences (IMAU), both of the University of Utrecht, and the Netherlands Institute for Sea Research (NIOZ).

In 1989, a research plan for the project "Earth Oriented Space Research at Delft University of Technology" was submitted to the Space Research Organization in The Netherlands (SRON) [Rummel, R., E. Vermaat, and K.F. Wakker, *Earth Oriented Space Research at Delft University of Technology*, Research plan 1990 - 1993, Faculty of Geodetic Engineering and Faculty of Aerospace Engineering, Delft University of Technology, Delft, June, 1989], which described the planned research activities in the framework of that project in the period 1990 - 1993. The present report summarizes the accomplishments within this project over that period.

Four major research areas have been identified in the Research Plan: crustal dynamics, earth rotation, ocean currents and gravity field from altimetry, and gravity field. Chapters 4 through 7 present the research which has been done, together with the major results being obtained, in each of these areas. Important supportive activities to each of these areas are the issues of satellite tracking and orbit determination. The significant developments and accomplishments in these areas are presented in chapters 2 and 3. Each chapter closes with a list of references, which are relevant to the topic. The publications produced by the team in this project in the report period, are listed at the end of the report in a separate chapter. Chapter 8 briefly reviews the present perspective for continued research in the area of Earth Oriented Space Research, referring also to the new Research Plan covering the period 1994 - 1997, which already has been issued in 1993.

The research described here has been supported through the regular research funds of Delft University of Technology (Voorwaardelijke Financiering TUD/GE-01/88-38) as well as through special University funding for pilot research (Onderzoeks Stimuleringsruimte). The project also received major financial support from SRON. In view of these major fundings, this report primarily serves the purpose of accounting for the work that has been carried out in the period 1990 - 1993. In addition there has been an overlap with a variety of smaller scale research projects, which have been supported by national and international scientific and industrial organizations, in particular through the Netherlands Remote Sensing Board (BCRS) and the European Space Agency (ESA).

2 Instrumentation and Tracking

The efforts in operations and instrument development at the Kootwijk Observatory for Satellite Geodesy (KOSG) aim at the continuation of the history of satellite geodesy in The Netherlands, contributing to maintenance and improvement of the state-of-the-art in the relevant observation techniques. Primarily these efforts concentrate on the technique of Satellite Laser Ranging (SLR) and the use of the NAVSTAR Global Positioning System (GPS).

The expertise in the SLR technique has been accumulated over two decades. In 1976, Technisch Physische Dienst TNO-TU (TPD) delivered a stationary SLR system, which had been developed in close consultation with the KOSG staff and was developed with the help of experience existing at that time in the U.S. and France. This SLR system of the so-called second generation was at that time a novelty in Europe. A decade later, TPD now jointly with KOSG, built two transportable SLR systems [1], one of which, the Modular Transportable Laser Ranging System (MTLRS-2), since has been deployed by KOSG. KOSG's contribution concentrated in particular on the design and development of the controller electronics and software. Recently, again about a decade later, the cooperation between TPD and KOSG has been renewed for the joint development of a fourth generation SLR system under contract with a foreign principal. Although there is a substantial industrial development at subsystem level (e.g. pulse lasers, detectors, timing systems), the application and integration of these developments in the technique of SLR demand active participation of the research groups, preferably in international cooperation.

With the technique of the GPS the situation is quite different. There is a very strong and competitive industrial development of integrated receivers, also for high precision applications. The scientific user does not need to participate in system development but must merely concentrate on understanding the observational process and its aspects of quality control. Scientific users can and should contribute to the development of (pre-)processing strategies in view of the high precision application.

The operational activities are intimately connected to the scientific objectives of the research in Earth Oriented Space Research at DUT, with emphasis to the applications in crustal dynamics, earth rotation and precise orbit determination for altimetry and gravity field determination. Below, the main activities in the areas of instrument development and operations, performed by the team at KOSG, are reviewed.

2.1 Development and acquisition of instrumentation

2.1.1 Upgrade and maintenance of MTLRS-2

The MTLRS-2 was delivered in 1984 and has been deployed in field campaigns since 1985. After some five years of operation under rugged field conditions, the system began to show malfunctioning, mostly as a consequence of aging of components. Trouble shooting activities and repair in the field began to limit the data acquisition capability. On the other hand the single shot precision of SLR systems was clearly advancing to the sub-cm level, while the efficiency in terms of acquisition rate considerably improved. These developments are primarily a consequence of shorter laser pulses and improved detector technology [2]. In the mean time MTLRS-2 still ranged at a typical 5 cm single shot precision, with about 10 % return rate. Both considerations urged the team to revisit the design at sub-system level and to develop a strategy for upgrade of some of the major sub-systems [3]. Budgetary constraints as well as the requirement to minimally interfere with the operational activities, dictated a stepwise upgrade programme, spanning at least several years to come. The major sub-systems considered in this planning were the pulse laser, the controller system and the detector system.

Pulse laser

The original pulse laser showed gradually more frequent malfunctioning, in particular of electro-optical subsystems (e.g. the Pockels cell trigger chain and the Mode Locking device) and the cooling system. Moreover, the pulse width of about 300 picoseconds would constitute one of the bottle-neck limitations for improving the range accuracy. Developments in pulse laser technology had by then resulted in pulse widths of typically 20 to 30 picoseconds at an energy level of 30 milliJoule. The Institut für Angewandte Geodäsie, which operates the identical MTLRS-1, was facing the same situation, and it was therefore decided to jointly select and procure a new pulse laser for both mobile systems. Because the laser in MTLRS is housed in the telescope cart, which is exposed to the full range of environmental conditions during operations, it must be of special, very compact design, and include active thermal stabilization and remote control on all critical optical components.

The system which has been selected is a Neodymium YAG pulse laser of the Self Filtering Unstable Resonator (SFUR) type, developed by the Quanta Systems company and modified by a German vendor. The emitted pulses have a "full-width-half-maximum" of 30 picoseconds at an energy level of 30 milliJoule. The order was placed by the end of 1990 and the system was delivered in mid 1991. Prior to the 1992 field campaign the system was implemented in MTLRS-2 and after an, initially severe, problem of electro-magnetic compatibility had been cured, test results indicated a performance according to the specifications. Since then the system basically performed well, although some problems were frequently encountered mainly with the pulse stability and the temperature control. Replacement of the switched mode power supply for the flash lamps and some modifications to the cooling system and system electronics resulted in a stable and reliable operation by the end of the report period. The shorter pulse width already resulted in some improvement of the overall range precision, but the major improvement to the 10 mm level or even better is now dependent on the detector upgrade.

Controller system

The original controller system of MTLRS, comprising a hardware unit controlling most real-time system functions, and two micro processors slaved to a central computer system for monitoring and data storage, has been designed by KOSG in the early eighties and has performed for many years without any substantial problems in field conditions [4]. After some five years of operation, the major drawbacks of this system became the aging of the electronics components and the loss of support from vendors of certain critical bought-out hardware components. In addition, the non-structured design and the limited capability of the processors to meet the operational requirements for the coming decade, called for a new design of the entire controller system.

The chief design goals which were formulated [5] concentrated on bringing down the costs of operations, minimizing the down-time in the field and enabling the observation of a multitude of new SLR satellites scheduled for launch in the nineties. The overall design which was completed in 1991, accommodates almost all controller functions in software, running in a network of parallel processors (Figure 2.1), which is linked to a standard PC hosting the graphics user interface under the MS Windows operating system. This novel design was also selected for the German MTLRS-1 and the manufacturing phase which started in 1991, aims at delivery of two identical controller systems for MTLRS-1 and MTLRS-2. This phase experienced some delay, mainly because of operational and other upgrade activities, but by the end of 1993 the system neared completion. Implementation in both laser ranging systems is foreseen prior to the field campaign of 1994.

Detector

The upgrade of the detector subsystem primarily aims at the improvement of the ranging accuracy to 10 mm or better at single shot and will be the key-stone of the stepwise upgrade programme, initiated in 1990. In essence two components of the detector system will be addressed, i.e. the wavelength filter which selects the laser wavelength out of the back scatter from the sky and the detector itself. This upgrade will be taken up after completion of the controller system.

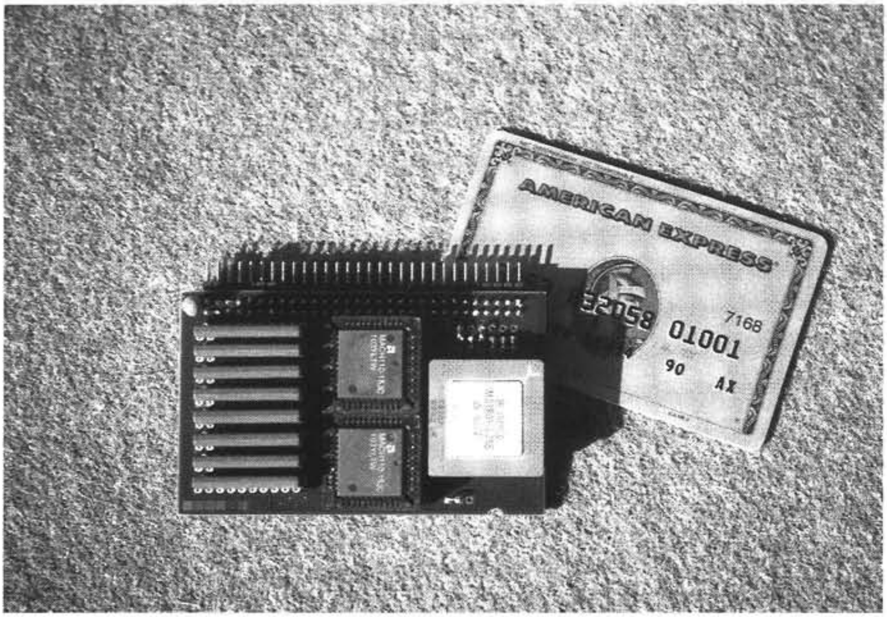

Figure 2.1 The "credit card" size processor board, designed and developed at KOSG, is the central board in the MTLRS controller system. This general purpose board houses the T805 transputer, with memory and fast I/O Bus.Presently four of these processor boards make up the parallel network in the controller system.

In the period covered by this report, the activities were limited to some preliminary modifications and preparatory investigations. The optical interface between the telescope and the detector has been expanded with an optical switch to accommodate two different detectors. This enables future testing of various detector options without jeopardizing the operational status of MTLRS-2. Experience has been obtained with a detector system designed by NASA comprising a micro-channel-plate photo multiplier. Test measurements were successful, although time critical problems were encountered in generating necessary high voltage gate signals for the multiplier, while observing very short ranges, as is required during internal calibration. The detector technology showed a significant development in the report period, in particular in the area of avalanche photo diode detectors. Experiences at other SLR stations (including the MTLRS-1 which already completed its detector upgrade) is being monitored closely, in preparation of the selection of a final strategy for the detector upgrade of MTLRS-2.

General maintenance

In particular during the 1992 campaign, it became evident that MTLRS-2 needed a general, major overhaul in addition to the stepwise upgrade of sub-systems. In particular the optics and mechanics of the telescope, which had been used for many years without virtually any specific attendance, needed a thorough cleanup and inspection to improve the system performance. The TNO Product Center assisted in this specialized activity in early 1993.

2.1.2 Global Positioning System

Since 1990, a coordinated strategy has been followed by the cooperating groups at DUT to make optimal use of the Global Positioning System, concentrating on high precision geodetic applications. In 1990 a SNR-8 ROGUE GPS receiver has been purchased jointly with SSR&T for stationary deployment at KOSG. This receiver, although at that time more or less still a prototype, was considered to be the state-of-the-art in GPS receiver design, in particular for high precision positioning. From the onset a close cooperation was established with the manufacturer and in particular with the NASA Jet Propulsion Laboratory (JPL) who originally designed this receiver. This cooperation aimed at rapid accumulation of expertise at DUT with this type of receiver technology and at optimizing the performance of the system. For installation at KOSG, the most optimal antenna location has been determined with great care, to minimize the multi-path effect and to ensure un-interrupted reception of the weak GPS signals, also at low elevation. At the short range radio test facility at ESTEC the phase centers of the antenna were accurately calibrated, enabling proper correction of the computed positions to the antenna reference point. The system came into operation at its definitive location at Kootwijk by the end of 1990. Ever since, some modifications and several firmware upgrades have been implemented in close cooperation with JPL. A software system for automatic down loading and submission of the data has been developed and implemented, resulting in a routinely operating, virtually automatic GPS station.

In 1992, as one of the first users outside the US, KOSG again jointly with SSR&T, purchased two TurboRogue SNR-8000 GPS receivers. This receiver, which is a follow-on development of the SNR-8, represents the state-of-the-art in miniaturized, high precision, field qualified GPS receivers. This purchase aims at enhancing the facilities for participation in international field campaigns for earth oriented space research and will also further contribute to the accumulation of expertise in GPS receiver technology for high precision work at DUT. Both receivers have been thoroughly tested and were expanded with ancillary equipment for deployment in field conditions.

2.1.3 PRARE

Already in 1989, SSR&T ordered a PRARE ground station to participate in the experimental phase of this novel tracking system after the launch of ERS-1, originally expected in 1990. The Precise Range and Range Rate Equipment (PRARE) is a satellite based tracking system, operating in the S- and X-band, designed to precisely determine the satellite orbit and in addition to determine positions of ground stations. The chief interests at DUT were to investigate its use for regional altimetry research and to contribute to the global tracking and orbit determination of ERS-1. Unfortunately, the PRARE space segment did not function properly after the launch in July 1991 and the experiment was cancelled. DUT intends to participate with its PRARE ground station in follow-on experiments, involving the METEOR-3 (launch fall 1993) and ERS-2 (launch 1995) satellites.

2.2 Kootwijk Reference Station

Late '73 the Faculty of Geodetic Engineering implemented the Kootwijk Observatory for Satellite Geodesy, marking the start of a Dutch space-geodetic reference station. In the beginning, the technique of satellite triangulation was deployed, but since 1976, distances to satellites were routinely observed from a stationary position with the technique of SLR. This led to a few decimeter accuracy coordinate determination in a world wide geodetic reference frame. Since 1984 the transportable SLR system MTLRS-2 was obtained, with which both at Kootwijk and elsewhere in international cooperation, positions at the cm level of accuracy are being obtained.

Since 1990 the radio positioning technique of the Global Positioning System is deployed as a permanent facility at KOSG. With continuous, high precision GPS observations the observatory participates in both global and regional networks of reference stations. This activity on the one hand supports the accurate determination of the orbit of GPS satellites as well as the orbit of low flying satellites carrying a GPS receiver (e.g. TOPEX/Poseidon) and on the other hand contributes to the maintenance of global and regional geodetic reference networks for studying crustal deformation and earth rotation.

In 1991 the station participated in the GPS IERS and Geodynamics Experiment (GIG'91), earmarking the advent of GPS in stationary deployment for research in geodynamics. One of the interesting issues was the feasibility of GPS to determine short periodic features in the rotation of the earth. This successful experiment led to the establishment of the International GPS Service for Geodynamics (IGS) under the auspices of the International Association of Geodesy and the International Union of Geodesy and Geophysics. The IGS aims at the determination of precision GPS satellite ephemerides, a terrestrial reference frame, earth rotation parameters, global and regional crustal motion and associated products. DUT successfully responded to a call for participation in 1991 and began the daily submission of the Kootwijk GPS data on a routine basis. This participation was renewed by the end of 1993, when the IGS was transformed into a formal and routine service, also embedded in the International Earth Rotation Service (IERS). Based on the performance of the international network up to then, the IGS Analysis Center Workshop [6], selected a subset of 13 IGS stations (Figure 2.2) of which the data is routinely processed by all seven IGS analyses centers. The products of this service, primarily GPS orbits and earth rotation parameters, are available at the NASA Crustal Dynamics Data Information System (CDDIS) on a daily basis, ultimately within two weeks of the date of observation.

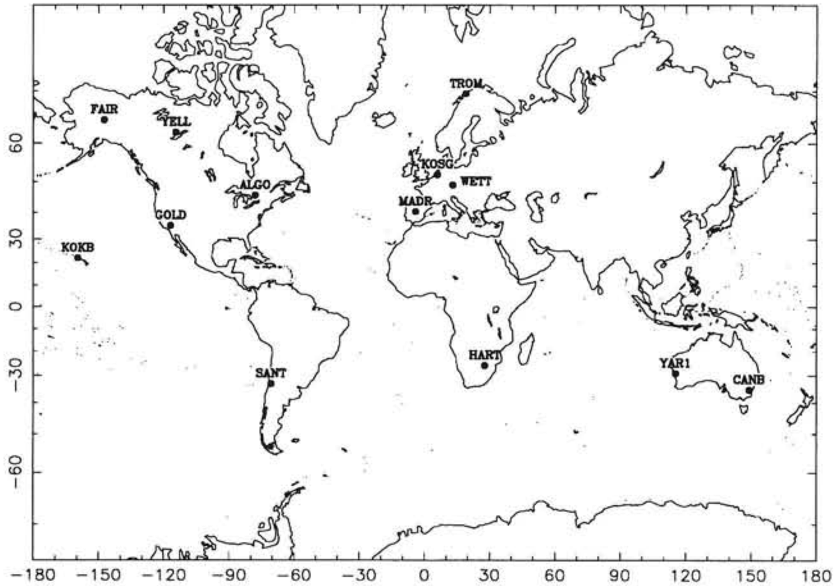

Figure 2.2 The 13 station global network of the IGS is the prime GPS geodynamics reference network.

The combination of permanent GPS measurements and regular campaigns with MTLRS-2 at the Kootwijk reference station, forms the basis of the maintenance of the international space-geodetic reference position in the Netherlands at state of the art level of accuracy.

Nationally, this position is connected to the National Triangulation Network (RD-network) and the height reference of the Survey Department of Rijkswaterstaat. The vertical component of position is of increasing importance in view of regional investigations on land subsidence or uplift and long-term variations of the mean sea level [7]. A gravimetric platform was implemented at KOSG in 1990, suitable for absolute and relative gravimetric observations for regional geoid determination and in support of the maintenance of a vertical reference. Absolute gravimetric observations were performed there (Figure 2.3) by the Institut für Erdmessung of the University of Hannover in 1991 and 1993 [8,9], connecting the station to the International Absolute Gravity Base station Network.

2.3 Field campaigns

The MTLRS-2 and mobile GPS equipment have been deployed in international observation programmes, supporting high precision station positioning and the monitoring of horizontal and vertical crustal movements as well as in support of precise orbit determination of application type satellites, supporting research in geodesy, geophysics and oceanography.

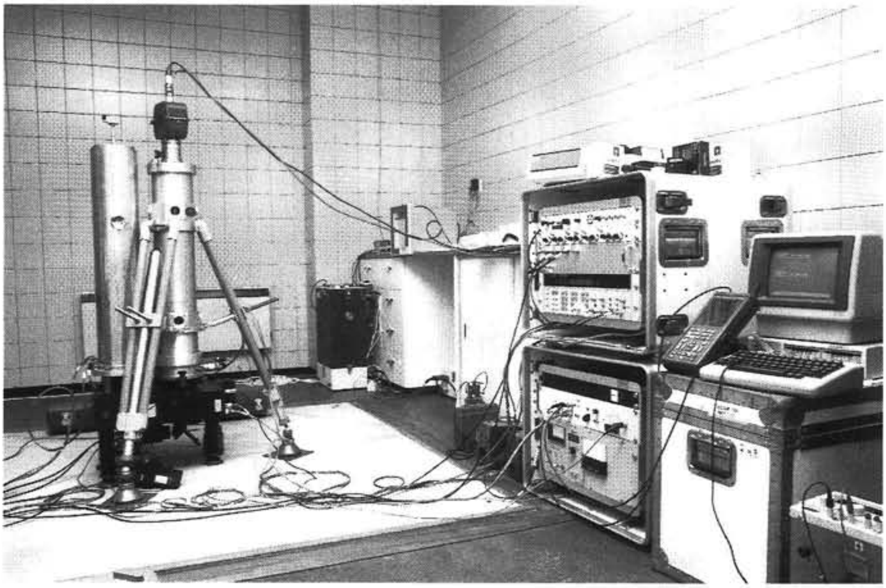

Figure 2.3 The JILAG-3 absolute gravimeter of the Institut für Erdmessung of the University of Hannover, observing at the gravimetry platform at KOSG.

2.3.1 MTLRS-2

In the summer of 1990, MTLRS-2 has been deployed at the Tromsø observatory in northern Norway, in a cooperation with the Norwegian Mapping Authority Statens Kartverk. The prime purpose of this campaign was to determine an accurate position of this Norwegian reference station in the global SLR reference frame. It provided in addition an important link between the techniques of SLR and Very Long Baseline Interferometry (VLBI), because Tromsø had been visited by a transportable VLBI system in 1989. The connection of the global SLR and VLBI networks is very important for the definition and maintenance of a global conventional terrestrial reference system to be used for the monitoring of crustal motion and earth rotation. Last but not least, this campaign has produced an SLR reference point in the far north of Europe, which can be used to support the long-term monitoring of vertical crustal motion (in particular post-glacial uplift) and of mean sea-level. The data analysis of this campaign was performed at DUT [10], resulting in an accuracy of station position better than 20 mm.

In the late fall of 1990, MTLRS-2 was transported to the astronomical observatory at Noto, Sicily (Figure 2.4). The observations there occurred in the framework of a bilateral agreement with the Italian Space Agency (ASI) under the umbrella of the WEGENER project. At this site a stationary VLBI system had recently been installed by ASI, thus providing an additional opportunity to contribute to the global comparison of the SLR and VLBI reference frames. This campaign also marked the inclusion of the Noto site in the WEGENER/MEDLAS network in the central and eastern Mediterranean (see also Chapter 4). After the installation of MTLRS-2 this occupation has been very successful, acquiring the critical dataset of 50 passes of the LAGEOS I satellite within 4.5 weeks, just prior to the occurrence of the 5.1 earthquake on December 13, 1991, with epicenter in the Gulf of Noto.

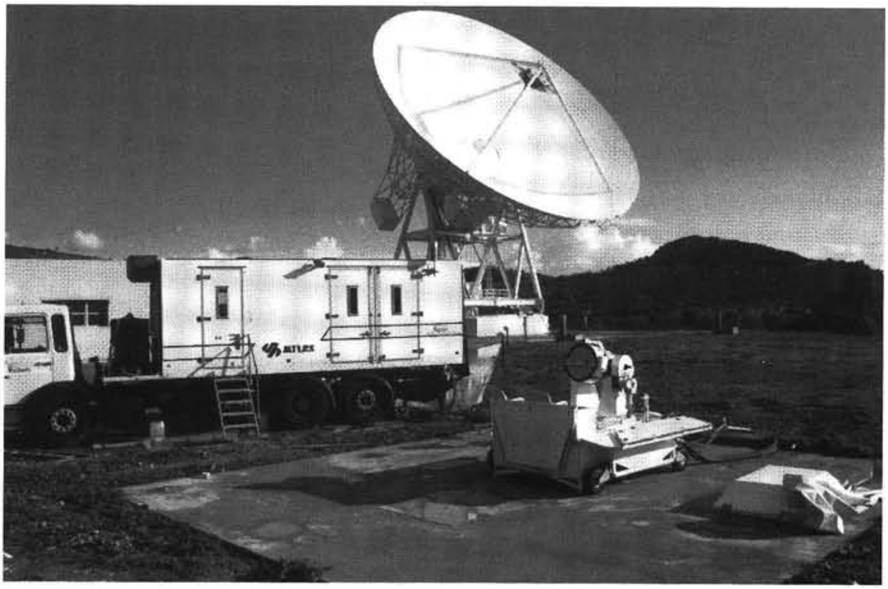

Figure 2.4 The transportable laser ranging system MTLRS-2 observing at Noto, Sicily, near the geodetic VLBI telescope of the Italian Space Agency.

In 1991 MTLRS-2 participated in the calibration experiment of the radar altimeter of the ERS-1 satellite [11]. The system was deployed at a military facility at Monte Venda near Padova in northern Italy from April to September. Initially, test measurements were performed to assess and eliminate the problem of electro magnetic compatibility caused by powerful radio transmitters in the area. After the launch of ERS-1 in July, 44 passes of that satellite were observed, of which 12 were actual overhead calibration passes. In addition, 69 passes of the LAGEOS I satellite were observed, which enabled the accurate determination of the global SLR position of this site.

In 1992 MTLRS-2 participated in the WEGENER/MEDLAS campaign and was deployed at the Greek Dionysos station from March. Data acquisition was lower than usual and this problem could not be sufficiently cured in the field, in spite of extensive trouble shooting. In August the system was brought back to Kootwijk for a major maintenance service in conjunction with the controller system upgrade.

Although all in all sufficient data had been collected at Dionysos, the remainder of the observation schedule for the system in Greece and Italy could not be completed that year.

2.3.2 GPS

In 1990 the team participated with two Trimble-SST mobile GPS receivers of the Faculty of Geodetic Engineering in an observation campaign connecting the European SLR stations to the Italian sites from which the radar altimeter of ERS-1 was to be calibrated in 1991. The Dutch receivers observed at the calibration site of Monte Venda near Padova and at the oceanographic platform of the Consiglio di Richerche Nazionale off the Venetian coast.

Furthermore, in 1992, two sites in Italy, viz. Basovizza and Medicina, were occupied with Trimble-SST receivers, in support of the WEGENER/GPS-92 campaign. This activity, which was part of the IGS Epoch'92 campaign, was organized by IfAG and supported by DUT. It represents the first coordinated effort to observe the entire WEGENER-MEDLAS network with GPS, enabling the comparison of SLR- and GPS derived station positions (see Section 4.3.1).

After the purchase of the SNR-8000 TurboRogue GPS receivers extensive test measurements have been carried out with these instruments at the Kootwijk Observatory and elsewhere in The Netherlands. Comparison experiments were performed with the stationary receiver of the IGS station at Kootwijk, in preparation of future replacement of the latter. In addition, these measurements supported on-going activities at the Faculty of Geodetic Engineering, in the development of an Active GPS Reference System (AGRS) in The Netherlands. The two TurboRogue receivers have been deployed in two campaigns in The Netherlands, organized jointly with SSR&T, to investigate the stability of the storm surge barrier in the Oosterschelde.

2.4 References

1. Visser, H., and E. Vermaat, *Description of a transportable laser ranging system MTLRS*, Rapport A 8289, Technisch Physische Dienst TNO-TU, Delft, 1985.

2. Degnan, J.J., *Millimeter Accuracy Satellite Laser Ranging: A Review*, In: Contributions of Space Geodesy to Technology, Geodynamics Series, **25**, American Geophysical Union, 133-162, 1993.

3. Beek, W. and K.H. Otten, *MTLRS-2 upgrade*, In: Proceedings of the Seventh International Workshop on Laser Ranging Instrumentation, Matera, October 1989, OCA/CERGA, Grasse, 329-336, 1990.

4. Vermaat, E., K.H. Otten and M. Conrad, *MTLRS software and firmware*, In: Proceedings of the Fifth International Workshop on Laser Ranging Instrumentation, Herstmonceux Castle, September 1984, GRGS/CERGA, published by the Geodetic Institute, University of Bonn, Bonn, 342-360, 1985.

5. Vermaat, E., J.W. Offierski, K.H. Otten, W. Beek, C. van Es, and P. Sperber, *Transputer based control system for MTLRS*, In: Proceedings of the Eighth International Workshop on Laser Ranging Instrumentation, Annapolis, May 1992, NASA Conference Publication 3214, Goddard Space Flight Center, Greenbelt, 12/40-12/48, 1993.

6. Kouba, J. (ed.), *Proceedings of the IGS Analysis Center Workshop*, October 1993, Geodetic Survey Division, Surveys, Mapping and Remote Sensing Sector, NRCan, Ottawa, 1993.

7. Kootwijk Observatory for Satellite Geodesy, *Position on Kootwijk*, Section Physical, Geometric and Space Geodesy, Faculty of Geodetic Engineering, Delft University of Technology, Delft, 1991.

8. Ree,R.E. van, *Absolute zwaartekracht in Nederland*, thesis, Section Physical, Geometric and Space Geodesy, Faculty of Geodetic Engineering, Delft University of Technology, Delft, 1991.

9. Lorenz, G.K., and R.E. van Ree, *Absolute zwaartekracht metingen*, in: NGT Geodesia, **35**, 2, Apeldoorn, The Netherlands, 1993.

10. Ambrosius, B.A.C., J.A. Bax, B.H.W. van Gelder, D.L.F. van Loon, R. Noomen, A.J.M. Verheijen, E. Vermaat, and K.F. Wakker, *Positioning of the Tromsø station by satellite laser ranging; Campaign 1990, Data acquisition and analysis*, Report LR-668/MFG-91.5, Faculty of Aerospace Engineering and Faculty of Geodetic Engineering, Delft University of Technology, Delft, 1991.

11. Francis, C.R. (editing author), *The calibration of the ERS-1 Radar Altimeter*, Report ER-RP-ESA-RA-0257, Issue 2.0, ESA/ESTEC, Noordwijk, March, 1993.

3 Orbit Determination

The understanding of the orbital mechanics and the accuracy of orbit determination of (earth) satellites is indispensable for the success of Earth Oriented Space Research. These topics have been studied extensively since the early seventies by Delft University and a wide experience in the field of orbit computations and its applications has been gained since. Initially, the investigations focussed primarily on the processing of SLR data for the precise orbit determination of satellites equipped with laser retro-reflectors. These fall into two categories; first of all, there are the "cannon ball"-type satellites, such as LAGEOS and STARLETTE, which are especially intended for crustal dynamics research, and secondly, another more conventional class of satellites exists, which also require precise orbits for their scientific mission. The latter category mainly includes most satellites carrying a radar altimeter instrument, such as ERS-1 and TOPEX/Poseidon.

More recently, two new tracking systems have been introduced successfully for precise orbit determination. One is the Doppler Orbitography and Radiopositioning Integrated by Satellite (DORIS) system, which was especially developed for the TOPEX/Poseidon mission. The other is the Global Positioning System (GPS). The latter is a general-purpose space-based radio navigation and positioning system, for which orbit determination of low earth satellites is only one of its many applications (other applications are discussed in Chapter 4 and 7).

Orbit determination of satellites using SLR data has more-or-less become an integral part of the overall data analysis efforts for crustal dynamics research and satellite altimetry investigations. Therefore, this topic will not be discussed separately in this Chapter, but the relevant issues will be included in the Chapters dealing with the applications. However, the DORIS and GPS investigations are relatively new and independent efforts, which warrant a separate treatment.

Because the DORIS system was designed to be the primary tracking system for TOPEX/Poseidon, it was first test-flown onboard the French SPOT-2 satellite. The aim was to validate the performance of the system, and to gain experience in the processing and analysis of this type of tracking data. DUT also participated in this effort and later became involved in the analysis of the TOPEX/Poseidon DORIS data as well. These activities are described in section 3.1.

The aim of the GPS orbit determination studies was to investigate the characteristics of the system and to explore its use, through numerical simulations and the actual processing of real observations. These consisted of data collected by an experimental GPS navigation receiver onboard the Landsat-5 spacecraft and measurements obtained by the first space-borne geodetic-quality receiver carried by TOPEX/ Poseidon. This topic is discussed in section 3.2.

3.1 Orbit determination with DORIS

Important contributions to the Global Change Studies, currently undertaken, are the oceanographic investigations using Earth orbiting satellites, such as ERS-1 and TOPEX/Poseidon. The aim of these missions is to get a better knowledge of the energetic exchanges between oceans and atmosphere. The satellites carry a precision radar altimeter which measures the oceans topography. To be able to interpret these altimeter measurements in valuable terms for oceanographers, the satellite orbit must be known to subdecimeter accuracy in the radial component. Traditionally, this has been a difficult problem, especially for low earth satellites, because their visibility is quite poor, in particular from a sparse tracking network. The problem is even worse for optical tracking systems like satellite lasers, which require clear skies. However, for a long time they were the only systems with sufficient accuracy. These limitations motivated the design of the new DORIS satellite tracking system.

DORIS is a satellite-based radio positioning and orbit determination system which has been designed, developed and is operated by CNES (Centre National d'Etudes Spatiales), GRGS (Groupe the Recherche de Géodésie Spatiale), and IGN (Institut Géographique National) [1].

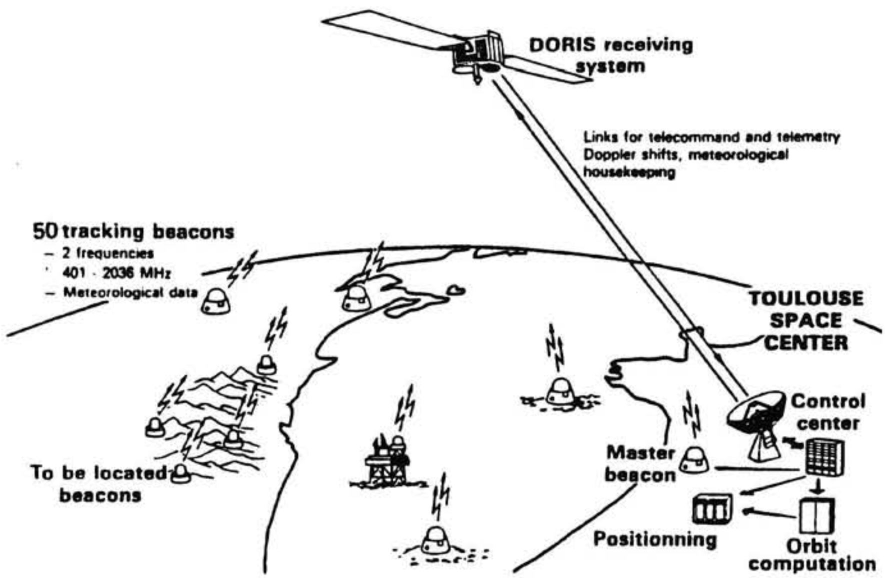

Figure 3.1 The Doppler Orbitography and Radiopositioning Integrated by Satellite (DORIS) system.

The system is based upon the one-way measurement of Doppler shifts on the radio signals transmitted by ground beacons and received by DORIS's onboard package as the satellite passes within range of these beacons. Every beacon transmits two signals with very stable frequencies: 2.03625 GHz and 401.25 MHz. The first signal provides the precise Doppler measurement and the second one the meteorological and housekeeping data. Together they provide a tool for eliminating the first order effect on the propagation of the signals through the ionosphere [2].

The complete DORIS system consists of the DORIS onboard package, a network of Orbit Determination Beacons (ODBs) and Ground Location Beacons (GLBs), a DORIS Control Center (DCC), and a Master Beacon (MB) which handles the communications between ground control and satellite [3]. Figure 3.1 gives a complete overview of the DORIS system.

The DORIS onboard package was placed on the remote sensing satellite SPOT-2 as a test experiment in preparation of the TOPEX/Poseidon mission. The satellite was launched into a sunsynchronous orbit on the 22nd of January, 1990. The first months of its mission were devoted to the system validation and instrument performance assessment [1]. Continuous operation started soon after and by the end of 1990, preprocessed DORIS data from all transmitting beacons in the time-frame of May 5 to May 18, 1990 were made available to all TOPEX/Poseidon principal investigators. Later, another data set, collected during the *asymptotic* campaign, which ran from January 2 to March 22, 1992, was made available.

Figure 3.2 shows the network of 39 stations that have been tracked by SPOT-2 during the *asymptotic* campaign. Included are the 15° elevation visibility contours. Note that the network covers more than 70% of the Earth's surface. During the first campaign, only a network of 29 stations was operational. In the first campaign only ± 50,000 measurements was collected, whereas in the second campaign this amounted to ± 300,000 measurements. The Doppler shift counts or radial velocity measurements in the stored data serve as input for the orbit determination and parameter estimation computations, which will be addressed hereafter.

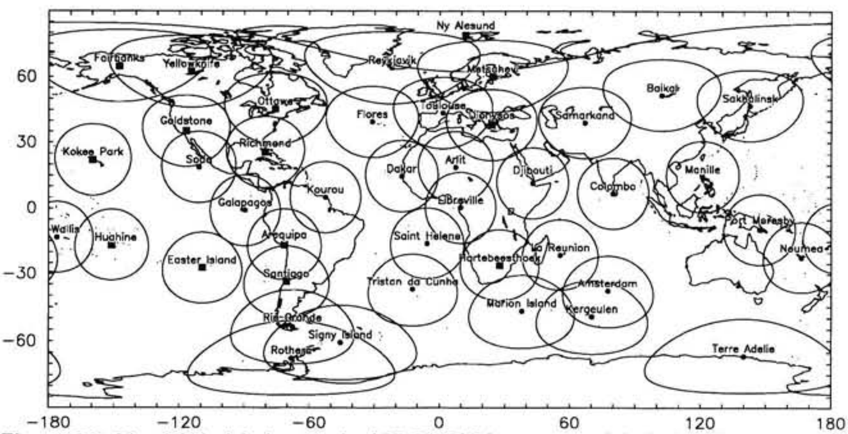

Figure 3.2 The 1992 global network of 39 DORIS beacons and their visibility contours for a 15° cut-off elevation (stations fixed to the ITRF90 solution are marked by ⊡).

3.1.1 Data analysis

The GEODYN II program, developed by EG&G [4], has been used for the orbit determination and the geodetic parameter estimation. The software has been in use for several years now, but until recently, primarily laser range tracking data had been processed. The DORIS data provided an interesting opportunity to test the capabilities of the program with one-way range-rate data.

Due to the enormous amount of data, a priori choices needed to be made about the analysis strategy. It was decided to process the data of the two campaigns in 7 and 39 consecutive batches of two days, respectively. The length of these so-called data arcs was limited to 2 days as a compromise, to prevent excessive build up of dynamic model errors on one hand, but to allow dynamic strength in the solutions on the other.

Earlier studies have shown that for low earth satellites, gravity field model errors produce by far the largest errors in the satellite's orbit, and that atmospheric drag is the second most important error source, in particular for the along-track position component [5,6].

The earth's gravitational field is represented mathematically as an infinite series of terms, their amplitude decreasing as their order in the series increases. The different coefficients represent the heterogeneities in the distribution of matter in the different layers of the earth. Recent solutions of the gravity field model did only permit satellite orbit determination with an accuracy of about 1 meter in the vertical direction. To achieve a higher accuracy, a model of the gravity field can be tailored specifically to the satellite's orbit. One of the institutes at which gravity models are being developed, is NASA's Goddard Space Flight Center (GSFC). Their models are usually referred to as Goddard Earth Models (GEM). At the time of this study, the most up-to-date general-purpose gravity model was the GEM-T2 model. This model was tailored for SPOT-2 using DORIS data gathered in the first months of its mission. The resulting model, Preliminary Gravity Solution PGS-4591, was expected to provide a radial orbit accuracy of better than 50 cm for SPOT-2, or any other satellite with the same orbit characteristics. This has been verified for ERS-1 [7], which is in an orbit at about the same altitude and inclination as SPOT-2. For the analyses, the full PGS-4591 model was used complete to degree and order 50.

As SPOT-2 orbits the Earth at a relatively low altitude of about 800 km, its orbit is affected considerably by atmospheric drag [8], and therefore up-to-date information on the atmospheric conditions is needed for the orbit computation. The atmospheric density model selected was the Jacchia 71 model, which uses daily 10.7 cm flux and geomagnetic A_p values to account for the solar activity. The uncertainties in atmospheric density cause significant errors in the computed orbits. A satellite such as SPOT-2 is subject to variations in atmospheric density as high as a factor 10 from the peak to minimum solar activity in the 13-yr cycle of this activity and to variations of 50% or so in a few hours resulting from short-period bursts of solar activity [9]. In general, unmodeled long-period variations in atmospheric density can be accommodated by the estimation of a scaling factor for the drag in the orbit computations. Usually, this is not sufficient, because local discrepancies and short-term variations also cause short-period perturbations. An engineering solution is to estimate a time series of drag scaling parameters, each covering only a fraction of the total arc-length. However, this is only possible for satellites with sufficiently dense tracking. SPOT-2 is a good example of such a satellite, since it is tracked almost continuously [9]. Earlier studies showed that adjusting the drag coefficient every four orbital revolutions is a good strategy [10]. The same strategy was adopted for the estimation of the drag coefficients.

The forces induced by atmospheric drag and solar radiation primarily act upon the cross-sectional area of the satellite. The cross-sectional area varies in time, because the satellite is three-axes stabilized and possesses a rotating solar panel of which the rotation axis is directed perpendicular to the orbital plane. The cross-sectional area is different, however, for each force. The area for drag is perpendicular to the satellite's relative velocity vector, while for the solar radiation it is perpendicular to the satellite-Sun vector. Because the relatively large solar array is always pointed towards the cum, the variation in cross-sectional area for the solar radiation effect is less compared to the variation in the drag effect. However, these variations tend to average out over a revolution, and since the position of the Sun relative to the orbital plane changes only very slowly with time, the variations will be similar for each revolution. Therefore, the solar radiation effect is accounted for by the estimation of a single solar reflection parameter (C_R) for each data arc.

The SPOT-2 satellite is frequently maneuvered to compensate for a loss of altitude due to atmospheric drag. These maneuvers, which occur at irregular intervals of several weeks, cause discontinuities in the orbital parameters, which may be modeled by introducing quasi-instantaneous accelerations at the maneuver times. Since the magnitude of the maneuver is usually only known with limited accuracy, it is best to estimate it from the observations. GEODYN has the possibility to account for these accelerations. As only one maneuver had to be accounted for and this maneuver consisted of two consecutive thruster firings with half an orbital period in between, a total of six acceleration parameters was solved for.

The station coordinates of the DORIS network pose another problem. To obtain highly accurate orbits, they need to be known with an accuracy of 5 to 10 cm. For some sites, where the DORIS beacon is collocated with other high accuracy tracking systems (< 2 cm) [11,12], this requirement is easily satisfied. Other sites, however, located in remote areas, which are often only surveyed with GPS (with an accuracy varying from 10 cm to more than 1 m), this is not so easy. Therefore, it was decided to fix some of the accurately known stations to their a priori positions and solve for the other ones. Not all the accurately known stations were fixed, so that an absolute comparison could be made of the DORIS results with the a priori coordinates for the other accurate stations. The fixed stations also provided a common reference frame for all arcs, simplifying the comparison of the results of the different arcs.

For the first campaign, the fixed stations were Arequipa, Goldstone, Hartebeesthoek, Metsahovi, and Yellowknife. Their a priori values were derived from the IERS Terrestrial Reference Frame coordinates (ITRF90) [12] interpolated to the epoch of May 5, 1990. In the second campaign these stations were Easter Island, Richmond, Hartebeesthoek, Metsahovi, and Yellowknife. Their a priori values were derived from the same ITRF90 solution advanced to the epoch of January 1, 1992. These stations were selected for the campaigns, because they were tracked best in every arc and had the best global distribution. Their locations are marked in Figure 3.2.

The coordinates of all other station were solved for with an a priori sigma of 1 meter. Their a priori values were taken from the JCOD1.3 station coordinate solution, denoted by CNES, for the first campaign and from another station coordinate solution by CNES for the middle of January 1992, for the second campaign.

Finally, to compensate for frequency offsets between the satellite and beacon oscillators, a range-rate bias was estimated for each pass.

3.1.2 Orbit determination results

The analyses generated an enormous amount of information. We have tried to select only the most relevant results and to summarize it into a few plots. Figure 3.3 shows the recovered values of the drag (C_D) and solar reflection coefficients (C_R) and the weighted root-mean-square (rms) values of the observation residuals, for the asymptotic campaign. The 1-sigma error bars of the drag and solar reflection coefficients are also plotted in the figure, but since they are generally very small and because of the small size of the plots they are hardly discernable, except for a few in the C_D plot. Finally, the daily 10.7 cm solar flux values and the geomagnetic index have been included in the figure as well. To save space, the comparable results for the first campaign are not shown. It suffices to mention that they are quite similar, although the rms is slightly worse (1.2 mm/s). This may be due to the smaller size of the network, in comparison with the asymptotic campaign.

The (weighted) rms of the range-rate residuals is a good measure of the success of the overall estimation process, indicating how well the computed orbit fits the measurements. It is emphasized that the rms values plotted in Figure 3.3 represent the results after automatic iterative data editing, in which bad data points have been eliminated from the estimation process. As can be seen, the residual rms averages about 1 mm/s for most data arcs. This is about 3 times higher than the system noise of DORIS, which is claimed to be of the order of 0.3 mm/s [2]. The difference can be attributed to deficiencies in the applied dynamic and measurement correction models. Overall, this result is considered to be quite good however, because from experience with SLR data of the LAGEOS satellite, which was especially designed to minimize these errors, it is known that the rms of fit is typically 3 to 5 times the data noise.

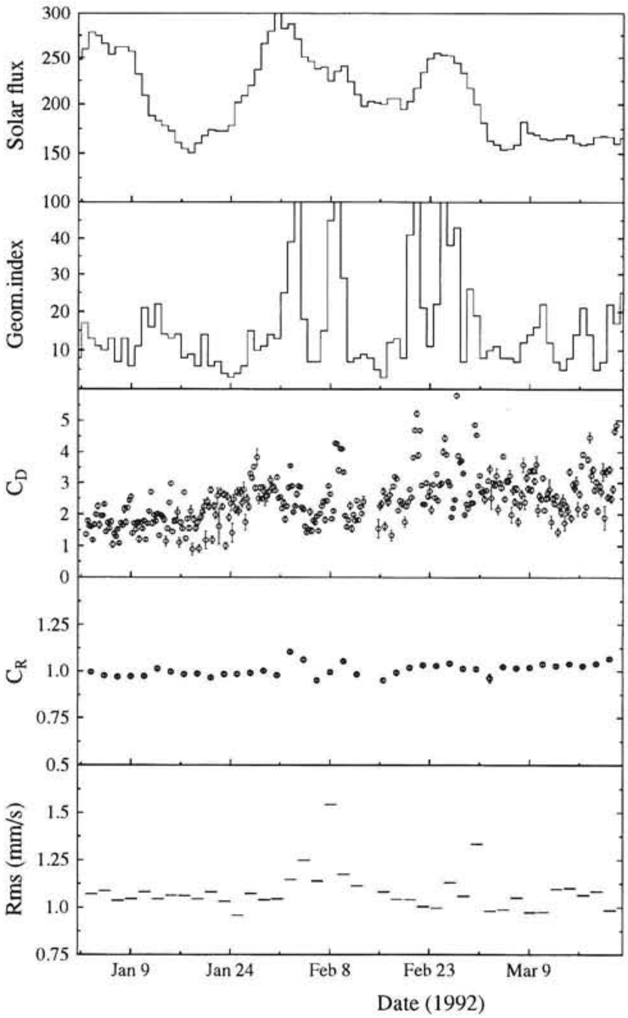

Figure 3.3 SPOT-2 orbit computation results involving drag coefficients, solar radiation coefficient and weighted rms values for the period of January 1, 1992, to March 22, 1992.

The effect of model errors is demonstrated nicely by a few arcs, in the beginning of February and near the end of that month, which exhibit a somewhat higher rms of fit. There seems to be a correlation between these worse fits and the peaks in the geomagnetic index, signalling strongly increased levels of solar activity, in particular for the arcs in early February. This can be interpreted as an indication that the Jacchia 71 atmospheric density model does not always account for these extreme effects correctly. Further evidence for this can be found in the C_D plot, which shows much larger values for this parameter, during the peaks in the geomagnetic index, than average, suggesting that the Jacchia 71 model underestimates the density in those cases. This effect is more pronounced for the arcs in late February than the earlier ones. Combined with the variations in the rms of fit, this means that the density model errors can sometimes be absorbed in the adjusted drag coefficients more easily than in other cases. This will be investigated further in the future.

The solar reflection coefficient, which is also plotted in Figure 3.3, is fairly constant with a mean value of about 1.0. The small variations, that can be seen, again mostly occur during the periods of increased solar activity indicated by the peaks in the geomagnetic index. They are yet another indication of deficiencies in the atmospheric density models, which prevent a good overall parameter solution for those arcs.

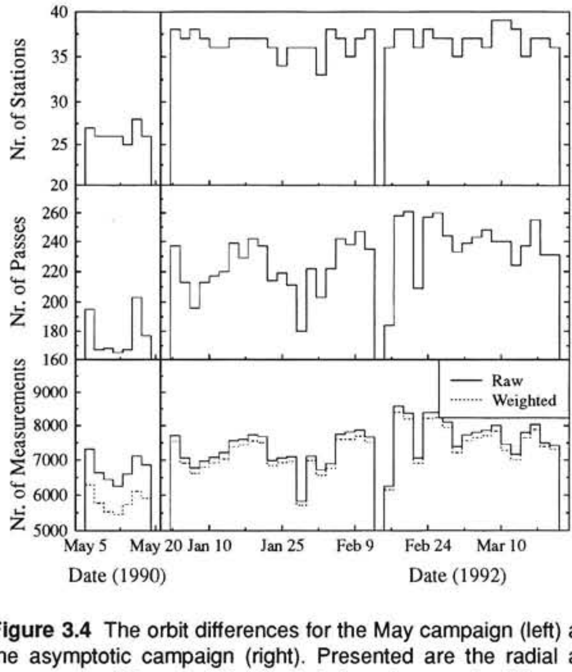

Figure 3.4 The orbit differences for the May campaign (left) and the asymptotic campaign (right). Presented are the radial and cross-track differences (top) and the along-track differences (bottom).

The accuracy of the orbit solutions may be assessed by examining the differences between the computed orbits of successive arcs, at the starting epoch of each arc. In Figure 3.4, these differences have been plotted, decomposed in radial, cross-track and along-track components. The results of both observation campaigns are included in the figure. For the radial and cross-track components, the maximum difference is only slightly larger than 1.0 m, the rms values being 50 and 25 cm for the first campaign, and 40 and 20 cm for the second, respectively. The variations in the along-track component are somewhat larger, in one case exceeding 7.0 m, with rms values of 3.0 and 1.5 m, respectively. The results for the May 1990 campaign are obviously slightly worse than for the asymptotic campaign. The individual differences can be considered to be the sum of the errors of the two orbits being compared. Therefore, the orbit accuracy is approximately equal to the rms values just given, divided by the square-root of 2. These results agree quite well with the accuracy predicted for the PGS-4591 gravity model, which, apparently, is the dominating error source.

As was mentioned earlier, in one of the arcs, an orbit maneuver took place. The velocity changes caused by both thruster firings were estimated along with the other parameters. This resulted in an orbital fit which was as good as all the others. The recovered velocity increments in the along-track direction of 4.45 and 4.42 cm/s agree almost perfectly with the nominal values quoted by CNES (4.46 cm/s for each velocity increment). We also found a statistically significant cross-track component and an in-significant radial component with a magnitude of about 10 percent of the along-track component, however. It is thought that the cross-track component is real and may reflect an offset of the thrust vector from the velocity vector.

Finally, the results of the station coordinate estimation process: from each 2-day arc a full global network solution was obtained. To compress the information and to increase the accuracy, the individual arc solutions were merged into two combined solutions, one for each data period. This was done using a special program, developed at DUT, which eliminates possible systematic differences between the individual solutions and uses the statistical information for weighing [13]. It is stressed that both sets of coordinates hold in the reference frame provided by the ITRF90 solution, advanced to the epochs chosen for both campaigns. Therefore, they cannot be simply compared, since crustal motions cause changes in the coordinates of up to 20 cm.

The formal errors from the solutions show that the coordinates of the asymptotic campaign are generally much more accurate than those of the May 1990 period. This is simply a statistical effect, caused by the larger amount of data in the second campaign. A better measure of the accuracy is provided by the residuals of the coordinates of the individual solutions with respect to the combination solutions. This information is also provided by the special program, and it was found that the rms of the residuals is about 15 cm in all three components, for both campaigns. This is quite a good result, considering the fact that SPOT-2 was never intended to serve as a platform for accurate ground station positioning.

An impression of the absolute positioning accuracy may be obtained from a comparison of the coordinates of those stations, for which also an independent solution based on other techniques is available. For this purpose the Arequipa, Dionysos, Fairbanks, Goldstone, Huahine, Kokee Park, and Toulouse stations were used, which were present in the ITRF90 solution, but which were not fixed in our analyses. At first sight, these results were somewhat disappointing, because the overall rms difference was of the order of 26 cm. However, when the a priori CNES solution was used, instead of ITRF90, the rms came down to 15 cm again. On closer inspection, it was found that the larger differences with ITRF90 were primarily caused by one or two stations. It is therefore suspected that some of the ITRF90 coordinates may be wrong, possibly due to errors in the local surveys between the positions of the various systems at a site.

3.1.3 First results for TOPEX/Poseidon

The accuracy with which the TOPEX/Poseidon orbits have to be computed imposes high demands on the applied orbit computation methodology and the used tracking system. To meet the orbit requirements of TOPEX/Poseidon, the effects of conservative and non-conservative forces on the satellite have to be modeled with extreme accuracy. Therefore, the most up-to-date models are used in the orbit computations. For the gravity field this is the post-launch JGM-2 model complete to degree and order 70 which has been obtained from JGM-1 using 15 cycles of SLR and DORIS data on TOPEX/Poseidon [14]. The Box-Wing Model was applied to account for the satellite's complex geometry, and attitude and surface properties in the modeling of solar radiation pressure and atmospheric drag [14]. For the latter, the French DTM density model with 3-hourly planetary geomagnetic index (K_p) values has been adopted. Also incorporated in the orbit computations are models for solid earth and ocean tides, the earth's albedo radiation pressure, relativity, and n-body perturbations from the sun, the moon, and the planets.

During the orbit computations, drag and solar radiation forces are held constant at nominal values. Model mismatches introduced by this approach are absorbed by a daily estimated set of 1 cycle per revolution (1-cpr) accelerations in the along-track and cross-track directions, and an additional constant acceleration in the along-track direction. Along with the epoch state-vector, pass-dependent range-rate biases and tropospheric scale biases are estimated for the DORIS data.

An important factor that influences the orbit accuracy and therefore should be mentioned is the geographic distribution of the tracking data. Currently, the DORIS data are supplied by a worldwide network of over 45 ground beacons. The fact that the isotropic distribution of the DORIS network and its all-weather capability enable the DORIS system to provide a nearly continuous monitoring of the TOPEX orbit, may serve as evidence that the geographic distribution of the DORIS tracking data are quite satisfactory.

One measure for the quality of an orbit is how well it fits the tracking data. The overall residual rms serves as an indicator for both model accuracy and data quality, as large residuals, relative to the theoretical noise level of the data, signify either model deficiencies or systematic data problems. Since the orbits are generated with the best force models currently available, the recently achieved range-rate residual rms of about 0.55 ± 0.02 mm/s, illustrate the current status for the level of fit of DORIS tracking data achievable in the TOPEX/Poseidon orbit determination.

Another measure for the quality of an orbit is the rms radial overlap. This quantity which is defined as the rms of the radial orbit differences between the last day and the first day of adjacent orbital arcs, gives an indication of how much the orbit shifts from one arc to the next to accommodate force and measurement model errors. Preliminary results for the orbital overlaps indicate that on average, the rms orbital overlap is better than 3 cm.

Individually, quantities like the rms radial overlap and the rms of fit of the residuals are not sufficient to assess the orbit accuracy, because the correlated errors are eliminated from the orbital overlaps, whereas the rms of fit is based on data residuals that are minimized in the orbit computations. Together however, these quantities provide a good measure for the orbit quality, indicating that the TOPEX/Poseidon orbits have a radial accuracy of 3-5 cm.

The introduction of additional parameters, such as the tropospheric scale biases per pass and the five general acceleration parameters, and the use of far more superior models than those used in the previous analysis with SPOT-2 (gravity field model, atmospheric density model, satellite macro model) resulted in a tremendous improvement in the orbit accuracy of this earth oriented satellite.

3.2 Orbit determination with GPS

The NAVSTAR (Navigation by Satellite Timing and Ranging) Global Positioning System (GPS) is a space-based positioning and navigation system, developed since the early eighties by the US Department of Defense. The system has three components, identified as the Space, Control and User segments. The Space or satellite segment consists of 24 space vehicles (SVs), including 3 active spares, optimally placed in 6 orbital planes. The satellites are in circular orbits with 12-hour periods and an inclination of 55°. The satellites transmit signals at two L-band radio carrier frequencies: L1 at 1575 MHz and L2 1227 MHz. The satellites also transmit a Navigation Message that provides users with the Broadcast Ephemeris, the Almanac, satellite clock information, time (UTC), satellite health, and ionospheric parameters. Modulated on the L1 carrier is a coarse acquistion code, or C/A code at 1.023 MHz, for rapid acquisition of the signal and the navigation message. In addition, each of the L-band carriers is modulated with a 10.23 MHzP-code, also known as the precision or protected code. [15,16,17].

These signals enable a user to determine his instantaneous position at any time and anywhere on and near the earth, with an accuarcy of 5 to 150 m, depending on the sophistication of the receiver equipment. Although this may be good enough for most applications, it is insufficient by 3 orders of magnitude for geodetic applications, such as geodynamics research and precise orbit detrmination of low earth satellites. These require sub-centimeter accuracy, which is beyond the basic performance of the system. However, it was soon realized that by using the GPS signals in a differential mode, the accuracy of the relative position determinations could be increased substantially. This effect was bolstered by the addition of measurements of the phase of the carrier signals. Because of the very short wavelength of these signals (ca. 20 cm), the measurement precision could be increased to the millimeter level. For this purpose, special receivers were developed, both for ground-based and space-based applications.

In the following Sections, two investigations on precise orbit determination with GPS will be presented. These activities were undertaken in support of the project Earth Oriented Space research, because GPS tracking of low earth satellites is expected to become an operational standard. In particular for satellite missions requiring precise orbits, such as altimetry missions, GPS is a very attractive tracking system. This will be demonstrated by the results obtained with the data from an experimental GPS receiver onboard the TOPEX/Poseidon altimetry satellite. The Landsat-5 study was a precursor study, in which the basic analysis techniques were developed. Some investigations concerned with ground-based applications and with applications for gravity field research will be discussed elsewhere in this report

3.2.1 Landsat-5 data analysis

In 1985, an experimental GPS receiver onboard the Landsat-5 satellite acquired some of the earliest GPS measurements from space by a network of 9 ground receivers in the continental United States of America. Although similar data had already been taken before, by the Landsat-4 satellite [18], the significance of the Landsat-5 data is due to the fact that some of it were collected concurrently with a large geodetic GPS measurement campaign in the continental US. This provided the first opportunity to process these datasets simultaneously, thus allowing to improve the accuracy of the GPS orbits and to estimate the Landsat-5 orbit at the same time. Data selected for the analysis was collected in the period 28 March to 5 April.

The collected observations consisted of P-code data only from the Landsat-5 receiver, and P-code and carrier phase data from a network of 9 TI-4100 ground receivers. All observations were processed with the DUT/SSR&T modified version of the GPS Inferred Positioning System software (GIPSY), developed at JPL [19]. GIPSY utilizes a so-called Kalman sequential filter to process the GPS measurements and to determine the estimates and corresponding uncertainties for the parameters.

To demonstrate the improvements due to the addition of the data of the ground receivers, the results of two orbit determination scenarios for Landsat-5, are described: one in which only the Landsat-5 orbit is estimated from highly-accurate GPS Satellite-to-Satellite Tracking (SST) P-code ranging measurements with respect to a GPS satellite transmitter reference network, and one in which both the Landsat-5 and GPS orbits are determined together from GPS SST P-code pseudo-ranges and GPS P-code pseudo-ranges and carrier phase measurements with respect to a ground receiver reference network. Also different strategies were tested to model the forces acting on the Landsat-5 satellite. Both, a purely dynamic and a so-called reduced-dynamic technique were applied. Finally, the accuracies of the results of the actual data analyses were compared with accuracy predictions from covariance analyses.

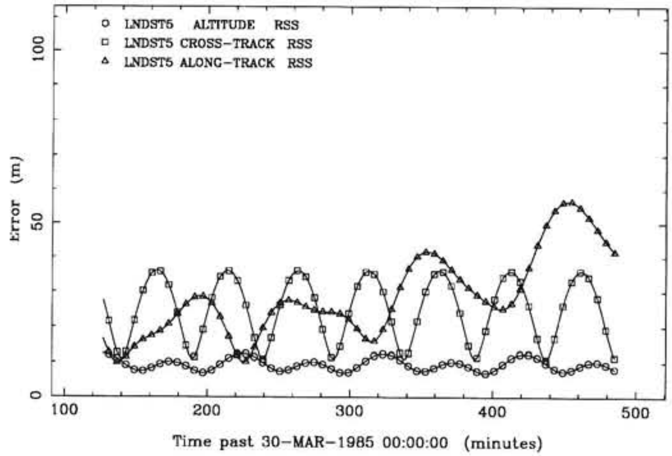

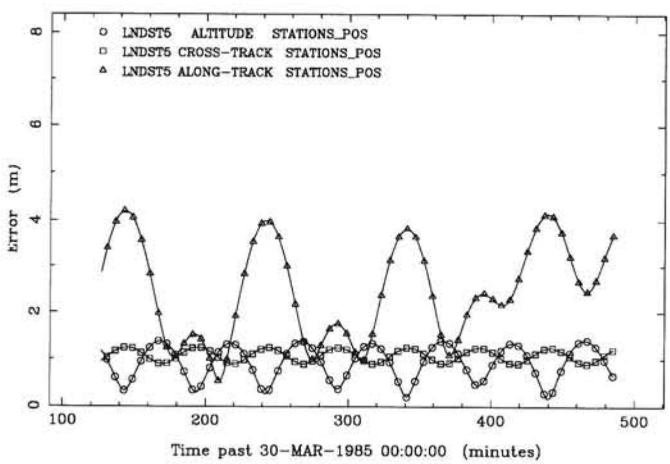

Figure 3.5 The variation of the overall (RSS) errors in the Landsat-5 position components for the first (top) and second (bottom) orbit determination scenario by application of the dynamic technique.

From covariance analyses of the first scenario for the dynamic case, it is shown that the Landsat-5 orbit determination accuracy is primarily limited by the GPS broadcast ephemeris errors, as can also be seen from the top plot of Figure 3.5. In this case, the orbital errors for Landsat-5 are of the order of 30 m in position and 30 mm/s in velocity. This is in contrast with the results obtained from actual analyses, which suggest that Landsat-5 position and velocity accuracies can be achieved below the 10-m and 10-mm/s level, respectively. However, these accuracies were determined by examination of the observation residuals and by comparison of the ephemeris differences of several contiguous data arc solutions over 3-hour and 4-hour overlapping time periods.

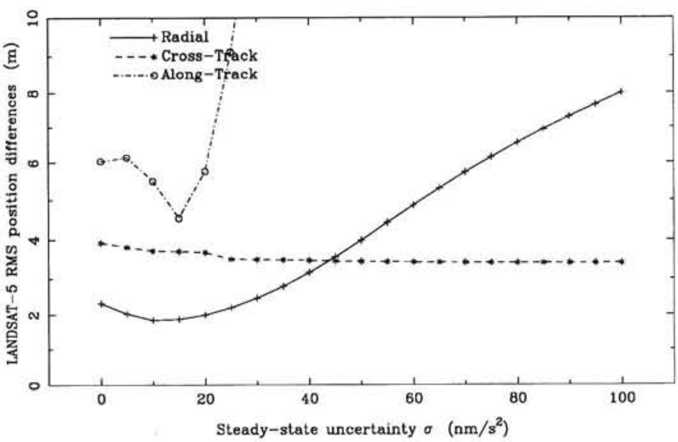

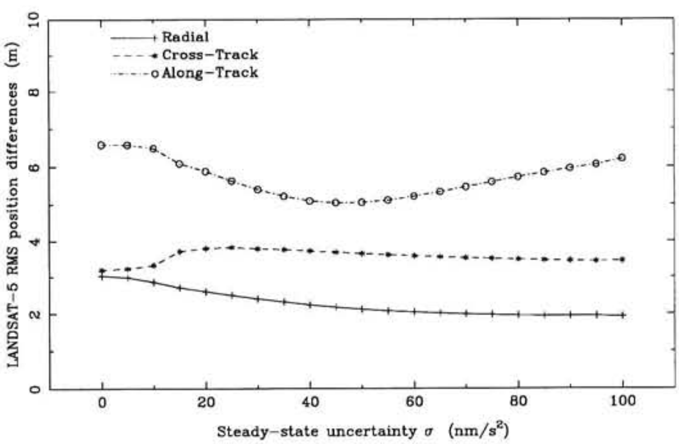

Figure 3.6 Rms differences in Landsat-5 position components for two 6-hour contiguous data arc solutions over a 3-hour overlapping time period with different weighting on dynamic models for the first (top) and second (bottom) orbit determination scenario. Results are obtained from actual analyses ($\sigma = \sigma_0$, $\tau = 98$ minutes). The dynamic case ($\sigma = \sigma_0$, $\tau = \infty$) is also represented in the figure.

By putting more weight on observing geometry, the SST scenario looses its strength, since the Landsat-5 orbital solution is much more affected by errors in the GPS satellite ephemerides. This is also demonstrated in the top plot of Figure 3.6, which shows that for values of the steady-state uncertainty σ greater than 25 nm/s^2 the rms position differences of Landsat-5 diverge in the along-track direction.

When the ground station data are added, the geopotential modeling errors and the uncertainties in the coordinates of the ground receivers become the major error sources. In addition, the location of the tracking stations appears to be a limitation too. In this case, the overall position and velocity accuracy for Landsat-5 improves to the 5-m and 5-mm/s level. Moreover, the highest orbit accuracy is obtained during the periods of 'good' observing geometry when Landsat-5 passes over or near the ground receivers in North America. The position accuracy then increases to better than 2 m. With this scenario, a good agreement is obtained between the results from covariance and actual analyses, as is demonstrated by the bottom plots of Figure 3.5 and Figure 3.6.

The results of this study give an indication of the overall capabilities of the GPS system for the orbit determination of low-earth satellites [20,21,22]. It is felt that this performance is also sufficient to meet the accuracy requirements for the orbit determination of the 'ARISTOTELES' or any equivalent satellite (STEP) mission from a scientific point of view. Since these 'future' low-earth satellites will carry a much more sophisticated GPS receiver that can also make carrier phase measurements, and because a global ground receiver network now exists, it is expected that the orbit determination accuracy will improve by almost an order of magnitude.

3.2.2 First results for TOPEX/Poseidon

Preliminary TOPEX/Poseidon orbits have been computed from the data obtained by the GPS Demonstration Receiver (GPSDR) on TOPEX/Poseidon and by a network of 10 globally distributed ground receivers. Half the number of these receivers have accurately known station coordinates and form the so-called fiducial network.

The data from the fiducial network are included to constrain the TOPEX/Poseidon orbit to the terrestrial reference frame. This could not be accomplished by the GPS constellation because the orbits of the GPS satellites are estimated along in the TOPEX/Poseidon orbit determination at.

The GPS measurements are processed in ten 30-hour contiguous solution arcs with a 6-hour overlapping period using the GIPSY-OASIS II (GPS Inferred Positioning SYstem - Orbit Analysis and SImulation Software II) software system, also developed at JPL.

Basically, two estimation strategies have been applied. The first is the dynamic technique, which relies on the accuracy of the dynamic models and is characterized by the fact that the transition of the satellite state at different observation times is accomplished by the integration of the equations of motion. The second is the reduced-dynamic technique, which takes full advantage of the geometric information content available from the GPS measurements and therefore is less dependent on the precision of the dynamic models. This technique is based on the fact that the satellite state transition at different observation times is accomplished by both the integration of the equations of motion and by the satellite positional change inferred from continuous GPS carrier phase measurements.

The GPSDR onboard TOPEX/Poseidon is the first highly sophisticated space-borne GPS receiver that can actually record both carrier phase and pseudo-range measurements at an extremely high data rate. The carrier phases are recorded every second, while the pseudo-ranges are recorded every 10 seconds. Since the GPSDR can take measurements from up to six GPS satellites simultaneously, it accordingly provides a continuous, global, and dense set of observations. At any instant of time, these observations are also in several directions.

For the orbit computations, the first-order ionosphere-free pseudo-ranges and carrier phase observations are formed which are assigned a data noise of respectively 1 m and 1 cm for the 10 ground receivers, and respectively 3 m and 2 cm for TOPEX/Poseidon. The carrier phase observations are decimated to a data rate of 1 observation per 5 minutes, while the pseudo-range observations are compressed to 5-minute normal points by smoothing them against the carrier over the entire 5-minute interval.

For both observation types, a cut-off elevation angle is used of about 0° for TOPEX/Poseidon and 15° for all ground stations. In the GIPSY-OASIS II software, all measurements are divided into finite discrete time intervals known as batches. The software makes use of a SRIF (Square Root Information Filter) filter, which is a so-called epoch state filter in which all measurements are processed sequentially.

The time update of the filter propagates the satellite state estimates and covariances from one batch to the next using a state transition model, while the measurement update of the filter incorporates a new batch of measurements. To obtain the optimal parameter estimates and covariances at all batch observation times from 100% of the measurements, a backward smoothing in time is performed. At the same time, it is possible to perform a forward mapping in time, since the filtered state estimates and covariances apply to the epoch state.

In the TOPEX/Poseidon orbit determination, the JGM-2 gravity field model is used. In comparison, the GEM-T3 model, truncated at degree and order 8, is applied for the computation of the orbits of the GPS satellites. The Box-Wing model is adopted for solar pressure, earth radiation, and atmospheric drag on TOPEX/Poseidon.

Furthermore, models for solid earth tides, ocean tides, and pole tides are applied. The estimated parameters include the TOPEX/Poseidon state vector at epoch, constant and 1-cpr accelerations in the cross-track and along-track directions for TOPEX/Poseidon, additional 2-cpr cross-track and along-track accelerations, the GPS state vectors at epoch, the constant GPS solar pressure scale factor, the constant and stochastic GPS solar radiation Y-biases, the stochastic GPS solar radiation scaling factors X and Z, the non-fiducial station locations, the random walk modeled tropospheric dry zenith residual delays, the X and Y pole position and corresponding rates, the UT1-UTC rate, the carrier phase biases, the TOPEX/Poseidon receiver clock (modeled as white noise), the GPS transmitter clocks (modeled as white noise) and the ground receiver clocks (modeled as white noise) except for one reference clock.

The starting values for the epoch state vector of the TOPEX/Poseidon orbit are taken from the results of the operational SLR analyses. Furthermore, the GPS orbits of IGS are used as a-priori information for the epoch states of all GPS satellites. These orbits, which have an estimated accuracy of about 30 cm, are the weighted mean of the orbit products generated by several different processing centers.

Finally, it is noteworthy to mention that it is possible to specify initial values for the empirical accelerations of the custom force model of TOPEX/Poseidon. Information about the constant accelerations and the sine and cosine 1-cpr and 2-cpr terms of the empirical force, can be obtained by first performing a dynamic filtering where these parameters are solved for. Then, the solved-for empirical force terms can be kept fixed in a subsequent reduced-dynamic filtering.

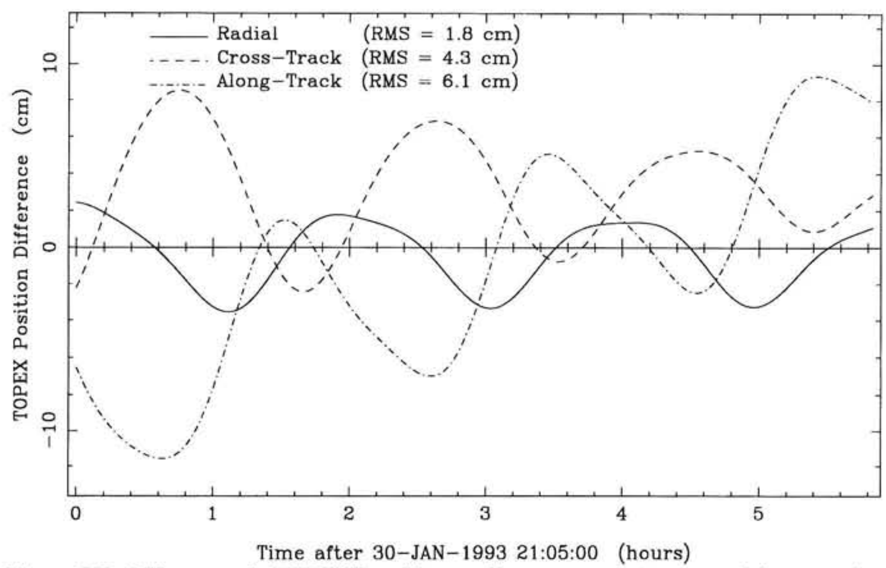

Figure 3.7 Differences in TOPEX/Poseidon position components over a 6-hour overlap between two 30-hour data arcs using dynamic techniques.

To obtain an indication of the TOPEX/Poseidon orbit accuracy, the observation residuals and the ephemeris differences over the 6-hour orbital overlaps have been investigated. Starting with the results of the dynamic technique, Figure 3.7 shows the TOPEX/Poseidon ephemeris differences in the radial, cross-track, and along-track directions over a typical 6-hour overlapping period. Since the rms difference is about 2 cm radial, 4 cm cross-track, and 6 cm along-track, it may be concluded that subdecimeter orbit accuracy can already be achieved with the dynamic filtering.

Examining the residual summary of the ten 30-hour data arcs that were processed, using the dynamic technique, the average overall rms of fit for the first-order ionosphere-free pseudo-ranges and carrier phase observations are found to be 39.0 ± 7.6 and 0.48 ± 0.04 cm respectively. For the TOPEX/Poseidon part of the corresponding data types they are found to be 70.1 ± 2.4 and 0.93 ± 0.09 cm respectively. On average, the number of observations is about 18000 for each data arc and each data type. Roughly 10% of the observations are taken on TOPEX/Poseidon.

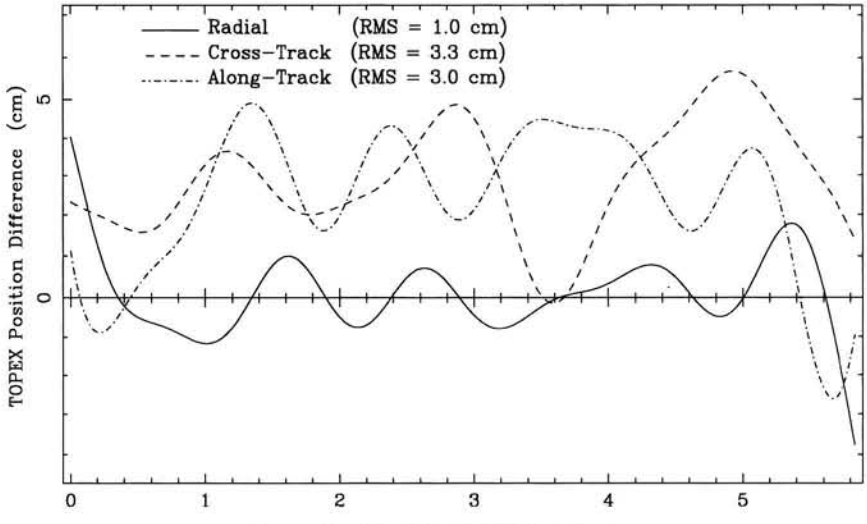

Figure 3.8 Differences in TOPEX/Poseidon position components over a 6-hour overlap between two 30-hour data arcs using reduced-dynamic techniques.

In case of the reduced-dynamic technique, a second filtering was performed to absorb the higher-order dynamic modeling errors. Using this approach, a so-called three-dimensional process-noise force consisting of fictitious accelerations was estimated for TOPEX/Poseidon to absorb the remaining small higher-order dynamic modeling errors. The correlation time of the estimated fictitious accelerations was set to 15 minutes and the corresponding steady-state uncertainty was set equal to the a-priori uncertainty. The uncertainties were assumed to be 10 nm/s^2 in the radial direction and 20 nm/s^2 in both the cross-track and along-track directions, and were taken from [23]. Furthermore, the data noise of the TOPEX/Poseidon carrier phase observations was tightened to 1 cm in order to give the tracking data on TOPEX/ Poseidon a higher weight. Figure 3.8 shows the overlap comparison using reduced-dynamic filtering for the same 6-hour period that is displayed in Figure 3.7.

Obviously, using the reduced-dynamic technique, better results are obtained with an rms difference in the TOPEX/Poseidon orbit of about 1 cm radial, 3 cm cross-track and 3 cm along-track. The corresponding residual summary for the same ten 30-hour data arcs, using a reduced-dynamic strategy, show that the average overall rms of fit only changes significantly for the carrier phase observations. The value reduces to about 0.4 cm. The same observation is made for the TOPEX/Poseidon part of the summary, showing a decrease of the rms of fit of the pseudo-ranges to about 66 cm while the rms of fit of the carrier phase measurements dramatically improves to the 0.4 cm level, which is due to the fact that the remaining higher-order dynamic modeling errors have been absorbed by the three-dimensional process-noise force. The rms of fit values of 66 cm and 0.4 cm now closely approximate the noise levels of the first-order ionosphere-free pseudo-range and carrier phase observations on TOPEX/Poseidon, which are about 70 cm and 0.5 cm respectively [24].

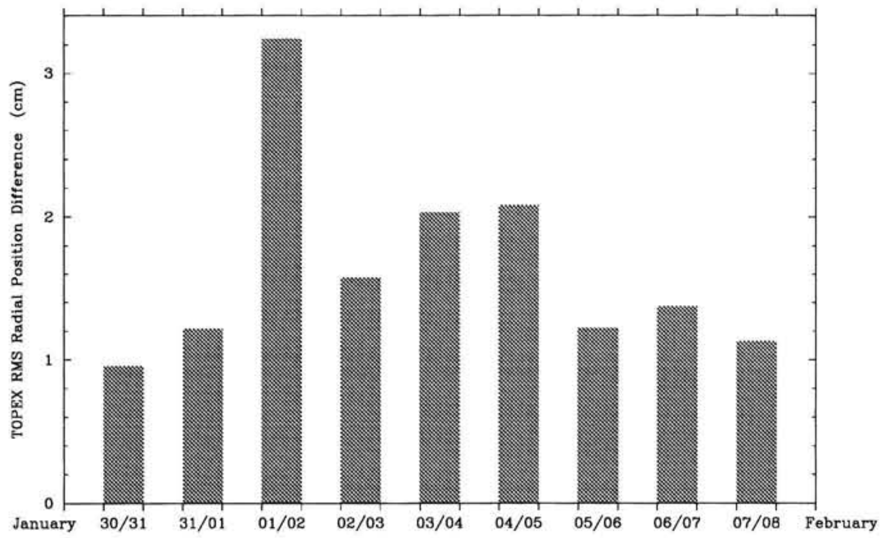

Figure 3.9 Radial orbit overlap rms for ten 30-hour consecutive TOPEX/Poseidon data arcs using a reduced-dynamic technique.

Finally, the radial rms overlap results for the 6-hour time periods between consecutive data arcs using reduced-dynamic filtering (Figure 3.9) are about 2 cm. This means that the internal consistency of the orbits is of the same level as the estimated 1-2 cm precision of the altimeter measurements [14].

3.3 References

1. Lefebre M., *DORIS status report*, CNES (Centre National d'Etudes Spatiales), GRGS (Groupe the Recherche de Géodésie Spatiale), France, 1989.

2. Dorrer M., B. Laborde, P. Duschamps, *DORIS (Doppler Orbitography and Radiopositioning Integrated from Space): System assessment results with DORIS on SPOT 2*, Acta Astronautica, **25**, 8/9, 497-504, 1991.

3. DORIS brochure, *Precision satellite-based orbit determination and beacon positioning*, CNES (Centre National d'Etudes Spatiales), GRGS (Groupe the Recherche de Géodésie Spatiale), IGN (Institut Géographique National), Fr, 1988.

4. Eddy W.F., J.J. McCarthy, D.E. Pavlis, J.A. Marshall, S.B. Luthke, L.S. Tsaoussi, G. Leung, D.A. Williams, *GEODYN-II system operation manual*, **1-5**, contractor report, ST System Corp., Lanham MD, USA, 1992.

5. Wakker, K.F., B.A.C. Ambrosius, L. Aardoom, *Precise orbit determination for ERS-1*, Delft University of Technology, Faculty of Aerospace Engineering, The Netherlands, ESOC contract report 5227/82/D/IM(SC), 1983.

6. Wakker, K.F., B.A.C. Ambrosius, R.C.A. Zandbergen, G.H.M. van Geldorp, *Precise orbit computation, gravity model adjustment and altimeter data processing for the ERS-1 altimeter mission*, Delft University of Technology, Faculty of Aerospace Engineering, The Netherlands, ESA contract report 6140/84/D/IM, 1987.

7. Gaalen, G.J.,van, *Operational analysis of ERS-1 SLR data*, Delft University of Technology, Faculty of Aerospace Engineering, The Netherlands, Technical thesis, Aug., 1992.

8. Kuijper, D.C, *Modeling of the aerodynamic forces for the Earth Remote Sensing satellite ERS-1*, DUT/SSR&T report, Delft University of Technology, Delft, The Netherlands, 1991.

9. Anderson, A.J., (red), A. Cazenave, (red), *Space Geodesy and Geodynamics: Doppler satellite measurements and their interpretation*, Chapter 3, R.J. Anderle, Academic Press, London, 1986

10. DORIS Newsletter, no. 2, 1991.

11. Boucher, C., J.-Ph. Dufour, *The DORIS tracking system - A progress report*, IGN (Institut Géographique National), France, 1991.

12. Boucher, C., Z. Altamimi, *ITRF90 and other realizations of the IERS Terrestrial Reference System for 1990*, IERS Technical Note 9, IERS/CB, Paris, France, 1991.

13. Noomen, R., B.A.C. Ambrosius, K.F. Wakker, *Crustal motions in the Mediterranean region determined from laser ranging to LAGEOS*, Contribution of Space Geodesy to Geodynamics; Crustal Dynamics, Geodynamics Series, **23**, American Geophysical Union, 331-346, 1993.

14. Putney, B.H., J.A. Marshall, R.S. Nerem, F.J. Lerch, D.S. Chinn, C.C. Johnson, S.M. Klosko, S.B. Luthke, K.E. Rachlin, T.A. Williams, R.G. Williamson and N.P. Zelensky, *Precise Orbit Determination for the TOPEX/Poseidon Mission*, Paper AAS-93-577 presented at the AAS/AIAA Astrodynamics Specialist Conference, Victoria, B.C., Canada, August 16-19, 1993.

15. Remondi, B.W., *Global Positioning System carrier phase, description and use*, Bull. Geod., **59**, 361--377, 1985.

16. Wells, D.E., N. Beck, D. Delikaraoglou, A. Kleusberg, E.J. Krakiwski, G. Lachapelle, R.B. Langley, M. Nakiboglu, K.P. Schwarz, J.M. Tranquilla, and P. Vanicek, *Guide to GPS Positioning*, Canadian GPS Associates, Fredericton, New Brunswick, 1987.

17. Hesper, E.T., *Operational principles and characteristics of the NAVSTAR/GPS satellite navigation system*, Delft University of Technology, Faculty of Aerospace Engineering, Delft, The Netherlands, January 1988.

18. Fang, B.T., and E. Seifert, *An evaluation of Global Positioning System data for Landsat-4 orbit determination*, AIAA paper 85-0286, January 14-17, 1985.

19. Lichten, S.M., *Estimation and filtering for high-precision GPS positioning algorithms*, Man. Geod., **14**, 159-176, 1990.

20. Wu, S.C., S.M. Lichten, W.I. Bertiger, J.T. Wu, J.S. Border, B.G. Williams, and T.P. Yunck, *Precise orbit determination of GPS and Landsat-5*, in: Proceedings of the Fourth International Geodetic Symposium on Satellite Positioning, Austin, Texas, 1986.

21. Yunck, T.P., W.I. Bertiger, S.M. Lichten, and S.C. Wu, *Tracking Landsat-5 by a differential GPS technique*, in: AIAA/AAS Astrodynamics Conference, Williamsburg, Virginia, August 18-20, 1986.

22. Hesper, E.T., B.A.C. Ambrosius, and K.F. Wakker, *GPS performance on Landsat-5 in a satellite transmitter and ground receiver reference frame*, ESA contract 9877/92/F/FL, Delft University of Technology, Faculty of Aerospace Engineering, Delft, The Netherlands, May, 1993.

23. Wu, S.C. and Muellerschoen, R.J. and Bertiger, W.I. and Yunck, T.P. and Bar-Sever, Y.E. and T.N. Munson, *Automated precision orbit determination for TOPEX/Poseidon with GPS*, AAS paper 93-576 presented at the AAS/AIAA Astrodynamics Specialist Conference, Victoria, Canada, August 16-19, 1993.

24. Bertiger, W.I. and Y.E. Bar-Sever and E.J. Christensen and E.S. Davis and J.R. Guinn and B.J. Haines and R.W. Ibanez-Meier and J.R. Lee and S.M. Lichten and W.G. Melbourne and R.J. Muellerschoen and T.N. Munson and Y. Vigue and S.C. Wu and T.P. Yunck and B.E. Schutz and P.A.M. Abusali and H.J. Rim and M.M. Watkins and P. Willis, *GPS precise tracking of TOPEX/Poseidon: results and implications*, J. Geophys. Res, 1993, submitted for publication to TOPEX/Poseidon special issue.

4 Crustal Dynamics

One of the major applications of space geodesy is its use for crustal dynamics investigations. Two different, though closely related activities can be distinguished here: data acquisition, which is discussed in Chapter 2, and data analysis, which is the subject of this Chapter. A second application of the space-geodetic technique is for studying the earth's rotation. This is discussed in Chapter 5.

The data analyses described below concern two different types of observations, viz. Satellite Laser Range (SLR) observations and Global Positioning System (GPS) tracking data. The SLR observations are acquired by a global international network that currently exists of about 30 fixed stations, supplemented by 6 mobile systems, including the MTLRS-2 system from KOSG. For GPS the situation is much more complicated because there is much less coordination in the many observation campaigns, which are frequently organized all over the world. Until recently, the technique has mostly been used for regional networks. For the purpose of the crustal dynamics investigations, described in this Chapter, only data collected during observation campaigns in the European region have been used.

The analysis efforts at DUT have focussed in particular on sites in the central and eastern Mediterranean area, which have been occupied by transportable SLR tracking systems a number of times, since 1986. Some GPS data have also been collected at these sites. This region is the meeting place of three major tectonic plates (Eurasia, Africa and Arabia), and is consequently the theater of many earthquakes each year. Both operational and analysis activities are typically carried out in the framework of the WEGENER project, which will be discussed in the next Section. This is followed by an overview of the analyses of the SLR observations. The Chapter ends with a discussion of the analysis of several GPS datasets.

4.1 WEGENER project

The WEGENER project [1] was named after Alfred Wegener, a German meteorologist, who postulated the tectonic plate motion theory in 1912 for the first time. The acronym stands for Working-group of European Geo-scientists for the Establishment of Networks for Earth-science Research. The project is aimed at the determination of crustal deformations in the central and eastern Mediterranean area [2,3]. Here, the Eurasian, African and Arabian major tectonic plates collide: Africa and Arabia move northward with respect to Eurasia at a rate of 8 and 24 mm/yr, respectively. These values are taken from NUVEL-1, a model for global plate tectonics derived from geophysical observations averaged over the last 3 million years [4]. The situation in southeast Europe is complicated by the existence of a number of smaller plates situated between the major plates. Examples of these so-called microplates are Adria (the African promontory covering the Adriatic Sea and its shorelines), the Aegean block and Anatolia. Whether Adria is rigidly attached to the major African plate or not, is still an issue under debate. Typically, microplates are not included in global plate tectonics models. The relative motions of the plates makes the area into the region within Europe most afflicted by earthquakes. As shown in Figure 4.1, the boundaries of the major plates and the microplates have been established quite accurately by mapping the focal centra of the earthquakes that have taken place in this area [5]. WEGENER is aimed at the determination of the actual deformation rates, both in magnitude and in orientation.

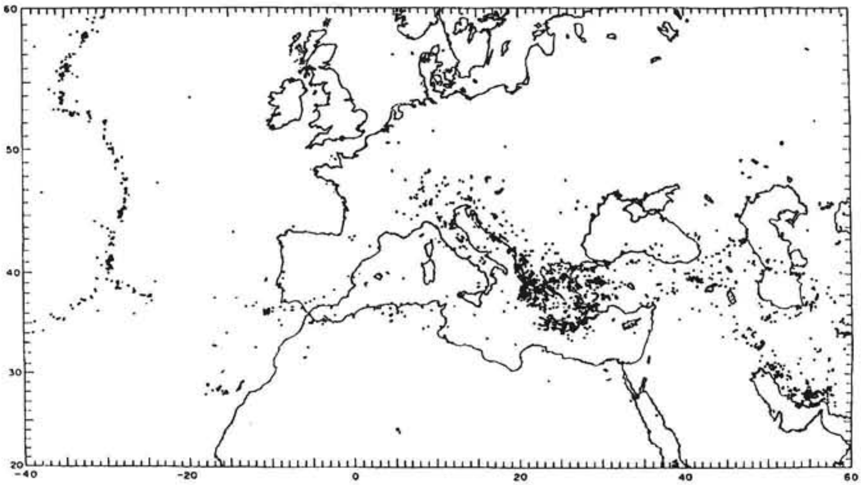

Figure 4.1 An overview of the epicentral of the earthquakes in the Mediterranean area which have taken place in the period 1961 - 1970.[5]

For this purpose, a special measurement project was defined, based on the SLR measurement technique. It was called WEGENER-MEDLAS. The fundamental idea behind the project is very simple. During observation campaigns, mobile laser systems visit some 15 sites in the region, and obtain a good set of range observations of the geodetic satellite LAGEOS-1 [6], which is depicted in Figure 4.2. This small and heavy spacecraft circles the earth at an altitude of about 5900 km. When combined with measurements that are acquired by the global network of SLR observatories, it is possible to reconstruct the satellite trajectory with an accuracy of a few centimeters. Once this model for the satellite orbit has been established, it can be used as a reference for the range observations to determine the position of the laser system in the Mediterranean with an accuracy of better than 20 mm. The occupations of the sites in the area are repeated at certain intervals, which results in a time-series of solutions for the position of each laser site. The deformations that are taking place at a certain location will show up as trends in the position solutions. On a global scale, this technique has been used successfully already to verify the tectonic models describing the major plate motions.

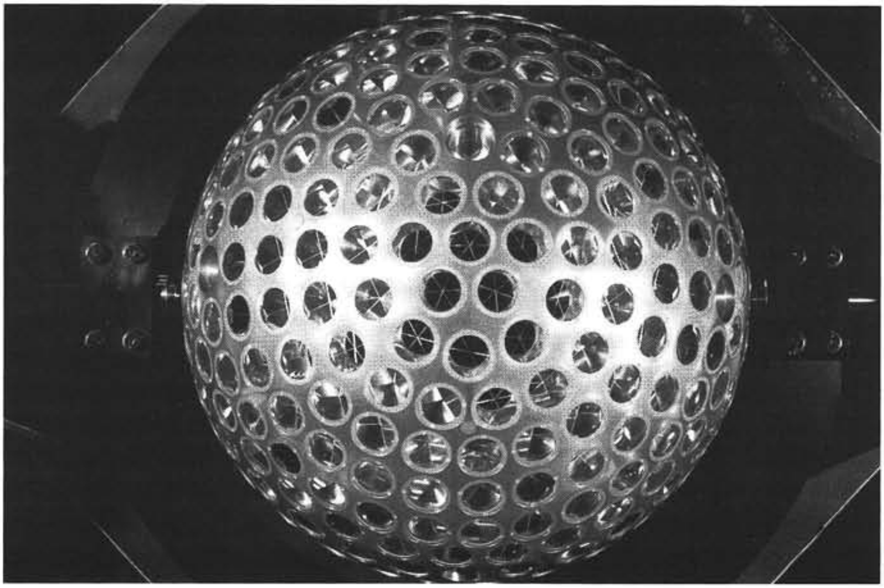

Figure 4.2 The geodetic satellite LAGEOS-1.

Three transportable laser systems participate in the observation campaigns of WEGENER: MTLRS-1 (Germany), MTLRS-2 (The Netherlands) and TLRS-1 (USA). Since the beginning of the project in 1985, four observation campaigns have been held, notably in 1986, 1987, 1989 (with an extension into the first months of 1990) and 1992. In the years in between, one of the mobile systems has also visited several sites in the area, in particular in the Italian part of the network. An observation campaign typically lasts for about 8 months. Mainly depending on the weather conditions, the SLR systems need 4 to 8 weeks to acquire a sufficient amount of observations on LAGEOS-1 to allow a precise computation of the station coordinates. LAGEOS-2, a satellite identical to LAGEOS-1, was launched in October 1992, and doubles the potential of SLR for crustal dynamics investigations. In principle, this redoubling can be used to reduce the required site occupation time. Since the most recent observation campaign in the Mediterranean was organized in 1992, the LAGEOS-2 observation are not relevant for the SLR operations and analysis results described here.

An overview of the sites in the area and their tracking history is shown in Figure 4.3. The plot clearly shows that the sites in Greece have been occupied most frequently: except for Karitsa, all of them have hosted mobile SLR systems during each of the 4 WEGENER campaigns. The crustal dynamics investigations are directly supported by the activities of the stationary SLR systems in the area, viz. Grasse, Matera, Bar Giyyora and Helwan.

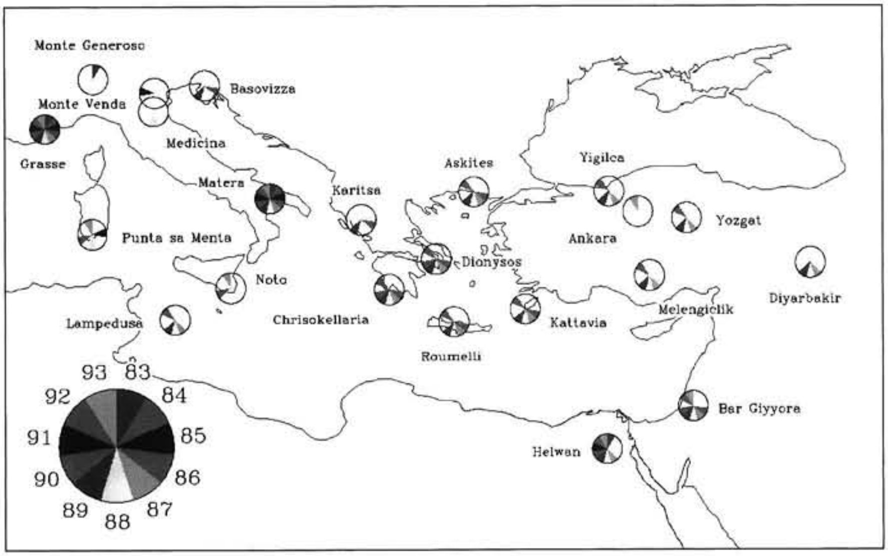

Figure 4.3 An overview of the SLR operations in the Mediterranean area. The color code indicates during which years sites in this region have been occupied by transportable SLR systems. Grasse, Matera, Bar Giyyora and Helwan host stationary SLR systems.

Later, the GPS technique was also included in the project. Initially, it was primarily used for densification, measuring smaller scale sub-networks. More recently, in 1992, the complete WEGENER-MEDLAS network has also been integrally observed with GPS for the first time. This made it possible to combine the results of both techniques.

4.2 SLR data analysis

DUT is involved in two types of SLR data analysis for the WEGENER project. First, the university acts as the Quick-Look Data Analysis Center (QLDAC). Second, it is one of the analysis centers for the processing of the full-rate SLR observations.

4.2.1 Quick-look

QLDAC is responsible for providing semi real-time information on the data quality of the range observations taken by the mobile laser systems, and the detection and reporting of potential data anomalies. The analysis is performed on a weekly basis, and involves a fine-screening of the SLR observations collected in the previous week. An essential element of this activity is the computation of the orbit of the satellites (since October 1992, both LAGEOS-1 and LAGEOS-2 observations are being processed), using the best models for the mathematical description of the forces acting on the spacecraft and the motion of the earth that are currently available. As an example, the representation of the positions of the SLR observatories, modeled as a linear function of time, typically has an accuracy of a few millimeters. The NASA/CSR JGM-2 model, which is used for the description of the gravitational attraction of the earth, includes provisions for the time-variation of this force, and is claimed to result in a radial accuracy of the LAGEOS orbits of better than 1 cm.

The observations are processed in batches of 10 days, which, in combination with the 1-week repeat period of the analyses, results in an overlap of successive analysis periods of 3 days. The main reason for choosing this arc length is the demand for a unique, yet continuous series of Earth Rotation Parameters (ERPs). This subject is discussed in Chapter 5. Solve-for parameters in the orbital analysis are the position and velocity of the satellites at epoch, related satellite-dependent parameters, ERPs and the positions of those SLR stations for which no accurate position information is available (yet).

Typically, the orbital analysis converges at an rms value for the SLR residuals (i.e. the actual range measurements minus their modeled counterparts) of 3 cm on average. This good fit facilitates the detection of data anomalies in individual passes of about 10 cm, and consistent systematic errors at a level of about 2 cm. The analysis results are summarized in a report, which is available within 3-9 days after the actual data acquisition. Stations for which data anomalies have been detected, are contacted directly.

4.2.2 Full-rate

The most important contribution to WEGENER consists of the analysis of the full-rate SLR observations [7,8]. These are the final data products of the SLR systems, fully calibrated and corrected for effects like tropospheric delay and the offset of the satellite laser-retroreflector w.r.t. the center of mass. In Delft, two different analysis methods have been explored. Both will be briefly described below.

The first method, which is based on a so-called long-arc approach using 1-week global data arcs, is very straightforward. First, the data period to be analyzed (the current interval runs from September 1983 to December 1992) is divided into a number of successive sub-intervals. The reason for this is due to the nature of the phenomenon under investigation itself: because of the ongoing deformations of the earth's crust, the positions of the laser stations continuously change with time. This is a very gradual process, although, in the case of earthquakes, sudden shifts also may occur

Since these deformations are not modeled in the data analysis and hence introduce an error which increases with time, it was decided to analyse the observations in batches that cover a relatively small period of time, where the change in the station coordinates is expected to be smaller than the a posteriori formal uncertainty of these parameters. On the other hand, a substantial number of satellite passes is required to precisely determine each laser station position. The selected time-span (three months on average) meets these requirements. The selection of the intervals has respected the deployment periods of the mobile laser systems at specific sites as much as possible. This way, a total of 38 sub-intervals have been identified, spanning three months on average each.

The analysis then starts by computing a simultaneous solution of the orbit of LAGEOS-1, the coordinates of the SLR stations and the ERPs, for each sub-interval separately. In this long-arc (dynamic) approach, all measurements of all global stations contribute to the determination of the satellite orbit during a significant time span. As a result, the modeled position of the spacecraft very closely follows the physical trajectory of the satellite. Consequently, this also holds for the geodetic parameters that are derived, such as station coordinates. This "physical truth" concept is optimized by using the best models for the description of the motion of the satellite and the earth that are currently available. The computation model closely follows the IERS Standards [9]. Exceptions are the use of the NASA/CSR JGM-1 solution for the modeling of the earth's gravity field and ocean tides potential, and the absence of models for representing the effects of long-term plate motion and short-periodic loading effects (atmosphere, ocean) on station positions.

The buildup of possible residual dynamic model errors is limited by opting for an arc length of 7 days, with all arcs starting on Sunday morning, 0.0 hr GMT. To fully cover the selected data periods, the data reduction and parameter estimation process is executed in a so-called multi-arc mode, where a number of independent 1-week satellite trajectories are adjusted simultaneously, whereas all tracking information is combined for the estimation of the relevant common parameters, such as station coordinates.

The actual data analysis is performed in two steps. First, for each arc separately, a normal equation is generated with GEODYN II, which is the NASA program for geodetic data reduction and parameter estimation [10]. The solve-for parameters included in each normal equation comprise the state-vector at epoch, a constant along-track acceleration parameter, acceleration parameters with a frequency of once per revolution, the coordinates of each observing laser station and the pole position and Universal Time at 5-day intervals. The solar radiation pressure force scaling parameter is kept fixed at a value of 1.13. Next, the normal equations are combined and inverted, and a complete parameter solution is computed for each individual 3-monthly sub-interval. For this purpose, we use the NASA program SOLVE II [11]. This way, a time-series of 38 independent, free global network solutions have been obtained. The parameter estimations typically converge with an rms of the observation residuals ranging from 20 to 40 mm. This is a first indication for the quality of the parameter solutions.

Another analysis method for the analysis of full-rate SLR data from a regional network is the so-called "spiral analysis method (SPAM)", developed at Delft. This method combines the advantages of dynamical long-arc solutions (stability) and pure geometric solutions (independency of dynamical model errors) with an efficient usage of data and computing power. It is based on relatively short data arcs of only a few orbital revolutions. By limiting the arc length, the errors due to inadequate modeling of the perturbing forces remain quite small. Furthermore, since only observations from simultaneously observing stations are used, the overall amount of data processed is also quite small.

The method proceeds as follows. First, in the data selection step, the "spirals" are composed. A spiral is defined by at least two consecutive passes from a station, of which at least one pass is simultaneously observed by another station from the dedicated network. A gap of one orbital revolution is allowed. As a special case, a single pass that is co-observed by three or more stations also defines a spiral. Subsequently, all consecutive passes observed by any other station are added to the spiral as long as that station has at least one pass co-observed with one of the initial stations or with a station which was previously added to the set. Thus, a station is only included in a spiral if at least one of its passes is simultaneously observed by another station. This implies that single passes from single stations, which indeed contain hardly any geometric information, are neglected in the analysis. Generally, some 80% of the data from a regional network is selected. For LAGEOS and the European network, including the Mediterranean sites, the spirals have arc lengths between 30 minutes and 18 hours. The spirals are clustered into batches of only 3 to 4 weeks, taking full account of the deployment periods of the mobile laser systems.

Then, starting from reasonably accurate a priori state-vectors, for example from the quick-look analysis, the orbit is adjusted for each cluster, providing a better estimate of this state-vector for each spiral. Finally, the state-vectors are adjusted again, but now together with the (relative) station coordinates in each cluster. An acceleration parameter is also solved for, in order to monitor the stability of the solutions. The dynamical model in these steps can be very simple. Each cluster of spirals thus produces an independent solution for the coordinates of a regional network of SLR stations. The spiral analysis method and its application to the WEGENER project is described in more detail in [7].

DEFORMATIONS

In principle, both methods described above can provide information on the deformations of the network, by studying time-dependent variations in the station coordinates solutions. However, the SPAM method only yields solutions for station combinations (baselines) that are occupied simultaneously. During the various WEGENER observation campaigns, these baselines were often different from year to year, so that the time-series of solutions becomes rather sparse. The long-arc method is not hampered by this problem, because it relies on independent station coordinate solutions. Therefore, the results discussed below are based on this method only.

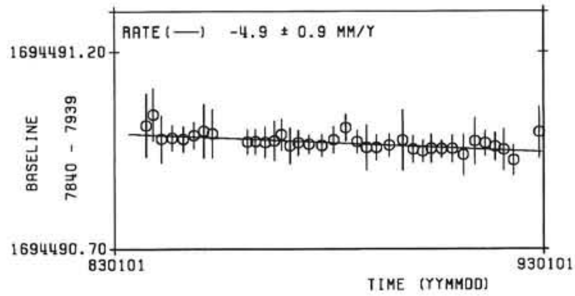

Figure 4.4 The history of the solutions for the linear distance between Herstmonceux (U.K.) and Matera (Italy). The error bars represent the 1-σ uncertainty of each individual solution. The scatter of the individual solutions around the trend line is 18 mm. The baseline values are in m.

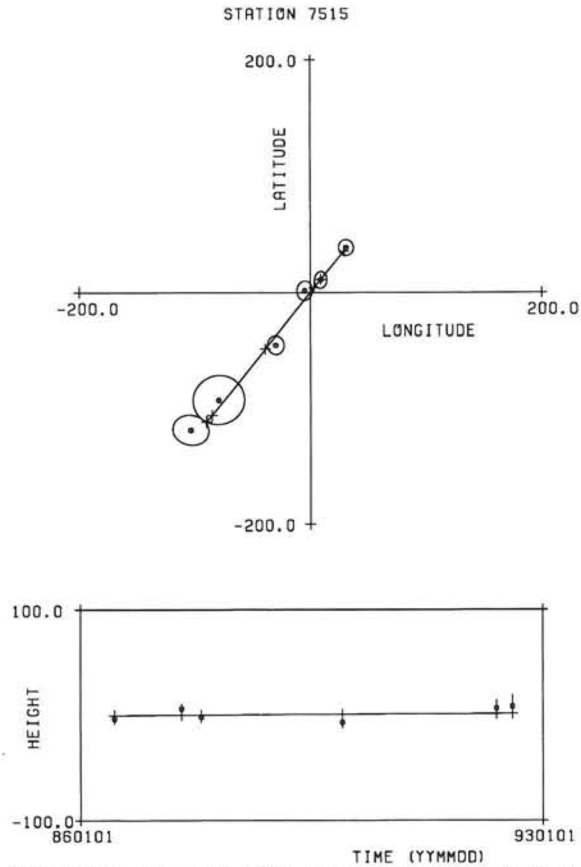

Figure 4.5 The horizontal (top) and vertical (bottom) position solutions for Dionysos. The solid line represents the deformation according to the linear model. Units: mm.

The crustal deformations, which are now manifest in the time-series of the SLR station positions, can be shown in two ways. First, one may look at changes in the distance between two sites. As an example, in Figure 4.4, the results for the baseline between the permanent SLR stations in Herstmonceux (U.K., near London) and Matera (southern Italy) are presented. The solutions, as determined for the period 1983 - 1992, show a gradual decrease of the distance at a rate of -5 mm per year. The scatter of the individual solutions around this trend is 18 mm only. Unfortunately, this method is not able to differentiate between deformations taking place in the UK. and those taking place in Italy.

To overcome this problem, a technique has been developed which makes it possible to derive motion vectors for each SLR station individually. This technique is based on the minimization of the sum of the squares of the differences between the individual station position solutions and a model for this position, which is allowed to change linearly with time. The coordinates at an arbitrary reference epoch and their time derivatives are estimated for each individual laser station, simultaneously with systematic offsets for each global network solution (in origin and orientation). As an example, Figure 4.5 shows the results of this technique for the Dionysos station in Greece. The original solutions (corrected for systematic offsets) are depicted with circles, and accompanied by the pertaining 1-σ uncertainty estimates. The crosses represent the positions for Dionysos according to the linear model, computed at the epochs corresponding to those of the original coordinates solutions. Full details of the estimation procedure can be found in [8]. The resulting motion vectors for the sites in the Mediterranean area have been decomposed into horizontal and vertical components. They will be discussed separately below.

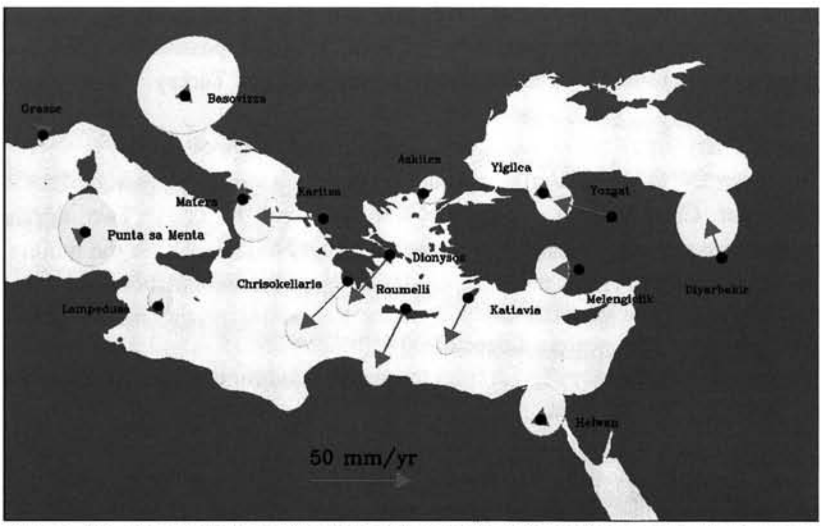

Figure 4.6 The solutions for the horizontal crustal deformations in the Mediterranean area. The vectors are relative to Eurasia. The ellipses indicate the maximum error of each solution.

Horizontal motions

In Figure 4.6, the horizontal motion solutions are given with respect to Eurasia. In this frame, stations rigidly located on the stable part of this major plate should exhibit a zero motion. The ellipses that accompany each solution indicate the maximum error that can be expected. Clearly, there is a direct relation between the dimension of these ellipses and the occupation history for each site.

Two different deformation regimes can be distinguished in the area of interest. First, the deformations in the eastern part are dictated by the convergence of Arabia and Eurasia. The solution for the SLR site in Diyarbakir, in eastern Turkey, shows a vector which is in reasonable agreement with the motion predicted by NUVEL-1: the longitude component differs by 1 mm/yr only, whereas the latitudinal component represents 60% of the NUVEL value (a difference of 9 mm/yr). However, considering the fact that this site hosted mobile SLR systems only twice (in 1987 and 1989), and assuming that the site is rigidly located on the Arabian plate (Diyarbakir is situated well south of the Bitlis zone, the area which is generally regarded as the border between Eurasia and Arabia), it is concluded that the SLR motion solution does not conflict significantly with the motion for Arabia as described by NUVEL-1.

Further to the west, both Yozgat and Melengiçlik exhibit a significant westward motion. Both stations are located on the Anatolian microplate, which is pushed to the west because of the convergence of Eurasia and Arabia. The magnitude of the velocity ranges from 13 to 29 mm/yr. The motion solution for Yigilca, which is situated along the Black Sea coastline, north of the North Anatolian Fault, shows that the westward motion of the Anatolian block is only partly transferred to this part of the country (the total vector having a length of 6 mm/yr). Unfortunately, because of lack of solutions for more stations in the area, it is not possible to draw more conclusions on deformation patterns in the northern part of Turkey.

The general pattern of the deformation in central and southern Greece is a motion ranging from 26 to 34 mm/yr in a southwestward direction, as indicated by the solutions for Chrisokellaria, Dionysos, Roumelli and Kattavia. Two different phenomena are generally assumed to act as the driving mechanism for the motion of the Aegean microplate: the push by Anatolia along the eastern boundary of the Aegean block and the gravitational pull of the slab subducting along the Hellenic Arc, the southern and western boundary. The magnitude of the motion vectors in Greece are statistically not different from those recovered for the Turkish sites, which leaves this question still open.

However, investigators from Cambridge (UK) [12] have recently proposed a so-called broken-slat model, which can explain the kinematics for Chrisokellaria, Dionysos and Roumelli, driven by Anatolia. Although not explicitly mentioned, the Cambridge model can also explain the motion of Karitsa, if it is assumed that a direct, stable link exists between this site and Anatolia which crosses the northern

Aegean. The problem is, that the motion vector solution for this site is based on two visits by SLR systems only. Therefore, it has to be regarded with some care, because the vector proves to be incompatible with the results recently obtained independently from GPS.

The broken-slat model fails to explain the SSW motion of Kattavia, so it is very well possible that the gravity pull plays a lead role at least in this part of the Aegean region. The latitudinal components of the horizontal motions for Chrisokellaria, Dionysos, Roumelli and Kattavia show a variation of 7 mm/yr at most, whereas the differences in the longitudinal direction are more significant. This may very well point to the existence of Creta, a separate microplate in southeast Aegea, on which Roumelli and Kattavia would be situated.

The series of occupations of Askites, in northern Greece, has resulted in a very small easterly directed motion vector, which must be regarded as insignificant considering the error estimate. This result suggests either that Askites is located on the stable part of the Eurasian plate, or that the net effect of deformations in the region between Askites and stable Eurasia is negligible.

The deformation pattern in the central part of the Mediterranean is significantly different, as can be seen from the solutions for the motions of the Italian laser sites. The motion solution for Matera and Lampedusa is directed almost due north, at a rate of 7 mm/yr. This value corresponds very well with the motion that is predicted by the NUVEL-1 model, provided these sites are assumed to be located on the (unperturbed) African tectonic plate. The motion solution for Punta sa Menta has a very large uncertainty, and can not be regarded as realistic. Additional occupations of at least this site are required to obtain more meaningful results.

The laser site in Basovizza, in northern Italy, has been occupied only twice, unfortunately both times resulting in rather sparse batches of observations. Consequently, no meaningful solution can be obtained here.

Grasse, the laser station in southern France, appears to be moving due south at a rate of 3 mm/yr. This motion vector solution is completely within the 99% confidence limits.

Vertical motions

In addition to the horizontal motions, the analysis of the SLR observations has also resulted in estimates for vertical station motions. A graphical representation is depicted in Figure 4.7. Generally, a value of 2-4 mm/yr is representative for these components, whereas the maximum value is -15 mm/yr (Diyarbakir).

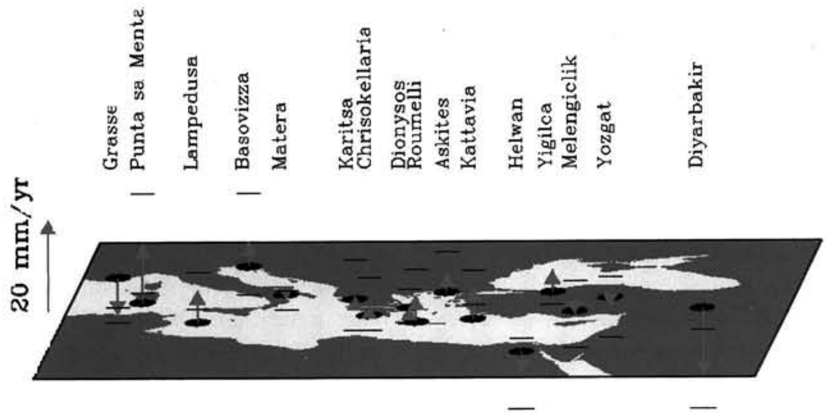

Figure 4.7 Solutions for the vertical crustal deformations in the Mediterranean area. The bars indicate the maximum error of each solution.

The results that have been obtained so far have to be interpreted with some care. First of all, the deformations in the vertical are typically one order of magnitude smaller than those in the horizontal directions. However, the uncertainties of the motion solutions in this direction are not significantly different from those for the horizontal components, as can be seen in Figure 4.7. This implies that most of the solutions are not statistically meaningful yet. A second reason for being careful when interpreting the results for the vertical direction is the fact that possible systematic errors in the range measurements of the satellite are generally absorbed in the solution for the station height. This susceptibility for ranging errors may be the reason for the unusually large value for the vertical motion solution for Grasse, and possibly also for Diyarbakir.

4.3 GPS data analysis

The Global Positioning System (GPS) is playing an increasingly important role as a high-precision geodetic positioning system, complementing the "traditional" space-geodetic techniques SLR and VLBI. As already mentioned, within the WEGENER project, it has been primarily used for small-scale densification projects, but in 1992, the first major GPS campaign was organized to observe the whole WEGENER-MEDLAS network. Furthermore, in 1989, a large GPS campaign was undertaken to connect the various national geodetic reference frames in Europe. This so-called EUREF project included many of the well-known SLR sites and in particular some of the WEGENER-MEDLAS sites. It provided the first opportunity to make a comparison between the SLR and GPS results for these sites. A similar test could be performed with the data from a much smaller GPS campaign that was organized in 1990. Its purpose was to link the positions of two new observation sites, which were established in Italy in connection with the calibration of the radar altimeter of ERS-1, with the European SLR network.

In the following, the results of the data analyses of these three GPS observation campaigns are presented. It will be shown that the agreement with SLR is quite good, demonstrating that GPS is a very useful system for crustal dynamics research.

4.3.1 WEGENER/GPS-92

During the IGS Epoch'92 campaign, which took place during a two week period centered around August 1, 1992, the WEGENER/GPS-92 subcampaign was carried out from July 29 until August 3, under the leadership of the Institute for Applied Geodesy (IfAG) in Frankfurt, Germany, in cooperation with DUT. All WEGENER-MEDLAS sites and one additional site on Cyprus, Dhekelia, were occupied with Trimble SST GPS receivers. This data set is of special interest due to the long experience with processing SLR data taken at the WEGENER-MEDLAS sites. It yields a unique opportunity to compare SLR derived coordinates with GPS derived coordinates since this is the first time that all sites of the WEGENER-MEDLAS network were measured simultaneously using GPS.

The dataset was analysed, using the GIPSY software developed at the Jet Propulsion Laboratory and the Bernese GPS software version 3.4. In the analysis a weighted combination of the orbits provided by the IGS was used to model the motion of the GPS satellites. The total number of stations processed in the GPS analysis was 21 from which 19 were located on or near an SLR marker. From these 19 stations 3 (Karitsa, Medicina, Noto) were downweighted in the comparison of the SLR and GPS solutions. The SLR solution for those sites was based on only 1 or 2 occupations and therefore the velocity vectors are not very reliable. Two other sites (Wettzell and Grasse) showed relatively large differences of up to several centimeters. Since this is much higher than the formal errors of both the GPS and the SLR solutions it is expected that these differences are caused by site tie problems. Using the remaining 14 sites the rms agreement between the SLR and GPS solutions is 12.1, 15.4 and 16.4 mm for the North, East and Up components after a 7 parameter Helmert transformation.

The very high accuracy of this comparison makes it useful to add the GPS solution to the SLR solutions considering it to be an additional occupation for all sites. This will greatly improve the accuracy of the velocity estimates since it increases the number of occupations with about 25% for most of the sites. In this way a new coordinate set and velocity field were obtained combining the GPS solution with the SLR solutions. Comparing the GPS solution with the new solution shows and rms agreement of 3.8, 5.2 and 12.5 mm for the North, East and Up components. This improved agreement is partly due to the fact the comparison is not independent, since the GPS solution has contributed to the combined solution, and is largely due to the better determined velocity vectors.

These results show that the GPS technique has matured to a point where it can now provide relative position solutions with an accuracy at least comparable to that of SLR for large regional networks. Therefore, it is expected that GPS will play an increasingly important role in the expansion and further densification of the WEGENER network, with SLR providing the fiducial reference frame.

4.3.2 The EUREF-89 dataset

In May 1989, the IAG Subcommission for the European Reference Frame (EUREF) organized the first EUREF GPS campaign to establish a common European Reference Frame [13]. During a 2-week period, lasting from 16 to 28 May 1989, various types of GPS receivers were deployed at about 100 different European sites. The network includes many national geodetic first order points and most of the well-known VLBI and SLR sites, with baselines ranging from less than 100 m to more than 2500 km in length.

Figure 4.8 Geographical location of the selected subset of EUREF-89 GPS sites.

The processing and analysis of this GPS data set was a major effort, which was finally completed by a group led by the Astronomical Institute of the University of Berne (AIUB). The results of this group, the 'official' EUREF/GPS 1989 solution, were presented at the March 1992 EUREF meeting in Berne [14]. Due to the amount of data, and the work involved, several other processing centers produced only partial solutions. The University of Nottingham computed a solution for a sub-network consisting of the stations in the United Kingdom [15]. Another two different partial solutions were generated at Delft University of Technology (DUT). The Delft Geodetic Computing Center (LGR) of the Faculty of Geodetic Engineering computed a solution for the stations in the Benelux area [16], whereas the Section Space Research & Technology (SSR&T) analyzed the measurements of a subset consisting of all the SLR and VLBI sites, and three additional points in The Netherlands [17,18]. The location of the selected sites is shown in Figure 4.8.

For the data analysis, the GIPSY software was used [19,20]. It is stressed that the study was an independent effort, which was primarily aimed at gaining experience with the GIPSY software, and exploring the capabilities of GPS to supplement SLR for the detection of tectonic motions. This investigation is a logical extension of the work of our group, which has been involved in the analysis of SLR data for many years now. This interest is reflected by the special emphasis on the comparison of the GPS results with our SLR solution, based on an analysis of 5 years of observations of the LAGEOS satellite. These analyses are of particular importance for crustal deformation studies in the framework of the WEGENER/MEDLAS project [8]. In addition the study also provided an interesting opportunity to assess the quality of the official EUREF solution.

The accuracy of the estimated station coordinates has been investigated by examining the repeatability of the daily solutions of all baselines between the stations. As can be seen from Figure 4.9, this repeatability is of the order of 0.5 - 2.0 parts in 10^8 for baselines up to 2500 km in length. This result is considered to be quite reasonable, in particular when it is realized that four different types of GPS receivers were used.

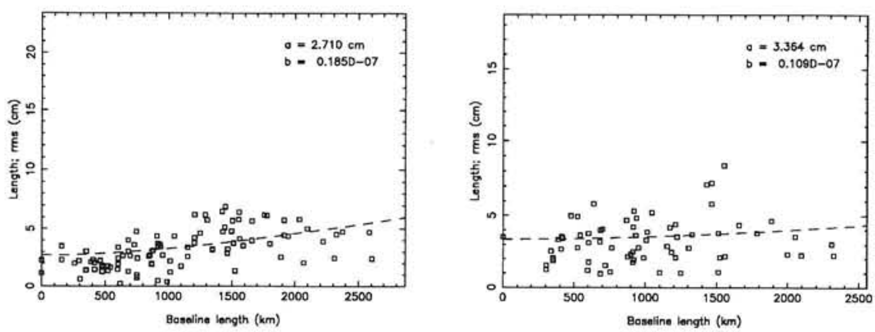

Figure 4.9 Baseline length repeatability (rms scatter about the weighted mean) for baselines between the selected EUREF-89 sites. The results for the first week (16-21 May) are at left, and for the second week (23-28 May) at right. Also plotted are the best fit curves.

The accuracy of the GPS estimates has also been investigated by comparing the GPS results with the a priori SLR coordinates solution. The GPS-computed and SLR-derived baseline lengths between common stations in both solutions agree on average to better than 2.0 cm. The comparisons prove that the fiducial coordinates used in the official EUREF solution, indeed were consistent with the overall European SLR Reference Frame.

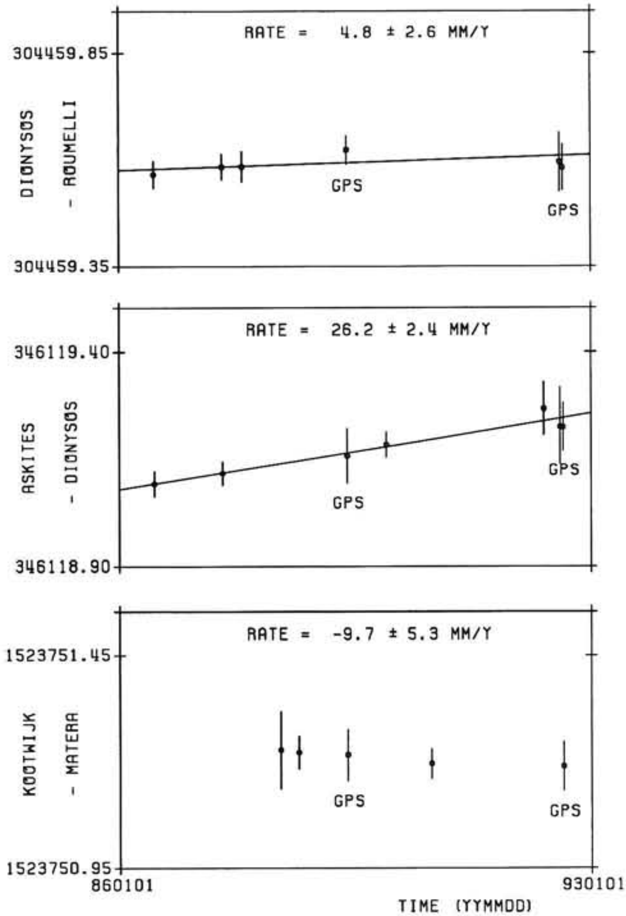

Figure 4.10 Time-histories of baseline length results for Dionysos-Roumelli (top), Askites-Dionysos (middle), and Zimmerwald-Kootwijk (bottom). Error bars indicate the 1σ standard deviation.

For the baselines involving the stations in Greece, the EUREF results seem to confirm the trends in baseline length changes emerging from SLR analyses, reflecting crustal motions in Greece. The individual solutions for these baselines, derived from an earlier SLR solution which was available at the time of the analysis, have been plotted as a function of time in Figure 4.10, along with the results obtained from the analysis of the selected EUREF-89 GPS data. Also shown are the best fit straight lines and 1σ error bars. The trends in the Greek baselines are quite evident and seem to be consistent with tectonic models of the area. It is most striking that the GPS data points fit quite nicely between the SLR results, demonstrating that both techniques supplement each other well [21].

EUREF'89 took place in 1989. At that time, only a small number of GPS satellites (7 instead of 24 in the final operational constellation) was available, and only about 7 hour daily observation sessions were scheduled. Therefore, from today's point of view the quality of the results presented in this Section are relatively modest. The accuracy of the computed coordinates is estimated to be at a level of about 4.0 cm in the horizontal and 6.0 cm in the vertical direction. Today it is possible to get much better results with continuous tracking and more available satellites. However, this analysis clearly demonstrated that at the time, GPS was already a promising technique with a great future. Given the requirements of EUREF, the results are certainly accurate enough to start with the establishment and maintenance of a common European Reference Frame, which will play an important role in the next decade in Europe.

4.3.3 Positioning of ERS-1 altimeter calibration sites

The first ESA European Remote Sensing satellite (ERS-1) was launched on July 17, 1991. Its mission is to map the earth's surface through a variety of space-borne down-looking sensors: a Synthetic Aperture Radar (SAR), a Wind Scatterometer (SCAT), an Along- Track Scanning Radiometer and Microwave Sounder (ATSR/M), and a Radar Altimeter (RA). The latter instrument was calibrated during the commissioning phase of the mission, when the satellite was in a 3-day repeat orbit. This orbit was controlled in such a way that once every three days, the satellite passed directly overhead the oceanographic platform 'Acqua Alta' in the Adriatic Sea, off the coast of Venice [22].

For the calibration, the sea level computed from the altimeter observations, taken during the brief passes over the Adriatic Sea surrounding the 'Venice platform', was compared with the real sea level. This altimetric sea level was derived from the altimeter measurements, corrected for atmospheric propagation effects and sea surface slope. In addition, the precise altitude of the ERS-1 satellite was obtained from SLR observations taken by several fixed European SLR systems and by the Dutch mobile SLR system, MTLRS-2, at Monte Venda, a site at about 50 km west of Venice. The real sea level was determined from tide gauge observations, using a fixed point on the Venice platform as a height reference mark.

This means that the height of this reference mark has to be accurately know in the geocentric reference system provided by the SLR stations. Also, since Monte Venda was a new mobile SLR site, especially established for the calibration, its position also needed to be determined within the network of the other stations. Because of the requirements on the precision of the bias calibration, the heights of these two markers had to be tied into the SLR reference frame with an accuracy of better than 5 cm. Therefore, a dedicated GPS campaign was organized, which took place in the period October 14-19, 1990. Figure 4.11 shows the network of points which were occupied by the GPS receivers. These consisted of a mix of Wild-Magnavox WM-102 systems, Trimble-SST receivers and one MiniMac.

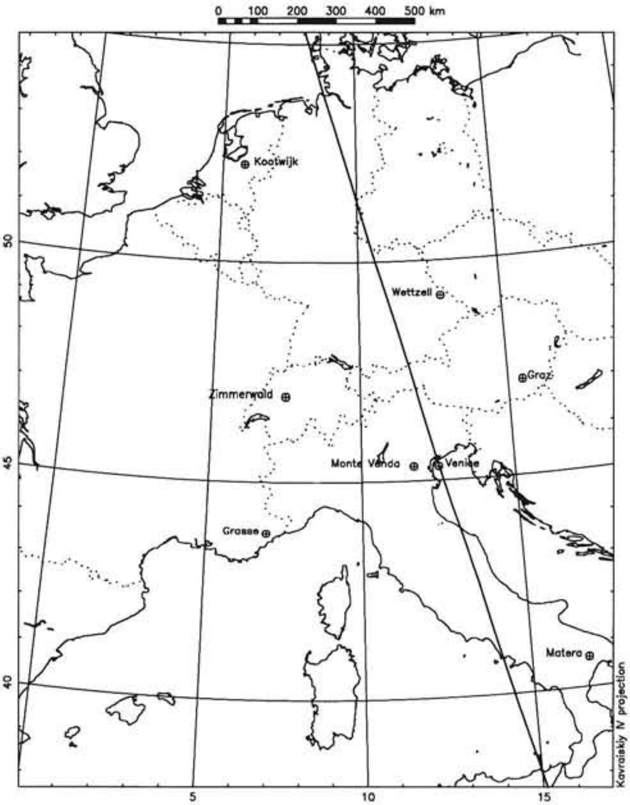

Figure 4.11 Sites occupied by GPS receivers for the calibration of the ERS-1 Radar Altimeter. The straight line indicates the 'Calibration Orbit' of ERS-1 overhead the Venice Tower.

The GPS measurements of this campaign have been analyzed at DUT. This activity was part of a larger effort which comprised the complete data analyses for the calibration of the ERS-1 Radar Altimeter [23]. However, it also provided an interesting opportunity to compare the results of this GPS analysis with the SLR solutions for the stations included in this campaign. In the following, the results of the analysis of the GPS data are presented.

Figure 4.12 shows the scatter of the five daily solutions (delta with respect to the a-priori coordinates) of the components of the baseline Monte Venda (WM90) - Venice (WM90). For each day the daily solution is indicated together with the 1σ formal error bar. The '+' in each plot indicates the weighted mean delta estimate of each baseline component.

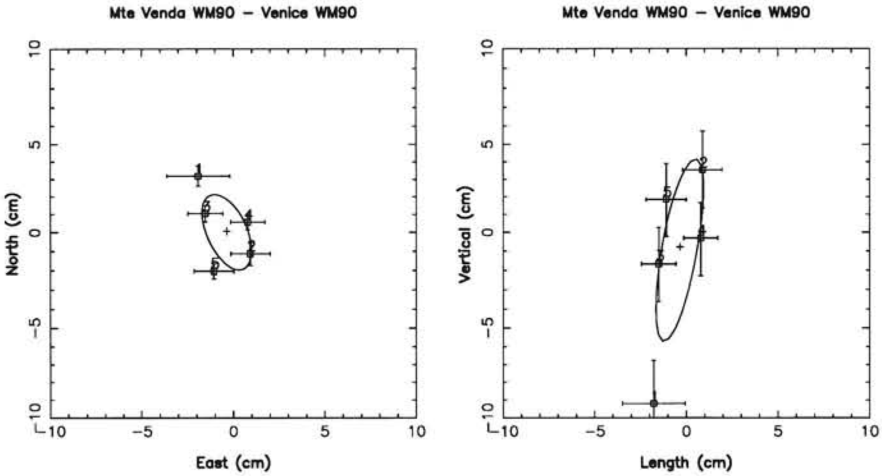

Figure 4.12 Scatter of the five daily delta estimates of the baseline components of the baseline Monte Venda - Venice, and the 1σ formal error bars. The numbers 1-5 correspond to 14-18 October, respectively. The '+' indicates the weighted mean delta estimate of each baseline component.

Figure 4.13 shows the scatter of the daily solutions of the height of the GPS marker at the Venice Tower, which is of the highest importance for the Altimeter Calibration analyses. For each day the daily solution is indicated together with the 1σ formal error bar. The dashed line indicates the stochastically combined solution of the height of the marker.

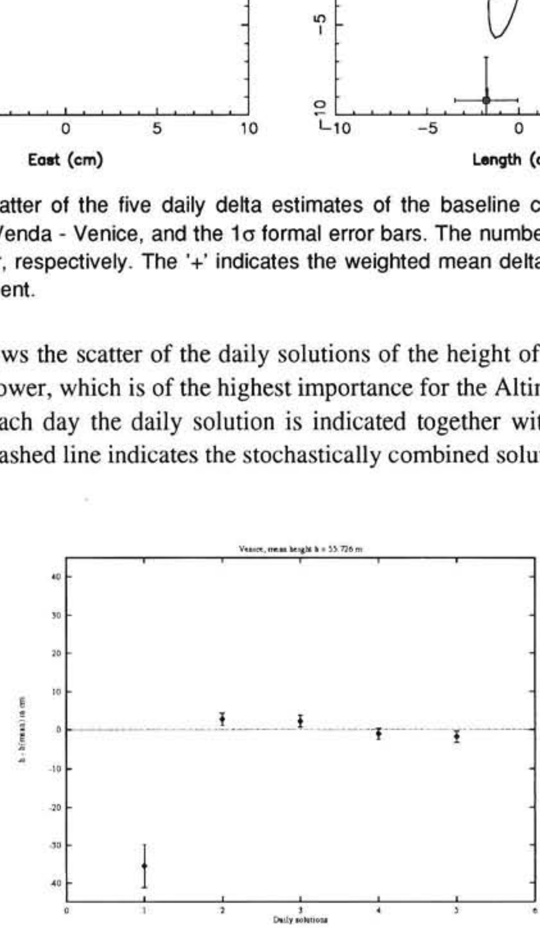

Figure 4.13 Variation of individual GPS height solutions with 1σ formal error bars for the GPS marker at the Venice Tower. The dashed line indicates the stochastically combined solution.

The results show that the coordinates of the GPS markers at Monte Venda and the Venice Tower, and therefore the coordinates of the SLR marker at Monte Venda, have been determined very accurately. The estimated coordinates of the SLR marker even agreed to within a few centimeter with the coordinates found after processing of LAGEOS quick-look SLR data of Monte Venda.

The results also compare favorably with those derived independently from the same data by the Astronomical Institute of the University of Berne (AIUB). Differences between DUT's and AIUB's solution are smaller than the 3σ uncertainties of the solutions.

4.4 References

1. Reinhart, E., P. Wilson, L. Aardoom and E. Vermaat, *The WEGENER Mediterranean laser tracking project: WEGENER-MEDLAS*, CSTG Bull., **8**, 145-162, 1985.

2. Aardoom, L., and B.H.W. van Gelder, *Satellite laser ranging to measure crustal motion in the Eastern Mediterranean area: instrumentation and network design*, Annales Geophysicae, **2**(3), 249-258, 1984.

3. Wilson, P., *Kinematics of the eastern Mediterranean region and the WEGENER-MEDLAS project*, Geojournal, **14**(2), 143-161, 1987.

4. DeMets, C., R.G. Gordon, D.F. Argus and S. Stein, *Current plate motions*, Geophys. J. Int., **101**, 425-478, 1990.

5. McKenzie, D., *Active tectonics of the Mediterranean region*, Geophys. J. R. astr. Soc., **30**, 109-185, 1972.

6. Cohen, S.C., and D.E. Smith, *LAGEOS scientific results: introduction*, J. Geophys. Res., **90**(B11), 9217-9220, Sep. 30, 1985.

7. Zwijger, H.E. de, and B.H.W. van Gelder, *Results of the WEGENER/MEDLAS 1986/1987 Campaign using the Consecutive Pass Analysis Scheme*, in: Proceedings of the Fourth International Conference on the WEGENER/MEDLAS Project, Scheveningen, The Netherlands, June 7-9, 1989, Delft University of Technology, Delft, The Netherlands, 1990.

8. Noomen, R., B.A.C. Ambrosius, and K.F. Wakker, *Crustal motions in the Mediterranean region determined from laser ranging to LAGEOS*, in: Smith, D.E., and Turcotte, D.L. (eds.), Contribution of Space Geodesy to Geodynamics; Crustal Dynamics, Geodynamics Series, **23**, American Geophysical Union, 331-346, 1993.

9. McCarthy, D.D., (ed.), *IERS Standards (1992)*, IERS Technical Note 13, Observatoire de Paris, Paris, France, 1992.

10. Eddy, W.F., J.J. McCarthy, D.E. Pavlis, J.A. Marshall, S.B. Luthke, L.S. Tsaoussi, G. Leung and D.A. Williams, *GEODYN-II system operations manual*, **1-5**, contractor report, ST System Corp., Lanham MD, USA, 1990.

11. Majer, V., *SOLVE program mathematical description*, NASA contractor report, Business and Technological Systems, Inc., Seabrook MD, USA, Dec., 1986.

12. Taymaz, T. , J. Jackson and D. McKenzie, *Active tectonics of the north and central Aegean Sea*, Geophys. J, Int., **106**, 433-490,1991

13. Seeger, H., W. Augath, R. Bordley, C. Boucher, B. Engen, W. Gurtner, W. Schluter, and R. Sigl, *Status report on the EUREF-GPS-campaign 1989*, Firence, Italy, 1990, submitted to the IAG EUREF-Subcommission.

14. Gurtner, W., S. Fankhauser, W. Ehrnsperger, W. Wende, H. Friedhoff, H. Habrich, and S. Botton, *EUREF-89 GPS campaign: Results of the processing by the 'Berne-Group'*, in: Report on the Symposium of the IAG Subcommission for the European Reference Frame (EUREF), March 4-6, 1992, Berne, 146, 1992.

15. Ashkenazi, V., C. J. Hill, G. M. Whitmore, and R. R. Christie, *The Nottingham processing of the EUREF-89 GPS campaign*, in: Report on the Symposium of the IAG Subcommission for the European Reference Frame (EUREF), March 4-6, 1992, Berne, 170, 1992.

16. Marel, H. van der, *Analysis of the EUREF-89 GPS data in the Benelux area*, in: Report on the Symposium of the IAG Subcommission for the European Reference Frame (EUREF), March 4-6, 1992, Berne, 197, 1992.

17. Overgaauw, B., B. A. C. Ambrosius, and K. F. Wakker, *Results of the analysis of the EUREF-89 GPS data from the SLR/VLBI sites*, in: Report on the Symposium of the IAG Subcommission for the European Reference Frame (EUREF), March 4-6, 1992, Berne, 179, 1992.

18. Overgaauw, B., B.A.C. Ambrosius and K.F. Wakker, *Analysis of the EUREF-89 GPS data from the SLR/VLBI sites*, Bull. Geod., **68**, 19-28, 1994.

19. Lichten, S.M., *Estimation and filtering for high-precision GPS positioning algorithms*, Man. Geod., **14**, 159-176, 1990.

20. Blewitt, G., *Carrier phase ambiguity resolution for the Global Positioning System applied to geodetic baselines up to 2000 km*, J. Geophys. Res., (B8), 10187-10283, 1989.

21. Ambrosius, B.A.C., R. Noomen, B. Overgaauw and K.F. Wakker, *Crustal motions in Greece determined from GPS and SLR observations*, in: Mertikas, S.P. (ed.), Proc. of the International Workshop on Global Positioning Systems in Geosciences, Chania, Crete, June 8-10, 1992, Technical University of Crete, Greece, 183-207, 1993.

22. Scharroo, R., K. F. Wakker, B. Overgaauw, and B. A. C. Ambrosius, *Some aspects of the ERS-1 radar altimeter calibration*, paper presented at the 42nd Congress of the International Astronautical Federation, Montreal, Canada, October 5-11, 1991, paper IAF-91-367, 1991.

23. Francis, C. R., A. Caporali, L. Cavaleri, A. Cenci, P. Ciotto, L. Ciraolo, W. Gurtner, F. H. Massmann, D. del Rosso, R. Scharroo, P. Spalla, and E. Vermaat, *The Calibration of the ERS-1 Radar Altimeter-The Venice Calibration Campaign*, ESA Report ER-RP-ESA-RA-0257 issue 2.0, ESA/ESTEC, Noordwijk, The Netherlands, March 1, 1993.

5 Earth rotation

For many millennia, the most accurate time-keeping instrument has been planet Earth itself, which was assumed to rotate evenly around a fixed axis. Astronomical observations were used as a means of accurate time-keeping. In the last decades of the 19^{th} century, technology caught up with nature: astronomers discovered irregularities in the behavior of the earth's axis. In the 1930's it became clear that the improved quality of clocks and other astronomical instruments made them agree better with each other than with the hypothesized perfectly simple earth rotation rate. These findings started the study of the irregularities in the rotation of the earth.

5.1 Theoretical background

Earth rotation studies can follow a geophysical or a geodetical approach: theoretical modelling of the earth's rotation, using the Euler-Liouville equations, or determination and interpretation of the Earth Rotation Parameters (ERPs), using space-geodetic observations.

Geophysically, variations in the earth's rotation can conveniently be separated into three parts [1]. Precession and nutation describe the rotational motion of the earth in inertial space. Polar motion is the variation in the position of the rotation axis with respect to the earth's crust. Variations in length-of-day or UT1 are a measure of the variable rotation rate about the instantaneous rotation axis. Precession and nutation are primarily caused by the lunar and solar gravitational attraction on the earth's equatorial bulge. Variations in polar motion and rotation rate are excited by geophysical processes originating within the earth. The distinction between polar motion and nutation is somewhat artificial because polar motion cannot occur without accompanying nutation and vice versa.

The Euler-Liouville dynamical equations describe the rotation of the non-rigid earth. Since, for the earth, the deviations from an uniformly rotating, rotationally symmetric rigid body are small, these equations can be rewritten in a perturbation form with rotation parameters on the left-hand side and excitation functions, including external torques, on the right-hand side. The rotation parameters can be determined from space-geodetic observations, while the excitation functions can be derived from geophysical observations and theory. Part of the earth rotation studies deal with explaining the observed rotation variations in terms of the available geophysical models, or, on the other hand, with deducing geophysical properties from the observed ERPs.

From a geodetical point of view, earth rotation describes the rotation between the conventional celestial reference frame and the conventional terrestrial reference frame [2]. In other words, earth rotation connects the motion of objects in inertial space, such as geodetic satellites, with the motion of the observing stations, located on the earth's crust. Earth rotation can be described as a coordinate transformation in the form of a series of rotation matrices, in which the fundamental components correspond with the three aspects of earth rotation. The International Earth Rotation Service (IERS) is responsible for the definition of the two conventional reference systems including the definition of the astronomical constants and dynamical models to be used in the analyses of space-geodetic data [3] and for the maintenance of the conventional reference frames and the determination of the ERPs to be used in the coordinate transformation [4].

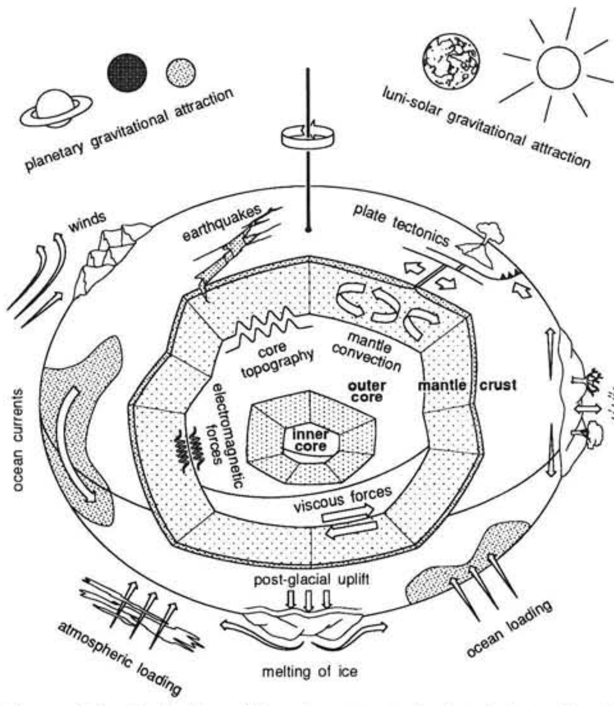

Figure 5.1 Illustration of the phenomena that perturb earth rotation.

The various components of earth rotation, as well as station positions and velocities, satellite motions and radio source positions, are routinely determined from space-geodetic observations. The situation is complicated, because different analysis centres use different analysis methods to process different datasets obtained with different techniques. The ERP and coordinate solutions therefore pertain to different reference systems, which is very important for the combination of the various solutions into an ERP series and the maintenance of the celestial and terrestrial reference frames. With the advent of high-frequency GPS solutions and the increasing temporal resolution of the other space-geodetic solutions (SLR, VLBI), short-periodic variations in earth rotation are becoming more important, while the distinction between polar motion and nutation is getting less clear. The ERP series can be analyzed using spectral techniques to determine the frequencies and amplitudes of the underlying processes. The ERPs can be correlated with auxiliary data to assess the type of geophysical processes which excite the earth rotation variations. For example, the short-periodic variations in polar motion and UT1 show a high correlation with atmospheric angular momentum data. The greater part of the studies concentrate on these geodetical aspects of earth rotation.

5.2 Determination of earth rotation

As mentioned in the previous Section, the determination of earth orientation parameters is an activity of IERS. This institute accomplishes this task by combining ERP solutions from numerous contributors, who analyze data from a number of different observation techniques. DUT is one of the SLR contributors, and reports to IERS on two aspects of earth orientation.

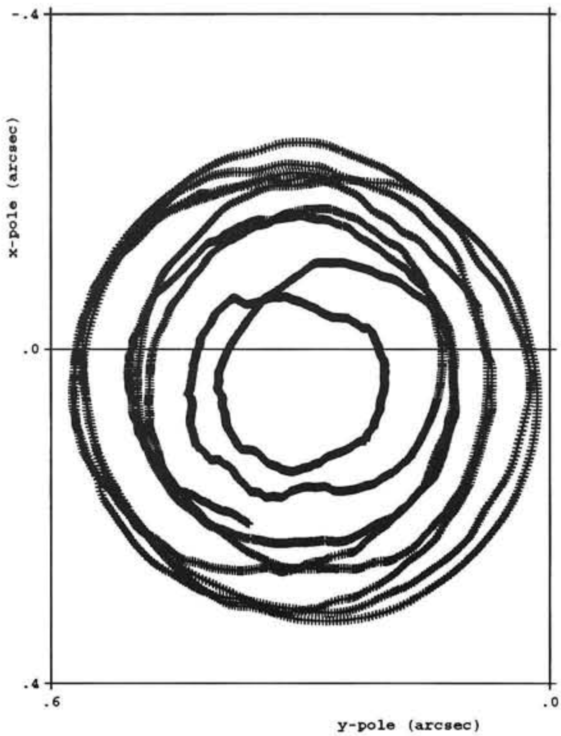

Figure 5.2 The daily position of the pole for the years 1983 through 1992. The positive x-axis points in the direction of Greenwich, the positive y-axis points in the general direction of New Orleans.

The first aspect is polar motion. Here, one can distinguish periodic components with periods of one year and of about 435 days, a linear trend, and additional high frequency irregularities. These add up to a variation in pole position of almost 0.6

arcseconds, as illustrated in Figure 5.2, which shows the position of the rotational pole for the years 1983 through 1992. This maximum variation of the actual pole position is equivalent to about 20 m, when expressed as a distance measured over the surface of the earth, and may result in similar variations for the actual position of a laser tracking station in its daily revolution around the earth's axis. This variation is reflected in the measured distances from the station to geodetic satellites such as LAGEOS-1, which position can be computed with an accuracy of a few centimeters.

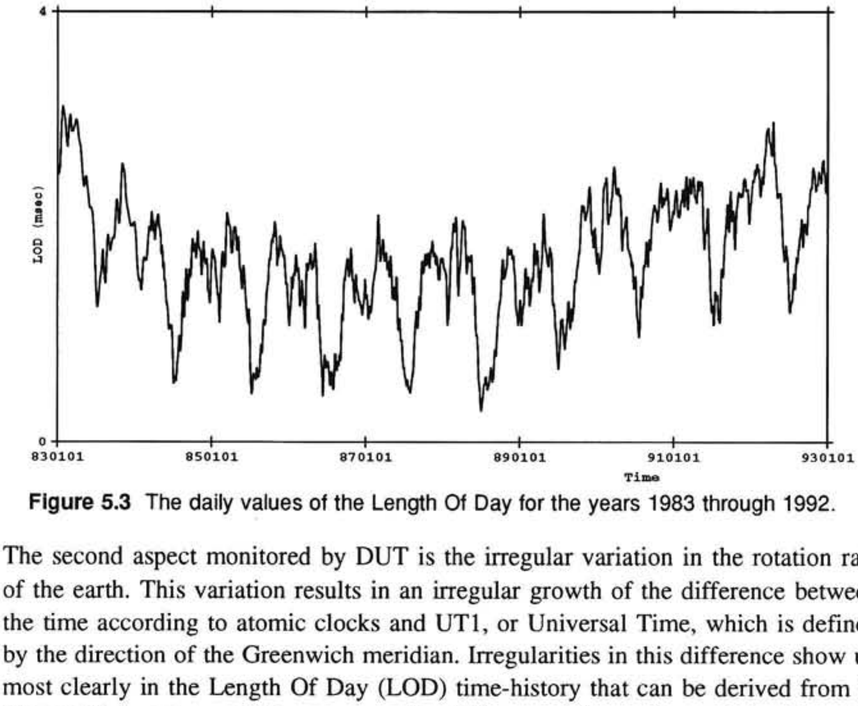

Figure 5.3 The daily values of the Length Of Day for the years 1983 through 1992.

The second aspect monitored by DUT is the irregular variation in the rotation rate of the earth. This variation results in an irregular growth of the difference between the time according to atomic clocks and UT1, or Universal Time, which is defined by the direction of the Greenwich meridian. Irregularities in this difference show up most clearly in the Length Of Day (LOD) time-history that can be derived from it. This LOD function, which represents the difference between the real duration of a day and its nominal duration of 24 hours, is depicted in Figure 5.3 for the years 1983 through 1992. After removing an easily distinguished seasonal oscillation, a slow trend and theoretically derived tidal effects, one is left with an irregular residual oscillation with amplitudes occasionally exceeding half a millisecond. At the equator this corresponds to a distance of about 20 cm. Since satellite orbits are not directly affected by variations in earth rotation rate, the effect can be easily discernible, even for laser tracking stations at the higher latitudes. However, it should be mentioned that deficiencies in currently available models for satellite orbital dynamics induce slowly evolving errors in the mathematical representation of the orbital plane: UT1 values derived from satellite tracking only will absorb the unmodeled slow rotation of the orbital plane.

As described in Chapter 4, DUT is an analysis center for laser ranging observations of the LAGEOS satellites, for which it needs accurate ERP values. However, these values are not yet known for the full data period under investigation. This holds in particular for the quick-look analysis, which is done almost real-time. The required precision of the actual satellite orbit and the instantaneous station positions can therefore only be achieved by including the ERPs as solve-for parameters. The two types of operational analyses performed at DUT, viz. quick-look and full-rate, yield ERP solutions of the kind that are useful to IERS. The characteristics of the two types of analysis are described in the next Sections.

5.2.1 Quick-look analysis

DUT performs a weekly analysis of LAGEOS-1 and LAGEOS-2 quick-look SLR data that are distributed in order to provide an early preview of the acquired measurements. The main functions of the quick-look analysis are computation of ERP solutions from observations of the LAGEOS satellites and monitoring of the performance of the SLR systems, in particular the transportable systems that are involved in the WEGENER/MEDLAS observational campaigns (cf. Chapter 4).

The quick-look data taken are generally made available within a few days after the observations have been recorded. This means that the activities represent a semi real-time operation, where the time of availability of the analysis results lags the events by no more than about 10 days. Since its establishment in 1987, ERP solutions for every fifth day have been reported to the IERS Sub-Bureau for Rapid Service and Predictions in Washington, and to the IERS Central Bureau in Paris as well. These solutions are a product of a weekly analysis of all available data for a period of one week plus the time tag difference of successive ERP values. The resulting overlap of analysis periods guarantees that every ERP value can be derived from satellite tracking data fully covering the time-span pertaining to that ERP data point (the data arcs start and stop at midnight, whereas the ERP intervals start and stop at noon). The results are included in both the weekly IERS Bulletin A and the monthly Bulletin B, and are used to compute the combined ERP series.

The ever increasing accuracy of SLR measurements and the improved models for satellite dynamics allow the computation of precise high frequency ERP solutions. Since June 1993, DUT submits 3-day ERP solutions to IERS, in addition to the standard 5-day solutions. These results are obtained in a 10-day data arc analysis, which still guarantees the computation of a unique, non-overlapping series of ERP solutions. In order to allow a smooth transition from 5-day to 3-day ERP solutions, additional 3-day solutions were computed for the first half of 1993. As a result, the 5-day series was phased out in January 1994.

5.2.2 Full-rate analysis

Starting in 1987, DUT has submitted an ERP solution to IERS every year. Each solution was derived from an analysis of all LAGEOS-1 full-rate data available at that time, occasionally complemented with more recent quick-look data. The most recently submitted solution, ERP(DUT) 94L01, encompasses the period from September 1983 to December 1992. For this time-interval, a continuous series of polar motion and UT1 solutions, at a frequency of 3 days, has been computed from SLR measurements of LAGEOS-1. The solution will be published in the 1993 IERS Annual Report [5]. Details of the computations are given in Chapter 4.

Even though ERPs are already solved for during the computation of positions and velocities of SLR stations for the WEGENER project, an extra step is added for the derivation of the final ERP solutions. In this additional step, a simultaneous solution is made of the pole position, UT1, and the orbit of LAGEOS-1. Stability is provided for this solution by constraining the ascending node of the LAGEOS-1 orbit to values that were recovered from the WEGENER analysis. The advantage of adding this final step is that it can also utilize the model for instantaneous station positions that was derived in the WEGENER analysis, and thereby make the solutions mutually consistent.

5.2.3 Results

The characteristics of the DUT solutions are illustrated by plots of the differences between those solutions and the EOP(IERS) 90C04 series, produced and distributed by IERS [5]. The latter series consists of a slightly smoothed combination of the solutions that were contributed by analysis centers for all relevant measurement techniques (i.e. very long baseline interferometry, lunar laser ranging, GPS and SLR).

For the latest full-rate results, Figure 5.4 displays the differences with the EOP(IERS) 90C04 solution. They tend to concentrate in bands with a number of interesting features. In the first place, the fact that the bands are getting narrower as time progresses, nicely illustrates that the number and quality of SLR observations has increased over the years. A second characteristic, the linear trend in the differences for the y-component of the pole position, can be interpreted as a consequence of differences in reference frame motions due to a disparity in assumed station velocities.

The UT1 comparison is only included for completeness' sake. The goals of the current WEGENER analysis do not include long term satellite orbit stability. The resulting irregularities in the longitude of the orbit's ascending node are echoed in the computed UT1 values, which makes them considerably less reliable than the pole position solutions.

For the quick-look results, the differences between DUT's 3-day solutions for 1993 and the EOP(IERS) 90C04 series are shown in Figure 5.5. This figure illustrates that the quality of the 3-day quick-look pole position solutions corresponds with that of the full-rate solutions.

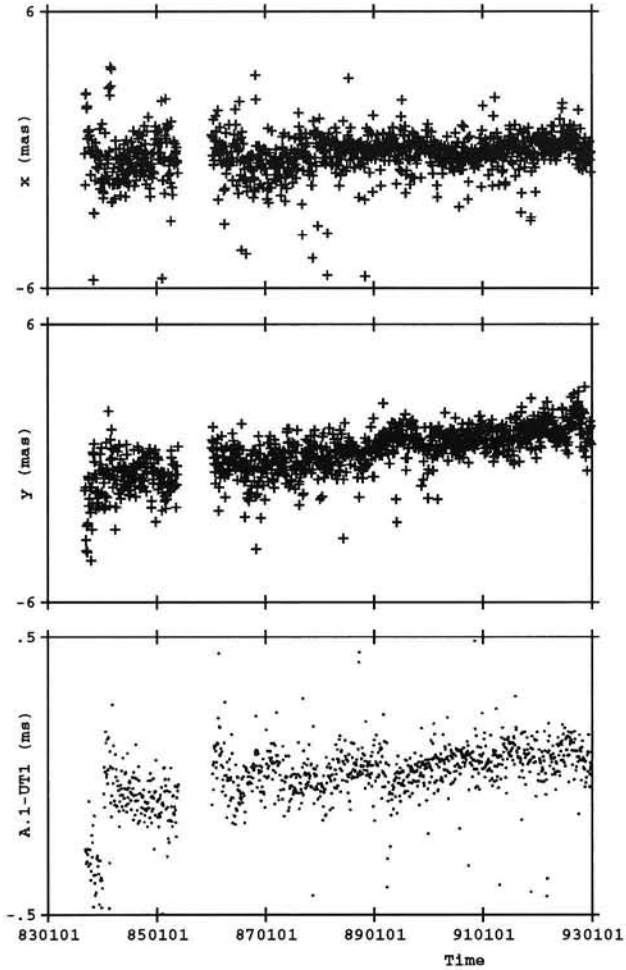

Figure 5.4 Difference between 3-day ERP solutions from the ERP(DUT) 94L01 full-rate solution and the IERS EOP 90C04 series.

The UT1 values, however, look completely different. For the quick-look analysis, the satellite orbits for successive weekly analyses are linked. This is done by setting the position of the LAGEOS-1 orbit's ascending node at the beginning of each analyzed period equal to the node position computed for that moment during the previous week's analysis. Although this technique avoids the high frequency irregularities resulting from using independent satellite orbits for successive analyses (that occur in the full-rate analysis), it leads to a significant trend in the UT1 values echoing the slow variations of the orbit's computed node position. The latter phenomenon is caused by imperfections in the dynamic models for the satellites. It is expected that improved models will alleviate this problem and possibly result in more useful UT1 values.

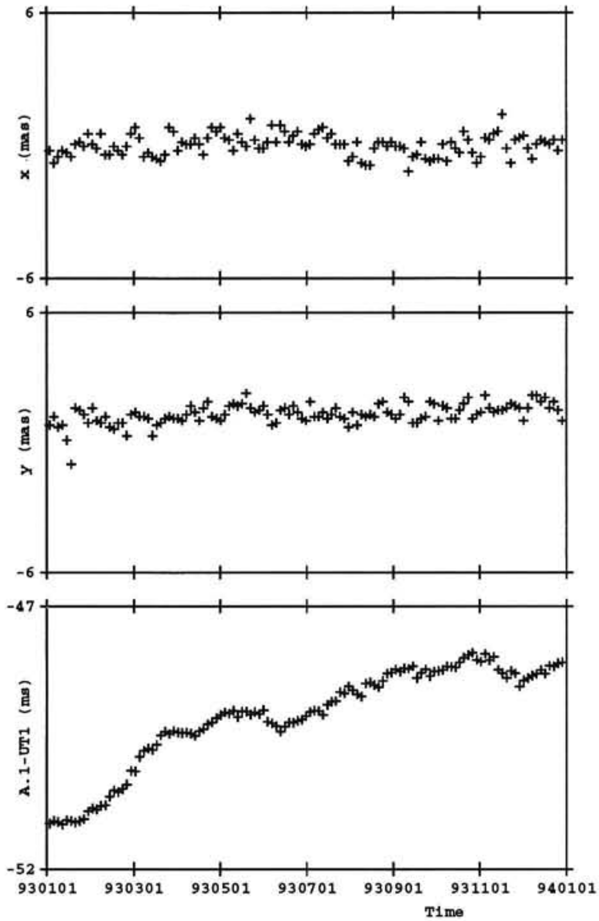

Figure 5.5 Difference between 3-day ERP solutions for 1993 from the DUT quick-look series and the IERS EOP 90C04 series.

5.3 References

1. Lambeck, K., *The earth's variable rotation: geophysical causes and consequences*, Cambridge University Press, Cambridge, UK, 1980.

2. Moritz, H. and I.I. Mueller, *Earth rotation - theory and observation*, Ungar, New York, 1987.

3. McCarthy, D.D., (ed.), IERS Standards (1992), *IERS Technical Note 13*, Observatoire de Paris, Paris, France, 1992.

4. IERS, *1992 IERS Annual Report*, Observatoire de Paris, Paris, France, 1993.

5. IERS, *1993 IERS Annual Report*, Observatoire de Paris, Paris, France, 1994.

6 Ocean Currents and Gravity Field from Altimetry

Various satellite radar altimeter missions, such as SEASAT, GEOSAT, ERS-1 and TOPEX/Poseidon, have provided or are still providing range measurements from the satellite to the sea surface, with uniform quality on a global scale. The indirectly derived sea level, or ocean topography, is of major interest to geoscientists, and can be regarded as the natural link between oceanography, geophysics, and geodesy. After more than a decade of research, satellite altimetry has proven to be of great importance in the field of plate tectonics, geophysical exploration, and for tuning and improving oceanographic and earth's gravity models [1]. An important step forward, during the last few years, is the more than one order of magnitude improvement in orbit accuracy both in global orbit determination [2] and in local configurations for altimeter calibration purposes, *e.g.*, that for ERS-1 near Venice [3]. This led to a better interpretation of the altimeter data, and at the same time enabled research for new applications. Optimal data editing and processing techniques have been developed in preparation of the ERS-1 and TOPEX/Poseidon missions [4]. Meanwhile, both satellites have been launched, and new challenges are accepted leading to the first promising multi-satellite results [5,6].

The progress in altimeter research during the past years allowed a better understanding of both the gravity field as well as the ocean circulation. The latter can be regarded as the recognition of a few of the pieces in the complex puzzle of climatology research. Clearly, measuring the sea level is of great importance in current and future studies on global change and in monitoring sea level change. In the following a detailed description is given of the altimeter research as conducted at Delft University.

6.1 Altimetry in perspective

To underline the importance of altimetric research it can be put in the framework of Global Change Research. People want to forecast natural and man-induced hazards like floods, tropical storms, and earthquakes, and to predict climate changes. For instance, global temperature rise and sea level rise will have a great impact on our environment. The climate is largely controlled by the oceans and the cryosphere. The oceans supply half of the total heat transport from the equator to the poles, resulting in mild climates at higher latitudes. The oceans absorb a great deal of the CO_2 and other greenhouse gases in the atmosphere. Furthermore, changes in the deep ocean circulation, the wind-driven circulation and the mesoscale circulation (*e.g.* El Niño), will directly and indirectly have an influence on the climate. The cryosphere contains 80% of the total available fresh water. In addition it regulates the hydrological cycle and sea level.

So, if we want to look at global change and understand it, a continuous observation of the ocean and the polar ice caps is indispensable. Therefore, calibrated measurements are needed of the total system (global), repeated within the time scales in which important changes occur (semi-synoptic). These measurements can then be used to obtain the boundary values of coupled dynamic ocean/atmosphere models in order to make reliable predictions possible. Clearly, only a satellite encircling the earth can meet the requirements of being global and synoptic. A way to monitor the ocean is simply monitoring the sea surface height, and this is done by the altimeter [7].

Altimetry started with an experiment on Skylab back in 1973. The first satellite carrying a radar altimeter was GEOS 3 (1975-1978), succeeded by SEASAT in 1978. These two satellites already demonstrated the feasibility of altimetry to be applied in ocean and gravity studies. However, it was only after the operation of the U.S. Navy GEOdetic SATellite GEOSAT that altimeter data could be fully exploited [1,8,9]. GEOSAT, launched in 1985, started its Exact Repeat Mission (repeating ground tracks every 17 days) in November 1986 and died in January 1990. More recent data come from the first European Remote Sensing Satellite ERS-1 launched in July 1991, and the NASA/CNES TOPEX/Poseidon satellite launched in August 1992. ERS-1 repeats its ground tracks every 35 days and TOPEX/Poseidon every 10 days. Already new missions are defined for the future to ensure an uninterrupted time series of sea level measurements; *e.g.* ERS-2, ENVISAT, and GEOSAT and TOPEX/Poseidon follow-ons.

Basically, altimetry has four areas of application. One is the study of the dynamic ocean topography and ocean circulation; both large-scale and mesoscale, and both semi-permanent and variable. One can think of the impact of ocean circulation on climate, weather, fishery, shipping, waste trajectories, and military or commercial sea operations. The vertical structure of the ocean circulation can be inferred from the ocean topography by using complex ocean models. Predictions for variations in the ocean circulation can be made. And also the changes in the global sea level can be monitored. Another area of application is the study of the geoid, *i.e.*, the mean sea surface with the mean circulation subtracted. Undulations in this equipotential surface are caused by hot spot distributions, lateral variations in the lithosphere, the mass distribution in the earth's crust, and sea bottom topography [10]. One can think of determining marine gravity, detecting ocean bottom topography, using it as one of the tools in modelling spreading ridges and fracture zones, or in geophysical exploration. The two other areas of application are the study of waves and wind, and the study of ice topography. Especially the latter is important for monitoring climate and sea level changes; the volume of the polar ice can be determined and its evolution can be observed by the altimeter.

Delft University is, in close cooperation with the Institute for Marine and Atmospheric Research of Utrecht University (IMAU), involved in the first two studies, *i.e.*, ocean circulation and gravity field studies [11,12]. Earlier studies mainly focussed on the precise orbit computation of altimeter satellites but the activities soon extended to the processing and interpretation of the altimeter data for the various purposes mentioned above. The research is conducted in cooperation with international groups like ESA, NASA, and CNES, and national groups like KNMI, NIOZ, and Rijkswaterstaat/RIKZ.

6.1.1 Altimeter data

The altimeter aboard the satellite measures the distance between the satellite and the instantaneous sea surface by recording the time needed for a radar pulse to be transmitted, reflected by the sea surface and to be received [13]. The travel time for a pulse transmitted from 800 km height is about 5 ms. To obtain an accuracy of 1 cm this travel time has to be measured with a precision of 30 ps. A short pulse of this size would require a carrier with to large a bandwidth, and it would be completely scattered at the sea surface and obscured by the sea waves. To be able to employ larger pulses, to put in enough signal strength, and at the same time to arrive at the 5 cm precision level special pulse compression techniques (chirped pulses) are used. The actual one-per-second measurement is formed by averaging over 100 to 1000 individual measurements of the time that is needed to receive half the ocean return power.

Additional information can be subtracted from the slope of the leading edge of the return pulse (wave height) and from the total ocean return power (wind speed). Because the pulse travels trough the atmosphere the derived distance has to be corrected for refraction effects, *i.e.*, the pulse will be delayed by free electrons, air molecules and water vapor. Also a correction is needed for the sea surface roughness; wave troughs are somewhat flatter and less steep than wave crests. The difference in reflection characteristics causes a bias in the timing of the return pulse, and therefore a bias in the estimated distance. When the corrected altimeter measurement is subtracted from the satellite orbital height, referenced to an ellipsoid fitted through the global sea surface, the sea height above that ellipsoid is found. The orbital height is computed at DUT/SSR&T independently using precise tracking data [14]. Finally, after subtraction of the contributions of solid-earth and ocean tides, ocean loading, and inverse barometer effects, the instantaneous sea level is obtained [15].

This sea level is a combination of the marine geoid and the dynamic ocean topography. The marine geoid is solely due to the gravitation and rotation of the earth and is on the order of tens of meters, from about -100 m to 70 m. Its topography is perpendicular to the local effective gravity. The variation in gravity is mainly caused by mass anomalies in the earth's interior which deviate from a homogeneous model earth. The dynamic ocean topography is due to ocean circulation and is on the order of 1 m. It can be divided into a semi-permanent part and a time-variant part. By studying the first the global ocean surface circulation can be inferred as well as secular changes in the global sea level can be monitored. By studying the latter, which is referred to as 'relative' dynamic ocean topography, both the meandering of large-scale ocean currents and the evolution of mesoscale ocean currents can be determined. Next to information on currents the sea level measurements also contain information on tides.

6.2 Orbits, peripheral models, and pre-processing

The application of altimeter measurements in oceanographic research is limited by the presence of errors introduced by uncertainties in the satellite position and in the marine geoid. Both uncertainties arise from the fact that the earth gravity field cannot be described sufficiently precise. To fully exploit the altimeter data in oceanographic research, methods have been devised that provide a suitable way to eliminate the radial orbit error of the satellite without eliminating too much of the oceanographic information, and by-pass the marine geoid model inaccuracies.

6.2.1 Orbit and geoid errors

The desired accuracy of the position of the satellite in its orbit is around or better below the altimeter noise level (< 4 cm). Normally, this is not true. Therefore many studies have been performed to improve the orbit accuracy [15,16]. The orbit errors are caused by uncertainties in the earth's gravity field and are concentrated at the zero and once per revolution frequency. One can distinguish several approaches to eliminate or reduce the effect of orbit errors. For ocean variability studies the orbit error can be eliminated quite easily by means of collinear polynomial fitting with respect to a mean track, or better to a reference track [17,18]. In the case of mean sea surface height (or geoid) determination, the orbit error is determined empirically from crossover analysis [4]. Also, in order to circumvent geoid model errors, local differences of altimeter measurements have to be processed. In these differences the time-invariant geoid and semi-permanent dynamic ocean topography contributions cancel. The collinear tracks technique uses the along-track differences from repeated ground tracks, whereas the crossover difference minimization technique uses crossover differences, *i.e.* the differences between measured sea heights at the location where two satellite passes cross.

Applications of these techniques indicate that the relative orbit errors can be removed up to the sea surface variability level. In practice these differencing techniques resolve only relative orbit errors, and therefore still suffer from datum problems. The differences are actually 'blind' for a common error to both measurements. The treatment and interpretation of the datum part of those errors in a global sense is often referred to as 'geographically correlated orbit errors', and has led to a lot of confusion in the literature. Recently, the misconceptions concerning the geographically correlated orbit error have been clarified to a certain extent [19] . Due to this error the resulting mean sea surface is as accurate as the chosen reference gravity field in those wavelengths that cause the major part of the orbit error [20]. Recent orbit computations for TOPEX/Poseidon, which has excellent tracking facilities, indicate that the absolute orbit error has been reduced so drastically, that other error sources like in tidal models have become more dominant. This has turned the TOPEX/Poseidon orbit into a reference for other satellites.

6.2.2 Collinear difference minimization

Sea level measurements along repeated ground tracks of a satellite are aligned at one second intervals measured from the time of the equator crossing. Relative height differences per point between two tracks, or between one track and a mean track are mainly due to relative orbit errors. These errors can be eliminated by removing an estimated first or second order polynomial, or truncated Fourier series. Obviously, it is important to eliminate blunders even though it may seem unnecessary in such a robust problem: thousand or more observations and only a few unknowns. From a w-test, testing the residuals against the a priori point standard deviation, it appeared that for GEOSAT and ERS-1 a reasonable number of blunders should be eliminated. The testing parameter can be found with an α of 1/2m, where m is the number of observations, which is a rule of thumb in deformation analysis. The erroneous data are usually caused by bad correction models such as tides, the ionosphere, or the wet troposphere in equatorial regions, near coasts and near ice. Because this kind of tests is based on normally distributed height differences, sudden sea level anomalies, e.g. caused by an eddy passing one of the satellite tracks, violate this assumption, and may cause biased orbit fits.

The w-test is not always sensitive for such cases, so additional tests have to be done based on Chauvenet's criterion, for eliminating this time variable signal [21]. These tests are performed iteratively to obtain the best orbit error fit, in order to derive from all repeated profiles the optimal mean profile. Clearly, the high frequency sea level variability has to be removed when estimating the orbit error, but need to be taken into account when analyzing the sea level anomalies after the orbit error removal. An other approach is to assign less weight to the along-track differences in the so-called high energetic ocean areas according to an a priori variability model [4].

6.2.3 Crossover difference minimization

In the crossover minimization the orbit error along tracks of up to 10,000 km length can be modeled adequately by a 2nd-order Fourier series whose base frequency is 1 cpr. As indicated earlier the orbit error has a long-wavelength nature: most of its power is clustered around this 1 cpr [20,22]. The parameters of the Fourier series are assumed to be constant along a track. Crossover differences, primarily a measure of the orbit error, are used as observations in the minimization process. Because there are more observations than parameters to be solved the solution is obtained by least-squares minimization. The parameters of each track are simultaneously adjusted such that the overall RMS of the crossover difference residuals is minimized. This crossover minimization does not incorporate an absolute reference for the individual tracks. Because each track is corrected with respect to all other tracks a mean sea surface is obtained that has a number of degrees of freedom. The whole surface in which the tracks lie can be tilted, rotated and deformed; *e.g.* lifting the entire surface by adding a constant to all measurements will not change the crossover differences. So, constraints and/or a priori information are needed. The adoption of the Bayesian weighted least-squares minimization allows the use of a priori values for the parameters to be estimated together with their standard deviations as constraints [18].

To generate the crossover data, pseudo-measurements have to be created at the crossover locations. Basically, this is done in two steps. One that guesses possible crossovers between tracks assuming a circular satellite orbit and taking into account the rotation of the earth. The initial longitude of a crossover is given by the average equator crossing of two crossing tracks. Then, in a Picard-iteration process the crossover location is found (2 or 3 iterations suffice). In the other step the actual crossover data are created by a quick-search (based on the crossover guess) of the 3 measurements on each side of the crossover along a track, by a fit of a cubic spline through the total of 6 measurements, and by differencing the sea heights in the computed crossover point.

6.2.4 Orbit error reduction and gravity model adjustment

Nowadays, orbit accuracies are better than 20 cm rms in radial direction. Taking into account that for wavelengths larger than some 2,000 km the geoid errors are still below the anticipated oceanographic signals, a separation of geoid signal and dynamic sea height is possible. In the so-called integrated approach a selected set of earth gravity model coefficients is adjusted and simultaneously models are estimated for the dynamic ocean topography and for the satellite initial state error (orbit error not due to the gravity model) [23]. The observation equations in this least-squares parameter adjustment are formed by the sea height residuals; *i.e.*, orbit minus altimeter measurement and minus geoid. The adjustment reduces at the same time the errors in the geoid model and in the radial orbit. Again constraints are needed here for the gravity coefficients (based on the variance-covariance matrix of the geoid model), for the dynamic ocean topography coefficients (based on the degree variances of an ocean circulation model or on hydrographic data), and for the initial state coefficients.

The model for the dynamic ocean topography is similar to that of the gravity field; a spherical harmonic expansion. Contemporary geoid models limit this expansion to about degree 20. This means that the smallest wavelength to be recovered in the global ocean circulation is about 2000 km. Such a resolution is sufficient to recover the large subtropical gyres, the eastern and western boundary currents, and the Circumpolar Current. The initial state error model is comparable to the radial orbit error model used in the crossover minimization. It has been extended, though, with the so-called bow-tie effect (typical for orbit integration methods) and terms that absorb resonance not modeled in the gravity model. In the set of parameters to be estimated the first zonal of the dynamic ocean topography model is inseparable from the 1 cpr term of the initial state. Therefore, also the coefficients of the initial state have to be constrained. For instance, by the variance of the a priori orbit error.

6.2.5 Interpolation to equidistant or equiangular grid points

The altimeter data gathered by the satellite are not synoptic, but distributed more or less irregularly in space and time. Altimeter satellites usually encircle the earth in repeat orbits, which results in a sampling of the oceans along repeated ground tracks. Consequently, the sampling density is high along the track but low across the track. Therefore, sophisticated interpolation techniques must be applied to yield a regular distribution in space and time.

Sea height residuals, corrected for orbit error, are transformed to sets of residuals at reference points, also referred to as normal points. All residuals within a 5 km radius from selected locations along the tracks are interpolated to these locations, based on distance weighting. After all the data have been grouped into the normal points, time series of the sea surface height are available in each of these points. Now, the mean sea height and the standard deviation can be computed in each of the normal points. The standard deviation or sea surface variability, gives a measure of the power of temporal changes in the sea surface height. These changes are mainly due to oceanographic phenomena, like meandering currents, the motion of eddies, Rossby and Kelvin waves, etc. When the mean is subtracted from all the data in a normal point a time series originates that reflects the history of the relative sea surface height, also referred to as relative dynamic ocean topography. By interpolating the differences from the mean in time the time series can be obtained at arbitrary intervals.

One of the last steps in the altimeter data processing is interpolating the results, *e.g.*, mean sea heights, relative sea heights, standard deviations, etcetera, to equidistant or equiangular points on a rectangular grid. Most of the data visualization software requires rectangular gridded data. For this purpose two gridding procedures were adopted.

One is objective mapping or Gauss-Markov interpolation, and is frequently used for mean sea surface grids. The shortest wavelength to be recovered from the mean sea surface data is about 30 km. However, the cross-track distance between the data is much larger. In order to map a high frequency signal between the tracks, an interpolation technique is needed that uses additional a priori information on the expected variance of the surface. Objective mapping makes use of the correlation between the measurements and the values at the grid points, not necessarily the same quantity (cross-covariance), and the correlation among the measurements and grid values themselves (auto-covariances). It gives the best linear estimate by minimizing the variance of the difference between the original signal and the signal to be estimated. This requires the computation of the inverse of the combined auto-covariances matrix. The matrix dimensions are determined by the number of measurements. When a geoid model is subtracted, the sea height residuals have characteristics comparable to unmodeled geoid undulations. In this case, the geoid undulation covariance function can be used to approximate the covariances between the sea heights in two points. The covariance then only concerns the commission errors - errors in the model coefficients given by the model covariance - and the omission errors - the unmodeled higher degree part, which is approximated by a gravity model power rule. In this way, short-wavelength features down to some 50-100 km can be recovered, especially when more satellites are combined. The implementation of this method in the software limits the number of measurements, and therefore the size of the grid, because large matrices have to be inverted to solve the normal equations. In practice, overlapping tiles are taken from the total grid and solved separately, assuming that measurements, that are reasonably far apart (> 3°) are uncorrelated.

The objective mapping can be extended to least squares collocation by including functional relations in the covariance functions. This makes it, for instance, suitable for obtaining the function derivative in each point of a grid in one computational step. In general, gravity anomaly grids are computed from the along-track sea height data like this [6]. The same principal is used for computing flow velocity grids from the relative dynamic heights. However, in both examples the proper choice of a covariance model is important. To show this, three different covariance models for the flow velocity have been compared and displayed significant differences in the computed grids. As a matter of fact, the most reliable case did not show much difference with a two dimensional spline interpolation.

The other gridding procedure is based on distance weighting, and is used for grids of sea surface variability and relative dynamic topography. The value in a grid point is the sum of all data in it's vicinity divided by the sum of the weights assigned to the data. These weights are reversely proportional to the distance between the measurements and the grid point. The decorrelation length in the weigh function determines the smallest wavelength to be recovered. The actual implementation consists of several steps. After each step residuals, *i.e.*, data minus grid values interpolated to the data points, are determined and interpolated in the next step with a smaller decorrelation length. The final grid is then the sum of all grids from the separate steps. Usually, three steps suffice. In this manner reasonable short-wavelength features can still be recovered without deforming long-wavelength slopes in the surface (stair-case effect). Also this procedure adequately deals with data gaps by using a high decorrelation-length in the first step.

6.2.6 Ocean tides

In order to study the ocean circulation or more locally currents like eddies and meanders, the tidal contribution need to be removed from the altimeter data. The global ocean tide models used are generally inaccurate in continental shelf areas or in nearly closed seas. From a comparison between the global Schwiderski ocean tide model with the Continental Shelf models of Rijkswaterstaat/RIKZ and Bidston, it could be concluded that the sea surface variability is drastically reduced when the local tide models are applied. Such tide models can even be improved when the altimeter is used as a kind of space-borne tide gauge [24]. Conventional tide gauges are mainly located near the coast, and the altimeter data are a welcome completion for interpolating tides between the individual gauges. At the same time, several studies showed that also global tide models can be improved by including altimeter data. For instance, in the study by Schrama and Ray [25], a joint effort of DUT and NASA, significant errors in the M2 tidal constituent were found and corrected based on TOPEX/Poseidon altimeter data. The main advantage of TOPEX/Poseidon over, for instance, GEOSAT, is the possibility to make a clear distinction between the tidal contribution and oceanographic information, since the tides are aliased at well known frequencies that do not interfere with the oceanographic seasonal and annual cycles. The comparison of the new tide corrections with tide gauge data (mainly for the M2 tide) shows an rms difference of 2.7 cm, whereas older models like Schwiderski or Cartwright/Ray do not get beyond 4 cm. The improved tide corrections allow a better detection and interpretation of oceanographic signals like Kelvin waves, and the annual and semi annual cycles [26].

6.3 Altimetry and oceanography

Quite a lot of oceanographic studies have been conducted in the framework of the Earth Oriented Space Research project. A number of these studies has been joint efforts between DUT and IMAU. In this Section some results will be presented covering several regions of interest, like the oceans around South Africa, and the North Atlantic Ocean. Next to these local studies, also some global studies will be discussed.

6.3.1 Ocean variability methods

Because several different methods circulate for determining ocean variability from satellite altimetry, the quality of variability results had to be established first [8]. For this purpose one year of Geosat altimeter data was used in order to compare three processing techniques for the determination of mesoscale ocean currents. Clearly, this is of importance, since observations like sea surface variability and relative sea height time series yield a valuable contribution to all kinds of oceanographical studies. In summary, the study gives an a priori estimate of the feasible spatial and temporal resolutions of the data by validating the techniques and comparing the results. The correlation between the different sea surface anomaly field solutions appear to be considerably high. The overall quality of the results obtained depend on the power of the sea level variability and therefore on what area is considered. For instance, for the Agulhas Retroflection area it was found that the rms difference of the relative sea level grids amounts up to only 4 cm, and that on the average the correlation is better than 0.90 (±0.04). The non-isotropic behavior was also studied in detail by analyzing the signal-to-noise ratio for two extreme sampling cases, *i.e.*, a quiet area, and a noisy area. Obviously, the best results are obtained when the variations in sea level are strong.

6.3.2 Oceanographic results around South Africa

Figure 6.1 shows a shaded image of a mean sea surface model computed from one year of GEOSAT altimeter data (July 1987 through July 1988), covering the South Atlantic and South Indian Ocean (top). Also shown is the associated standard deviation or sea surface variability (bottom). It will be clear from this figure that the mean sea surface, on this scale equal to the geoid, is correlated with ocean bottom topography. Most of the major ocean ridges left their signatures in the sea surface; *e.g.* the Ninety-East Ridge, the South-East and South-West Indian Ridge, and the Mid-Atlantic Ridge with the Falkland and Rio-Grande fracture zones. Also smaller features like seamounts and plateaus are represented: *e.g.* the Discovery Tablemount, the Meteor Seamount, the Schmitt-Ott Seamount, the Kerguelen Plateau, and the Agulhas Plateau. The high levels of variability are caused by changes in the position of the Agulhas Current and the Agulhas Retroflection Front, by moving eddies, and by meandering of the Agulhas Return Current. This meandering is a result of the interaction of the currents with bottom topography, especially the Agulhas Plateau, and the variation of the Coriolis force with latitude. A similar reasoning applies to the East Madagascar Retroflection and Madagascar Return Current. Here eddies are produced, which enter the Agulhas Current along the African coastline. Two branches of variability can be noticed west of South Africa in the vicinity of the Walvis Ridge stretching out to the Mid-Atlantic Ridge. This is due to the westward motion of large anticyclonic eddies that were shed from the Agulhas Retroflection Front.

To study the mesoscale currents in detail, GEOSAT relative dynamic sea height grids have been converted to relative flow field grids by imposing geostrophic equilibrium, *i.e.*, the Coriolis force (rotating earth!) balancing the surface pressure gradient or the sea surface gradient. Vector plots of the relative flow field, representing flow magnitude and direction, allow detection, qualification (cyclonic or anticyclonic motion) and quantification (swirl velocity) of coherent structures, such as eddies and current meanders. The motion of these structures can be followed in time when a time series of vector plots is studied in detail.

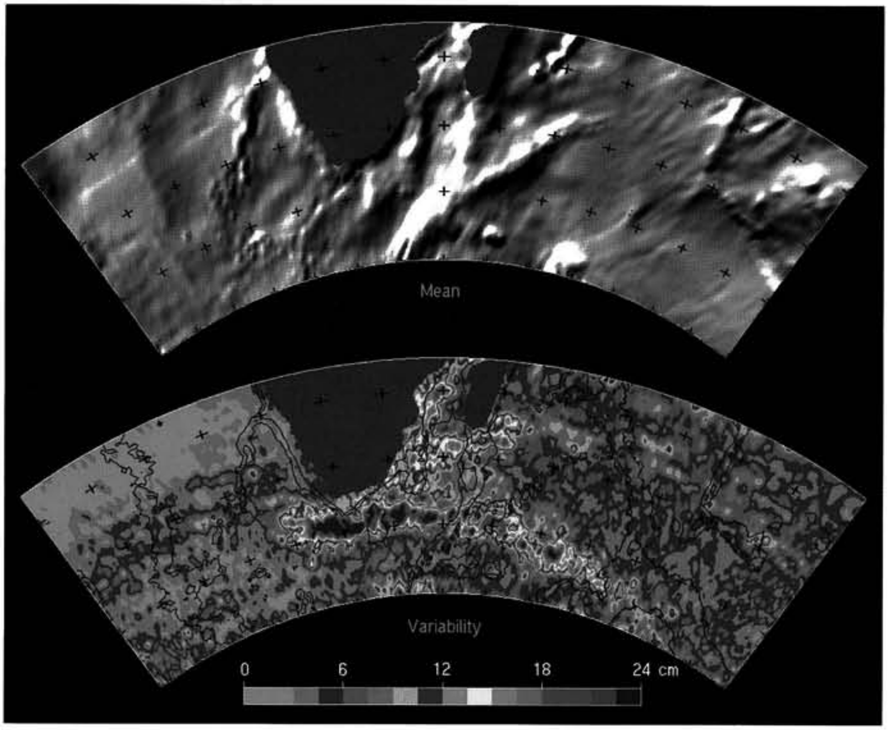

Figure 6.1 GEOSAT Mean sea surface (top) and sea surface variability (bottom) covering part of the South Atlantic and Indian Ocean.

This procedure was adopted for the eastern part of the South Atlantic ocean. A considerable number of anticyclonic and cyclonic mesoscale ocean features were detected and found to be moving in a general westward direction. The diameter of these eddy-like features range from some 100 km to 350 km. Figure 6.2 shows the established trajectories of 13 large eddies, of which most are anticyclonic. Also drawn are the 2000-m and 3500-m isodepth contours.The beginning of each trajectory is indicated by a large circle and the plotted dots represent successive eddy locations separated by 10 days. Open dots indicate cyclonic motion and solid dots anticyclonic motion. For the southern hemisphere an anticyclonic motion is associated with a counterclockwise rotation. From ship CTD (Conductivity, Temperature and Depth) measurements it was demonstrated that eddy "A" is a typical Agulhas eddy originated from the Agulhas Retroflection area [27]. Agulhas eddies are generated south of South Africa by a temporarily short-circuited Agulhas Retroflection; the most western part of the Retroflection is cut-off and becomes an independent anticyclonic ring-shaped current system. A comparison with Figure 6.1 (bottom panel) confirms that the trajectory of eddy "A" falls within the most northern branch of increased variability, that stretches out to the Mid-Atlantic Ridge.

A computer animation of the relative dynamic ocean topography time series has enabled us to visualize the temporal evolution of the mesoscale ocean currents in this region, and to study the eddy/eddy interaction and eddy/bottom-topography interaction effects, as well as the effect of bottom topography on eddy trajectories [28].

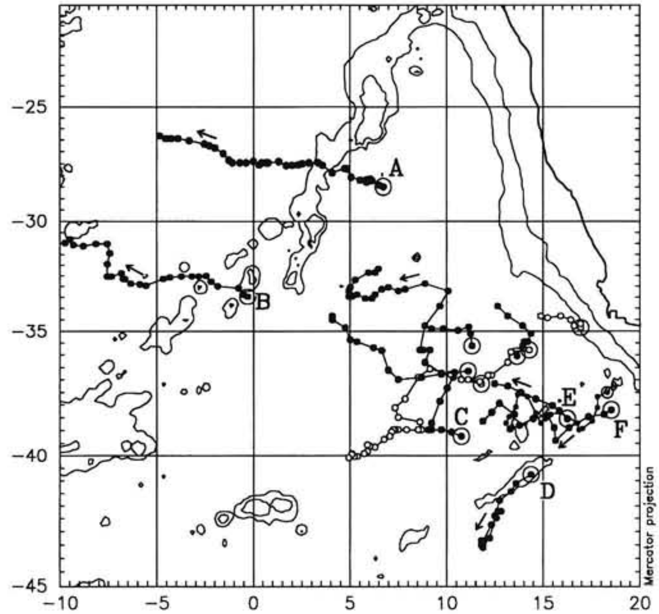

Figure 6.2 Eddy trajectories in the South-east Atlantic as deduced from GEOSAT altimetry.

Some eddy characteristics have been plotted in Figure 6.3 for two anticyclonic eddies in the South-East Atlantic. Presented are the translation velocity and the swirl velocity histories, for eddy "A" (left) and eddy "D" (right). Eddy "A" has a mean translation velocity of 4 cm/s. The regression line through the velocities of both eddy "A" and "D" suggests a gradual decay of the eddies. This might be due to internal friction, exchange of heat with the atmosphere, or interaction with the main flow. A rough estimate of the eddy's lifetime can be obtained by extrapolating the regression line. For instance, eddy "A" should live for about two years, which is sufficient to allow it to cross the entire South Atlantic and to reach South America, where it may be absorbed by the Brazil Current. Such a long lifetime indicates that the eddy motion is quasi-two-dimensional, rather than three-dimensional. Remarkable is the relatively low swirl velocity, and therefore smaller gradients in the relative dynamic sea surface topography, when eddy "A" moves over the Walvis Ridge and the water column beneath decreases. This is likely to be associated with a temporarily increase of eddy radius to conserve angular momentum.

Most of the detected large anticyclonic eddies have their origin in the Agulhas Retroflection and enter the South Atlantic at a rate of about 8 eddies per year, carrying a large amount of warm Indian Ocean water. Evidently, they play a key role in the dynamics and the heat budget of the South Atlantic. In general, these Agulhas eddies pass north of the Schmitt-Ott seamount and Cape Rise, but some have a more southwest trajectory and cross the subtropical convergence. The Cape Basin is found to be an area with a dense population of cyclonic and anticyclonic eddies that seem to interact. North of 35° South these eddies generally move with an average translation velocity of 5 cm/s in a westward direction and many have to cross the Walvis Ridge. The ocean bottom topography, in particular that of the Walvis Ridge, plays an important role in the eddy motion and eddy behavior. It seems that the eddies have preferential trajectories over the deeper parts of the Walvis Ridge, which was already observed from Figure 6.1 (bottom panel) and Figure 6.2.

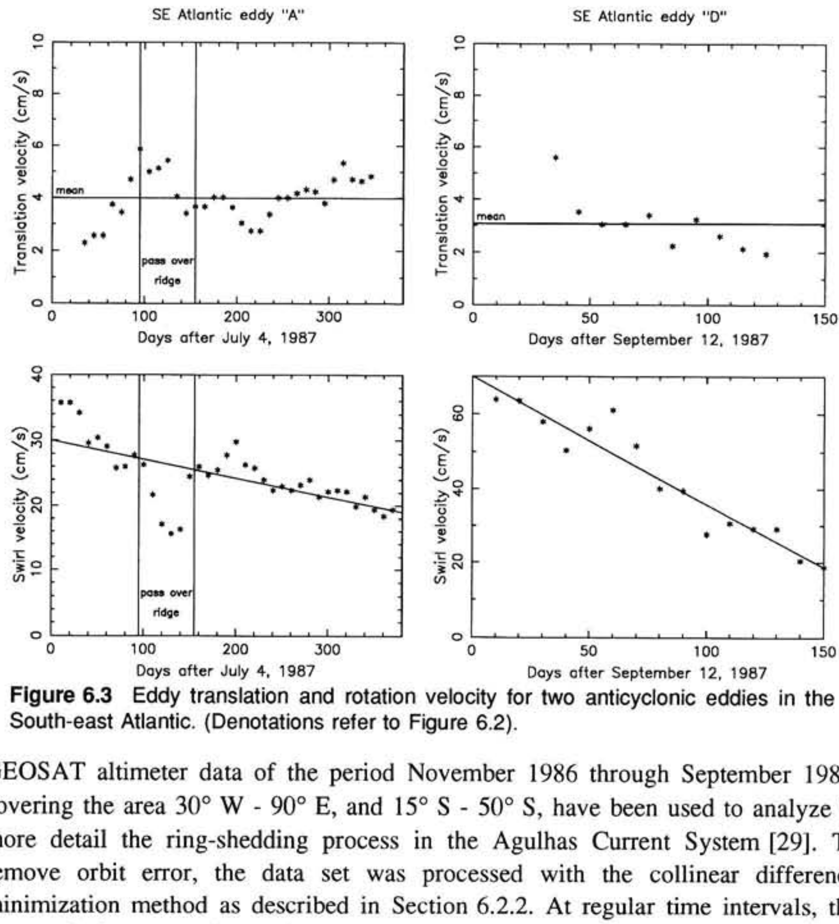

Figure 6.3 Eddy translation and rotation velocity for two anticyclonic eddies in the South-east Atlantic. (Denotations refer to Figure 6.2).

GEOSAT altimeter data of the period November 1986 through September 1989, covering the area 30° W - 90° E, and 15° S - 50° S, have been used to analyze in more detail the ring-shedding process in the Agulhas Current System [29]. To remove orbit error, the data set was processed with the collinear difference minimization method as described in Section 6.2.2. At regular time intervals, the corrected data were interpolated to rectangular grids of 1°× 1°, using objective mapping. Figure 6.4 presents the power density spectra of the temporal variations in the relative sea height for an active area (AR = Agulhas Retroflection) and a quiet area (SA = South Atlantic). These spectra were calculated for each grid point available in an area and averaged. The *stdev* or the standard deviation represents the variation per spectral component. The South Atlantic results are multiplied by 10 for a better visualization. The Agulhas Retroflection spectrum (AR) shows two peaks around 11 and 14 weeks. In order to investigate the origin of these peaks, especially in relation to the ring-shedding process, a combination of different statistical tools is needed. For this reason, the harmonic analysis and principal component analysis techniques were adopted to extract the characteristic frequencies in the Agulhas Retroflection from the 3 years worth of GEOSAT data.

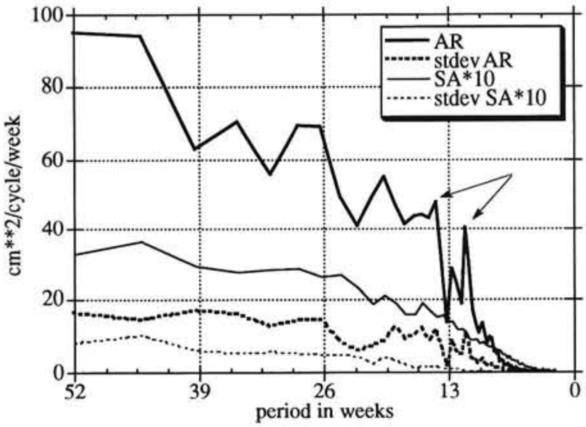

Figure 6.4 Power density spectra and standard deviations of the relative sea height time series in the Agulhas Retroflection (AR) and in the Southern Atlantic (SA).

The analyses indicate that 11 or 12 dominant events took place over the 3-year period. The number of events vary from year to year. February, March, and April (austral summer/autumn) are identified as anomalous months in which the relative sea height signal is not as well defined as in the other part of the year. It can be shown that the first three modes of variability (explaining 25%, 20%, and 12% of the variance, respectively) are dominant. The structure of the spatial and temporal scales leads to the hypothesis that these modes are to be associated with periodic Agulhas front movements, culminating in the formation of the Agulhas rings. Sharp changes (pulses) in the stability of the sea level pattern give an indication of the time a ring is pinched off. A number of 18 (±2) pulses over the 3-year period was found in which an anomaly in the average decorrelation time occurred. If these pulses really can be attributed to the formation of Agulhas rings, they are of great importance in the study of the large-scale circulation, because these rings contribute significantly to the energy and freshwater flux between the Indian Ocean and the South Atlantic.

The next logical step in analyzing altimeter data is to compare the results with the results from analyzing a contemporary oceanographic model. The ocean variability in the major western boundary current systems of the Southern Ocean was studied by comparing results from the United Kingdom Fine Resolution Antarctic Model (FRAM) to 3 years worth of GEOSAT data [30]. For this purpose, several analysis techniques, like harmonic analysis, principal component analysis, and principal oscillating pattern analysis, were applied to both the modeled sea levels and the *real* *ocean* altimeter data. The results from the analysis of the altimeter observations were verified, and the interpretation of the GEOSAT data in the three southern ocean western boundary systems could be improved significantly.

The hypothesis that ring formations can be catalogued and studied from variations in the decorrelation time of successive sea level anomaly fields, is confirmed by FRAM. Applying the techniques to altimeter data of the Agulhas, Brazil/Malvinas, and East Australian Currents showed that regular ring formations take place, roughly every 100, 150, and 130 days, respectively. The first period is close to the empirical value of 14 weeks shown in Figure 6.4. FRAM only generates periodic ring formations in the Agulhas and East Australian Current, both with a very regular 125-130 days period. This period is clearly a model favored harmonic (1/3 year) which is however sufficiently close to the *ground-truth* altimeter observations.

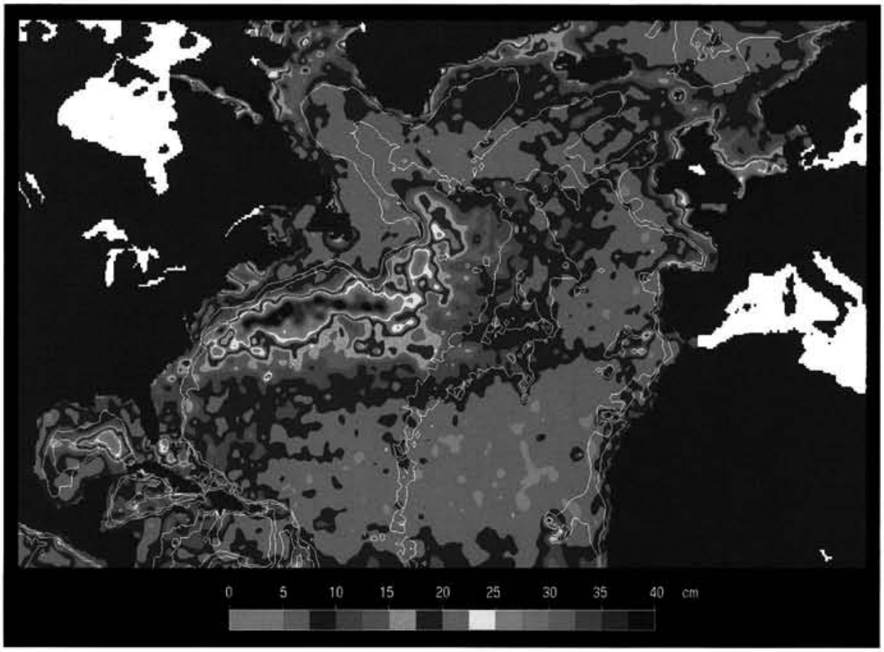

Figure 6.5 Sea surface variability in the North Atlantic as computed from two years of GEOSAT data.

6.3.3 Oceanographic results of the North Atlantic

Figure 6.5 shows for the North Atlantic the sea surface variability computed from 2 years of GEOSAT data (November 1986 to November 1988). It ranges from 6 cm in the Atlantic Basin, west of Africa, to about 40 cm in the Gulf Stream and Gulf of Mexico. The highest variability levels can be associated with the shifting positions of the core of the Gulf Stream and Gulf Stream Extension, and the formation and motion of Gulf Stream eddies. These eddies are pinched off from Gulf Stream meanders both to the north (anticyclonic: warm-core) and to the south (cyclonic: cold-core). High variability is also found where the cold waters of the Labrador Current interacts with the warmer Gulf Stream water. Remarkable is the fact that almost no variability exists over the Grand Banks, which indicates that the motion of eddies here is confined to the deeper parts of the ocean.

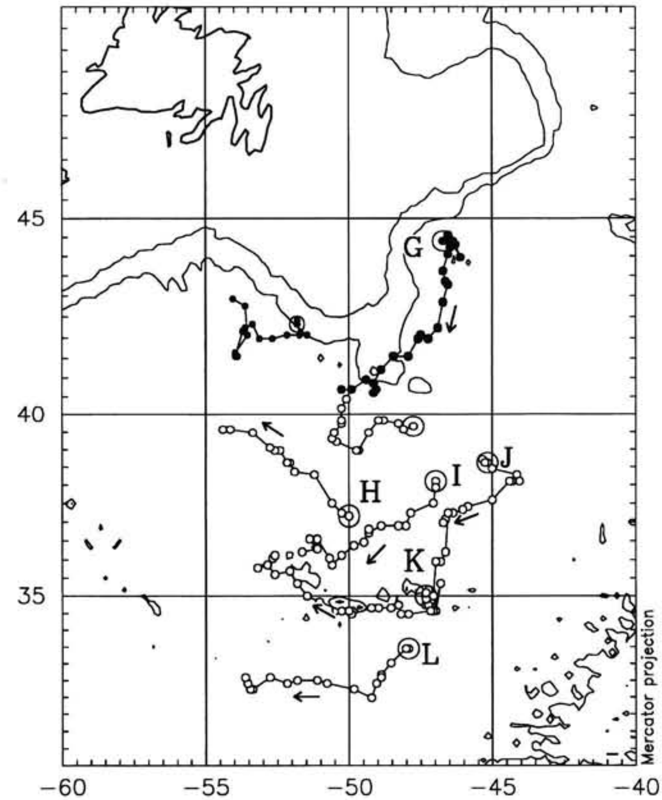

Figure 6.6 Observed eddy trajectories in the North-west Atlantic from GEOSAT data.

The variability associated with the Gulf Stream seems to bifurcate southeast of the Grand Banks. One broad branch extends to the southeast, a narrower and more energetic branch of variability extends northward. The southeastward branch consists of a recirculation component which flows back along the Gulf Stream itself and an eastward component extending over the Mid-Atlantic Ridge south of the Azores feeding the Canary Current. The activity in this area may be caused by the propagation of Rossby waves. The high levels of sea surface variability that occur in a band between Scotland and Iceland were at first thought to be due to the shifting positions of the thermal front between the Arctic and Atlantic waters. Analyzing time series of the differences from the mean sea surface, based on GEOSAT data, learned that a strong semi-annual signal is present in this area, which was identified as a M2 tide error aliased close to the annual cycle. Tide modeling errors also are to be expected in shallow waters, for instance near the British and northern Canadian isles and in the North Sea.

For the western part of the North Atlantic time series of the relative flow field were computed from the GEOSAT data and the resulting grids were studied in detail. Figure 6.6 shows the observed trajectories of 6 large cyclonic and 2 large anticyclonic eddies. The eddy diameters range from 50 km to 250 km. Apparently, the motion of these Gulf Stream eddies is generally westward. At first sight this might look a bit strange, because the main stream flows eastward. However, it is in agreement with fluid dynamics [31] and this behavior has already been observed from drifting buoys and infrared images. The lifetime of the observed Gulf Stream eddies is rather short. It was found that most of the eddies are absorbed again by the Gulf Stream after a few months. Typical translation and rotation velocities that have been found are 4 cm/s and 30 cm/s, respectively. Unlike the behavior of the above-mentioned Agulhas Eddies, there is no clear decay in time; eddy "G" was even found to gain vorticity. This must be due to interaction with Gulf Stream meanders. No evidence was found for a correlation between eddy translation velocity and rotation velocity. Although, in theory there should be a correlation, this result was not surprising, because the eddy propagation depends on the eddy behavior itself (vorticity, merging, instability, pulsation, nutation, Rossby wave generation, etc.), on the influence of the surrounding fluid, and on the presence of ocean bottom topography.

The same kind of analysis was repeated when ERS-1 became available and resulted in similar results. Figure 6.7 presents a relative flow field for part of the North Atlantic on 24 June 1992 (left panel). The *z*-component of the rotation of the velocity grid, also referred to as relative vorticity, is plotted in the right panel. The contour interval is $0.2 \times 10^{-5}\ s^{-1}$, and the dashed lines indicate negative vorticity, and the solid ones positive vorticity. In these figures one can quite easily identify a number of cyclonic and anticyclonic features such as Gulf Stream rings and meanders.

To study spatial scale characteristics of the sea surface currents in the North Atlantic, mean wavenumber spectra were derived from 5 months worth of ERS-1 data. For two $15° \times 15°$ areas, one representing an energetic area (Gulf Stream area) and one representing a less energetic area (Azores area), spectral analysis was performed on the relative sea heights in the normal points along each track passing the area. This was done for ascending and descending tracks separately. However, the difference between the two did not reveal any significant anisotropic effects, and the results were combined. Figure 6.8 presents the spectra for the two areas. For both areas a white noise level of approximately 300 cm^2/cycle/km ($\approx$ 5 cm) is found for wavelengths below some 50 km. Interesting differences, however, are to be found in the red part of the spectrum between 80 and 500 km wavelength. The difference in the spectrum slope indicates a difference in the mechanism of eddy energy

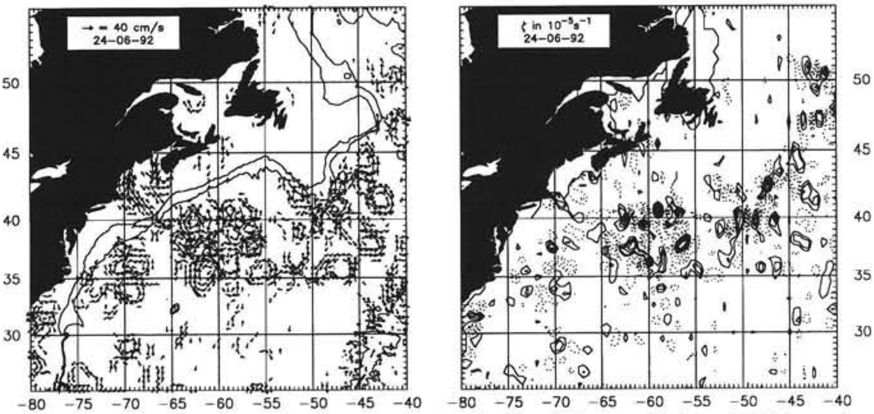

Figure 6.7 Relative flow field (left) and relative vorticity (right) on 24 June 1992 based on ERS-1 data.

generation. In the Gulf Stream area a possible mechanism is the instability of the mean currents causing turbulence, whereas in the Azores area a more plausible mechanism is wind forcing.

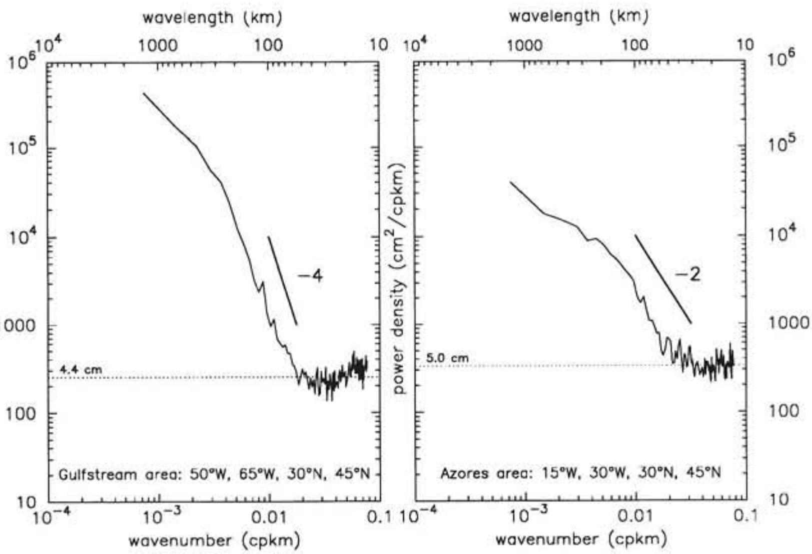

Figure 6.8 Spatial power density plots for two areas in the North Atlantic based on ERS-1 data.

6.3.4 Global oceanographic results

A mean long-wavelength dynamic ocean topography model is shown in Figure 6.9 on page 86. It is based on the first ten 10-day repeat cycles of the TOPEX/Poseidon mission. For every cycle a spherical harmonic model of the semi-permanent dynamic ocean topography up to degree and order 20 was computed using the integrated approach mentioned in Section 6.2.4. The constraints applied to the models come from the degree variances of the Levitus model which is based on 75 years of hydrographical data. This forces the solution to be close to zero over land. The mean dynamic topography, computed from the ten individual solutions, was mapped on a globe and is viewed here from four different angles. Bearing in mind that the water flows along the lines of constant height (similar to the atmosphere, where wind blows along lines of constant pressure), we notice many known features of the global ocean circulation like the Circumpolar current and the western boundary currents: the Gulf Stream in the Northwest Atlantic, the Kuro Shio in the Northwest Pacific, the Agulhas Current in the West-Indian Ocean, and the Brazil Current in the Southwest Atlantic.

When time series of such dynamic topography models are studied, the evolution of currents can be monitored and ocean phenomena like El Niño can be observed. For this purpose computer animations out of sequences of the dynamic ocean topography were made. In addition, secular changes in the first parameter of the initial state error or bias give insight in changes in global sea level. It will be clear, that one must be very cautious in choosing the different constraints to stabilize the solutions, if phenomena are studied that have an amplitude of a couple of centimeters. Also a better a priori gravity model or a more precise satellite orbit is a prerequisite; better than 5 cm, the challenge for the near future.

Recently, another study was performed to obtain the mean dynamic topography from horizontal eddy fluxes derived from altimeter measurements [32]. A method based on the quasigeostrophic instability theory [33] was developed to estimate the mean topography from its observed fluctuations in time or temporal variability. Basic turbulence closure (K-theory) was applied to express the unknown mean relative vorticity gradients in terms of relative vorticity fluxes. The mean potential vorticity can than be calculated, from which the mean topography can be derived. For the boundary conditions an a priori mean topography model like Levitus' model can be used. In contrast to the previous method it is possible to arrive at a higher spatial resolution for the mean topography. Subsequently, this field can be merged with the eddy field, *i.e.*, relative dynamic topography, to be able to derive the total geostrophic surface velocity field. In this manner a rigorous improvement in oceanographic interpretation of the ocean dynamic topography can be achieved. At the same time, due to a better knowledge of the ocean circulation, an improvement of geoid models in the wavelengths between 200 and 2000 km is expected.

6.4 Altimetry and gravity field research

Figure 6.10 shows for the North Atlantic a mean sea surface model illuminated from the northwest. This model is based on five months of ERS-1 data (8 April to 19 September 1992). Areas with no data or data over land are coded black. Because of the dense pattern of the ERS-1 satellite ground tracks the spatial resolution is very high and many bathymetric features can be identified in more detail than from a 3-years averaged GEOSAT mean sea surface. The steep edge of the American Continental Plateau can be seen all along the American East Coast, from the Grand Banks of New Foundland to the Puerto Rico Trench. Evidently, islands (Bermuda, Canary Islands, Azores, Cape Verde Islands) on the tops of largely submarine mountains cause the sea surface to sloop. Also submarine mountains at large depths, such as the New England Sea Mount Chain can be seen in front of the American coast near New York. The depth of the mountain tops varies from 1500 to 2500 meters in the 5000 meter deep North American Basin.

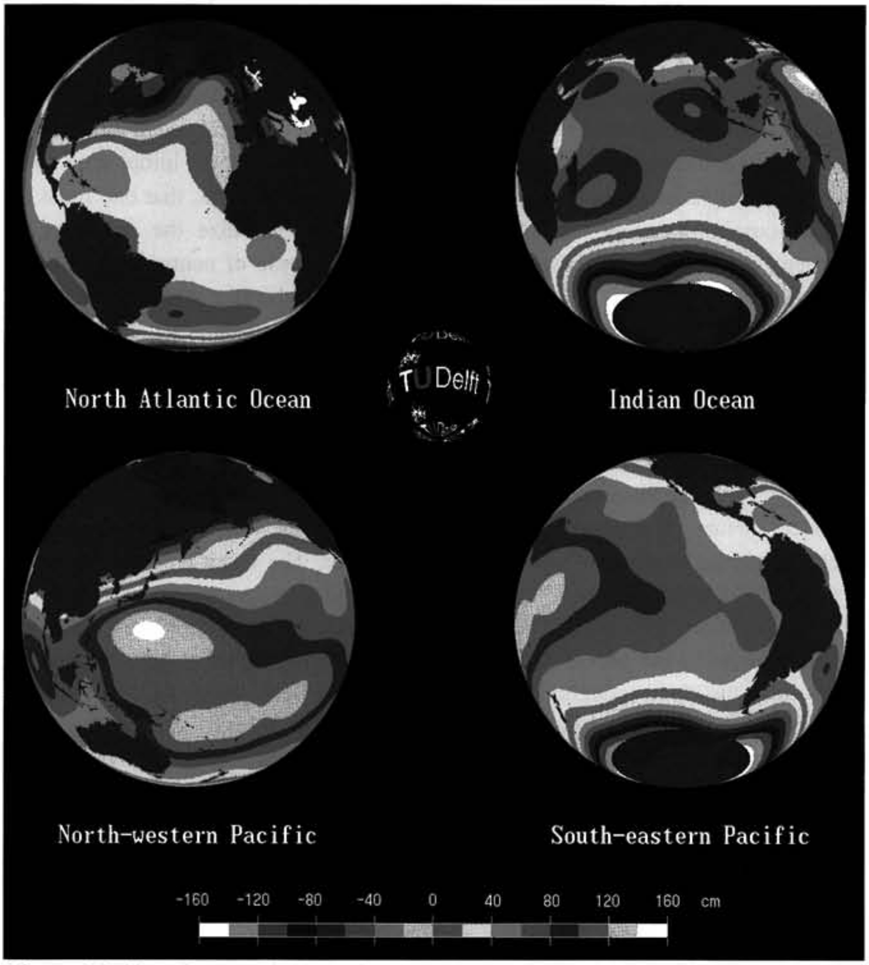

Figure 6.9 Mean large-scale dynamic ocean topography model based on TOPEX/Poseidon data. The model is viewed from four angles.

The most striking feature is the Mid-Atlantic Ridge running vertically through the picture from Iceland down. Clearly, the ridge is intersected by many fracture zones. The largest of them, the Gibbs Fracture Zone, splitting the Reykjanes Ridge from the rest of the Mid-Atlantic Ridge, runs all the way from the Labrador Sea to the edge of the European Continental Shelf. Apparently, the fracture zone is rather wide and has a U-shaped cross-section. Apart from the smaller Oceanographer and Atlantis Fracture Zones, the Cape Verde Fracture Zone is quite interesting, as it appears to have a very fine extension throughout the Cape Verde Basin. There is also a noticeable difference in the texture between the rough mountainous areas and the smooth 5000 to 6000 meter deep Canary, Cape Verde and North American Basins. Even the Bermuda Rise seems to be more rough than its deeper surroundings. Moreover, the Reykjanes Ridge seems to have a structure which is quite unlike the rest of the Mid-Atlantic Ridge.

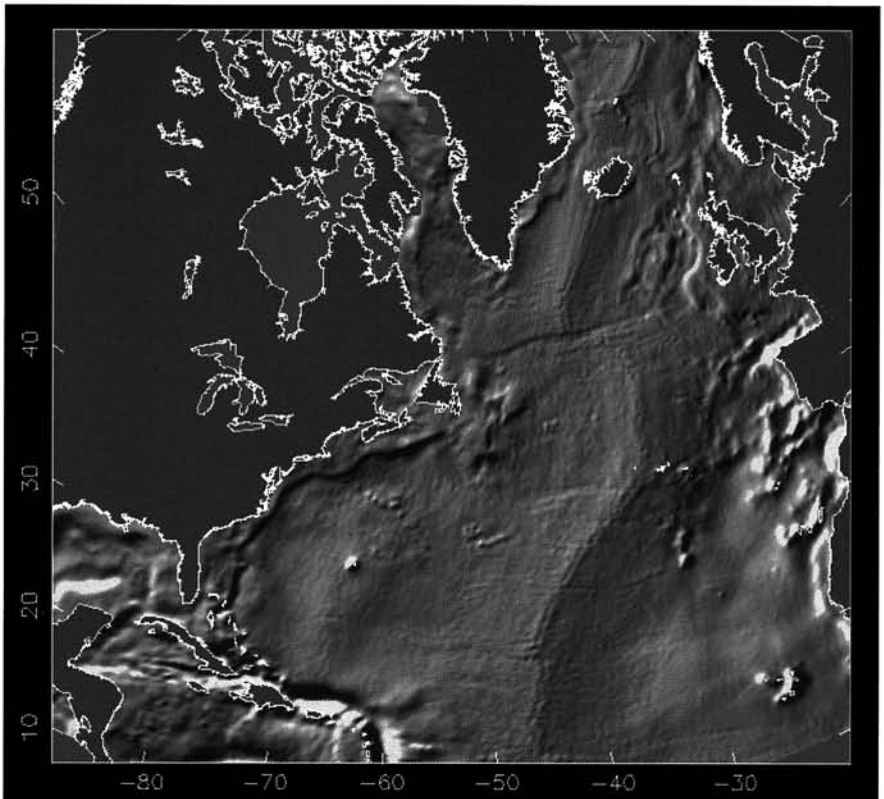

Figure 6.10 ERS-1 Mean sea surface covering the North Atlantic Ocean.

Another region of interest is the North Sea; a relatively shallow sea surrounded by land masses, covering part of the European Continental Shelf. Altimeter data from three satellites have been combined and processed through crossover difference minimization; *i.e.*, three years of GEOSAT data (Nov. 1986 - Nov. 1989), more than one year of ERS-1 data (April 1992 - June 1993), and 7 months of TOPEX/Poseidon data (September 1992 - April 1993). The combination of the data resulted in a very dense network of satellite ground tracks, and therefore a very high spatial resolution of sea height measurements. In addition, the large number of tracks resulted in a large amount of crossovers. It will be clear that this is beneficial for the least-squares minimization. The applied tide model is a local model for the North-east Atlantic and North Sea, obtained from the Proudman Oceanographic Laboratory [34].

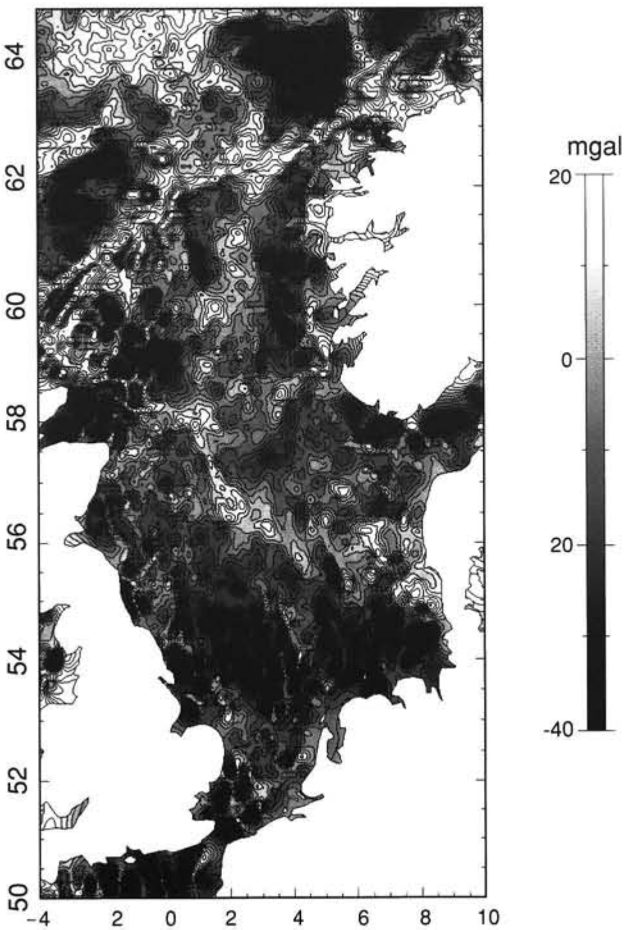

Figure 6.11 Gravity anomaly map of the North Sea as computed from GEOSAT, ERS-1 and TOPEX/Poseidon altimeter data. Contours plotted at 5 mgals interval.

Figure 6.11 gives a gravity anomaly map of the North Sea. It was computed from the mean sea heights at the normal points as discussed in Section 6.2.5, by applying the functional relation between geoid and gravity anomaly in the objective mapping scheme. A comparison with a map based on ship gravimetric data shows excellent correspondence. As a matter of fact, due to the dense coverage of the altimeter data more detail is obtained from the altimetric gravity. It is interesting to know that the bathymetry is quite flat in this area, which means that most of the undulations we see in Figure 6.11 are due to mass fluctuations beneath the ocean bottom. When the mean sea surface is compared with a geological map of the same area, a correlation with geological structures that were formed several million years ago is noticed. Visible are, for instance, some faults like the Horn Graben, the Central Graben and the Viking Graben. These faults were later filled with sediment and can therefore not be detected from bathymetry only. However, also a few bathymetric features are present like the Grandpian High, The Ringkobing-fyn High, and the Brabant Massive.

For the gravity field research, also other techniques have been developed that create grids of geoid heights and gravity anomalies from the altimetric sea heights [35]. At first, these developments were based on the inverse Stokes' formulation in combination with an appropriate interpolation method. Later, it seemed more profitable to obtain the along-track first derivatives of the potential and combine those to gravity anomalies by means of an inverse Vening Meinesz formulation [36,37]. Both methods rely on a proper evaluation of the integral equations and on a sensible choice of a prediction technique. The evaluation should, in principle, be carried out over the entire world, but in practice it is restricted to regional or even local computations. That the prediction technique is very important is due to the specific spatial sampling characteristics of the altimeter: a high resolution along-track, but low in cross-track direction. To exclude the subjectivity of *objective* interpolation techniques, we tried to extract information about the vertical component of the gravity field in an alternative way.

In theory the vertical component can be deduced from along-track second derivatives of the geoid profiles. The combination of two orthogonal horizontal components at a crossover point yields the gravity gradient through Laplace's formula [38]. The satellite tracks at a crossover do not intersect orthogonally, so that Laplace's equation for a local oblique frame has to be used. This means the inclusion of two additional terms consisting of cross components depending on both directions, and a factor depending on the angle of intersection. The theoretical framework of this method is rather simple being based on this local formula. This in contrast to the methods mentioned before. Furthermore, no gridding or interpolation is involved. The pointwise evaluation at the crossovers is advantageous near coasts and in closed basins, where conventional two-dimensional integration techniques fail, and also in case data from different satellites are combined. Nevertheless, not the gravity anomaly is obtained but the vertical gravity gradient which cannot be compared directly with ship gravimetric data. So, the anomalies have to be derived in a additional step, if desired.

To validate the implementation of the method and to show its feasibility, a first test with SEASAT data was carried out. Since in each differentiation step the noise is amplified, a proper filter has to be chosen. For this purpose, Fourier techniques, with simple differential operations and filters in the frequency domain, and smoothing splines, with the best approximation properties, have been tested thoroughly. This resulted in a preference for optimal smoothing splines, because point standard deviations and non-regular data sampling can easily be included, and a continuous smoothed function value, its first and second derivative, can be extracted at every point. In addition, no trends have to be removed and restored like in discrete Fourier transformations.

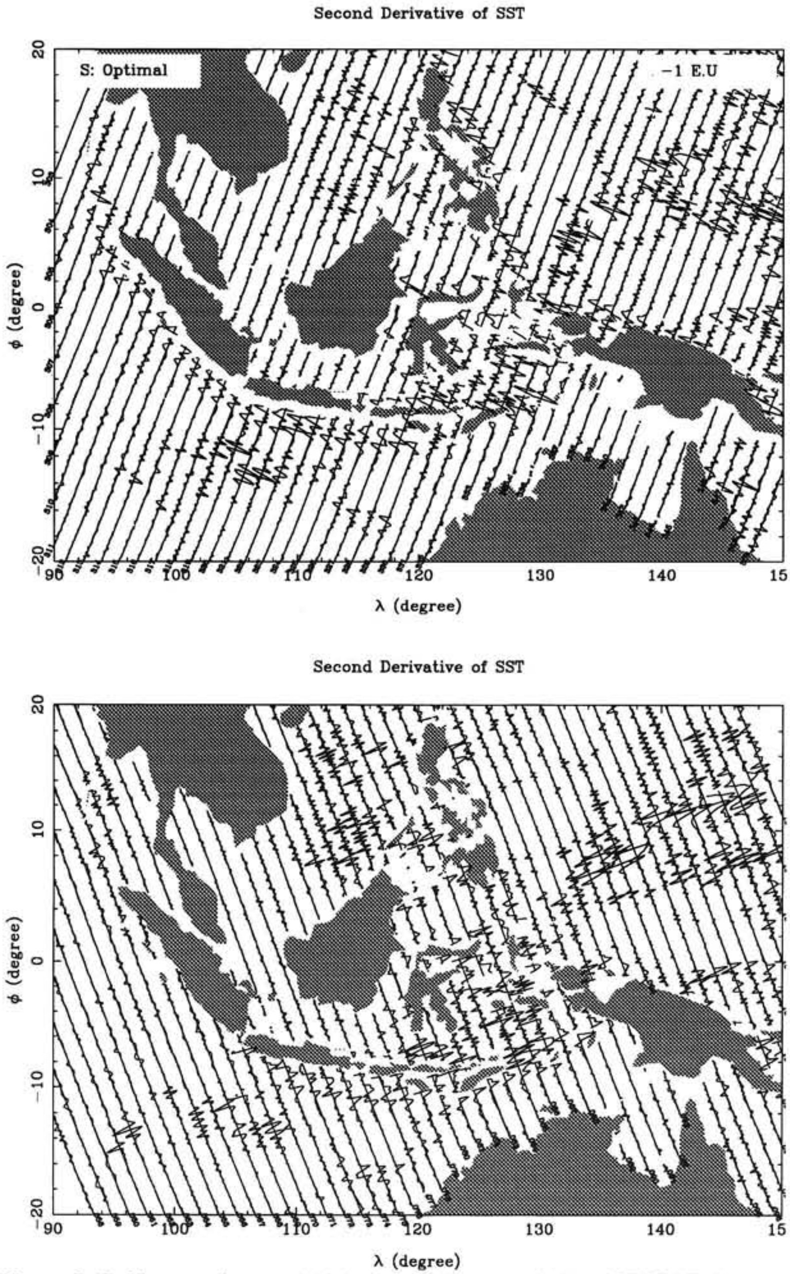

Figure 6.12 Along-track second derivatives of the potential from GEOSAT altimeter data (top: descending tracks, bottom: ascending tracks).

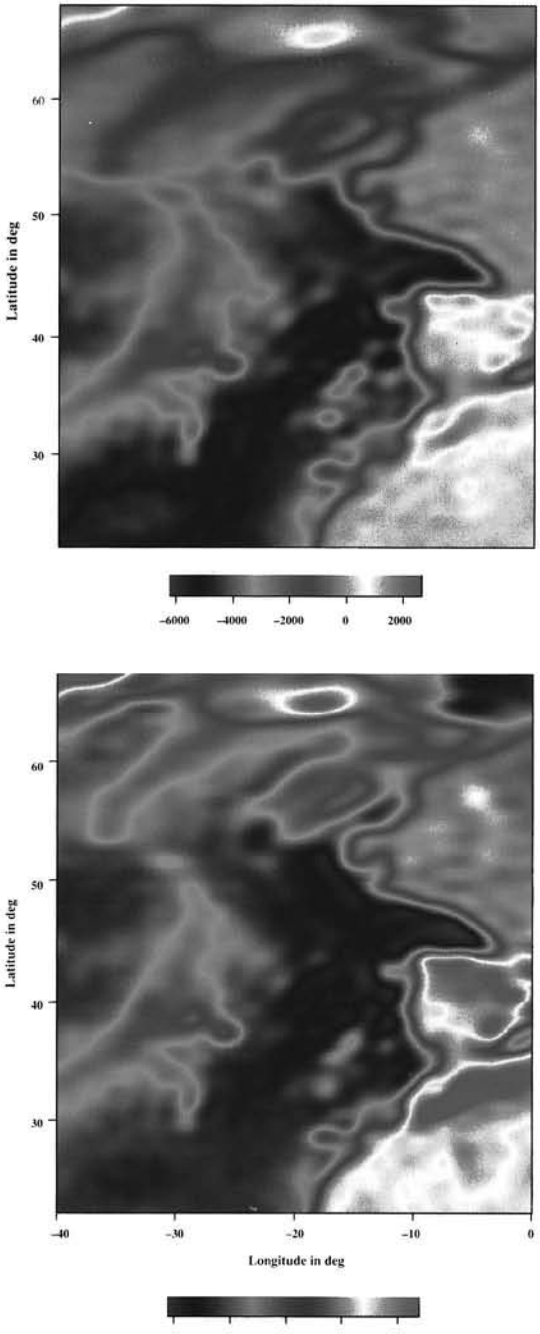

Figure 6.13 Topography and bathymetry in m. (top) and its topographic-isostatic contribution to the geoid in m. (bottom).

The degree of smoothing for every individual sea height profile is determined by the method of Generalized Cross Validation (GCV) as proposed by [39]. A first simple implementation of the iterative search for the minimum of the GCV function, which corresponds to the optimal degree of smoothing, appeared to take up far too much computer time. Therefore, the implementation was optimized using a *moving inverse* instead of the real inverse. This approximation has led to a 30 times faster algorithm with a maximum deviation of 0.001 in the smoothing parameter, which generally lies between 0.5 and 1.5 for altimetry. The associated maximum change in the along-track second derivatives is 0.02 E (1 E = $10^{-9}/sec^2$), which is negligible compared to the overall precision of the computation of 0.9 E. The GCV procedure appears to be rather sensitive for blunders in both data and standard deviations, so that six more or less robust tests had to be designed to eliminate those erroneous data. A practical drawback of smoothing splines is that originally no error propagation was available. Therefore, we developed and implemented this error propagation ourselves [40].

After the test with SEASAT data, GEOSAT data, covering the Indonesian Waters, were processed. Per individual track 3-5 % of the observations was rejected. This number seemed to be correlated with the percentage of surrounding obstacles along-track, like islands. Obviously, islands have an influence on various corrections, like humidity, pressure, temperature or tides. From 3 years worth of data we derived, along-track, the mean sea height profiles, the deflections of the vertical, and the second derivatives. The relative precision of these quantities is estimated at, respectively, 1.7 cm, 0.5 μrad (≈ 0.5 mgal), and 0.9 E. The results for the second derivatives for ascending and descending tracks are shown in Figure 6.12. Due to the nature of the second derivatives, displaying only local variations of the gravity field, one can easily recognize the signature of the deep trench south of Java. The trench is more distinct in the descending tracks since these cross the trench almost perpendicular. The repeatability of yearly averaged profiles can be examined from the difference between the years and the point precision. It appeared that the differences between the mean sea surfaces, the first derivatives, and the second derivatives remain within a $\pm$ 1.95σ error margin. Details preserved in the second derivative reflect information from all wavelengths of the gravity field down to 22.5 km where the signal to noise ratio becomes one. This indicates that the method is capable of filtering the signal adequately to obtain good signal to noise ratio for mean sea surface heights, mean first and second along-track derivatives. At the same time, it is able to preserve as much signal as possible, even in the high frequencies.

In cooperation with Norsk Hydro Research Centre one year of ERS-1 35-day repeat data have been processed to obtain gravity gradients in the Barents Sea in a similar way. The high inclination of the ERS-1 orbit offered the unique possibility to study an area that was not yet covered by other altimeter satellites. The average precision of the computed mean sea height profiles could be estimated at about 4 cm, whereas the vertical deflections have a precision of about 1.2 μrad, and the second derivatives of 2.1 E. The difference in quality between the GEOSAT and ERS-1 results can be explained by the difference in the number of repeated tracks. The ratio of the empirically determined variances of the combinations N_{xx} and N_{yy}, and N_{xy} and N_{yx}, and of N_{zz}, follows largely the theoretical rule from gradiometry. For the sake of completeness; N represents the geoid height, and subscript xx the d/dx^2, and so on.

Finally, to study geology from the gravity field quantities as computed from altimeter data, a first attempt was made to model the anomalous potential field, and the corresponding attraction, solely caused by the isostatically compensated bathymetry, according to a Airy-Heiskanen isostatic model. Newton's law of attraction was evaluated in terms of spherical harmonics representing the so-called equivalent rock topography. This corresponds with topography on land and bathymetry at sea, where the sea is filled with solid rock so that equal rock density is used on land and sea. An expansion based on this equivalent rock topography and isostasy was developed up to degree and order 180, corresponding with 1°× 1° a grid. The bathymetry for the North Atlantic and its topographic-isostatic contribution to the geoid is shown in Figure 6.13 on page 91. The height values range respectively from -6200 m to 2700 m, and from -1 m to 19 m. The fine topography and its compensation up to 5'× 5' was subsequently obtained from a three dimensional layered model solved by numerical integration in the z direction and by two dimensional FFT in the x,y planes [41]. This model needs to be extended for all first and second derivatives of the potential or geoid, so that all altimetry results mentioned above can be corrected for the bathymetric attraction. The remaining signal displays geological phenomena like fractures or density distributions.

6.5 References

1. *GEOSAT special issues*, Journal of Geophysical Research, **95**, no. C3 and C10, 1990.

2. Scharroo, R., K.F. Wakker, and G.J. Mets. *The Orbit Determination Accuracy of the ERS-1 Mission*, Proceeding of Second ERS-1 Symposium - Space at the Service of our Environment, Hamburg, Germany, ESA SP-361, 1993.

3. Francis, C.R., A. Caporali, L. Cavaleri, A. Cenci, P. Ciotto, L. Ciraolo, W. Gurtner, F.H. Massmann, D. del Rosso, R. Scharroo, P. Spalla, and E. Vermaat. *The Calibration of the ERS-1 Radar Altimeter - The Venice Calibration Campaign*, ESA Report ER-RP-ESA-RA-0257 issue 2.0, ESA/ESTEC, Noordwijk, The Netherlands, 1993.

4. Wisse, E., M.C. Naeije, R. Scharroo, and K.F. Wakker. *Processing of ERS-1 and TOPEX-Poseidon Altimeter Measurements*, Interim report, BCRS study 1.2/OP-01, Delft University, p. 75, June, 1993.

5. Naeije, M.C., E. Wisse, R. Scharroo, and K.F. Wakker. *Ocean Dynamics from the ERS-1 35-day Repeat Mission*, Proceedings of Second ERS-1 Symposium - Space at the Service of our Environment, Hamburg, Germany, ESA SP-361, 501-506, 1993.

6. Wisse, E., R. Scharroo, M.C. Naeije, and K.F. Wakker. *Mean Sea Surface Computation from ERS-1 Data*, Proceedings Second ERS-1 Symposium - Space at the Service of our Environment, Hamburg, Germany, ESA SP-361, 1993.

7. Koblinsky, C.J., P. Gaspar, and G. Lagerloef eds. *The Future of Space Borne Altimetry: Oceans and Climate Change*, Joint Oceanographic Institutions Inc., Washington DC., p. 75, 1992.

8. Feron, R.C.V., M.C. Naeije, and D. Oskam. *Quality of Ocean Variability Results from Satellite Altimetry*, Marine Geodesy, **15**, pp. 1-18, Taylor & Francis, 1992.

9. Naeije, M.C., K.F. Wakker, R. Scharroo, and B.A.C. Ambrosius. *Observation of Mesoscale Ocean Currents from GEOSAT altimeter data*, ISPRS Journal of Photogrammetry and Remote Sensing, **47**, pp. 347-368, Elsevier, 1992.

10. Sandwell, D.T., *Geophysical Applications of Satellite Altimetry*, Reviews of Geophysics, supplement, pp. 132-137, 1991.

11. Haagmans, R.H.N., *Satellite Altimetry: the Ocean Surface as a link between Oceanography, Geophysics and Geodesy*, Geodetical Info Magazine, **5**, no. 11, 1991.

12. Haagmans, R.H.N., M.C. Naeije, and R.C.V. Feron. *TOPEX/POSEIDON and ERS-1: New Dimension in Satellite Altimetry Part1 and Part 2*, Geodetical Info Magazine, **7**, no. 11 and 12, 1993

13. Chelton, D.B., *WOCE/NASA altimeter algorithm workshop*, Tech. Rep. 2, US Planning Office for WOCE, 1988.

14. Scharroo, R., K.F. Wakker, B.A.C. Ambrosius, R. Noomen, W.J. van Gaalen, and G.J Mets, *ERS-1 precise orbit determination*, in: Proc. 1st ERS-1 Symposium (Space at the service of our environment), Cannes, 4-6 November 1992, ESA SP-359, **1**, pp. 477-482, ESA, 1993.

15. Rummel, R., *Principle of Satellite Altimetry and Elimination of Radial Orbit Errors*, in: Lecture Notes in Earth Sciences 50, Satellite Altimetry in Geodesy and Oceanography, ed. R. Rummel & F. Sansò, Springer, Berlin, 1993.

16. Zandbergen, R.C.A., *Satellite Altimeter Data Processing: From Theory to Practice*, PhD thesis, Delft University of Technology, January, 1991.

17. Oskam, D., *Sea surface variability in the North Sea as derived from Seasat altimetry*, Geophysical Journal International, **100**, 1-7, 1990.

18. Wakker, K.F., R.C.A Zandbergen, M.C. Naeije ,and B.A.C Ambrosius. *GEOSAT Altimeter Data Analysis for the Oceans around South Africa*, J. Geophys. Res., **95**, No. C3, pp. 2991-3006 & 3421, March 15, 1990.

19. Schrama, E.J.O., *Some remarks on several definitions of geographically correlated orbit errors: consequences for satellite altimetry*, Manuscripta Geodaetica, **17**, pp. 282-294, 1992.

20. Schrama, E.J.O., D. Oskam, und R. Rummel. *Geodätische Aspekte bei der Verarbeitung von Satellitenaltimetriedaten*, Zeitschrift für Vermessungswesen, **1**, 1990.

21. Tailor, J.R., *An Introduction to Error Analysis; The Study of Uncertainties in Physical Measurements*, University Science Books, Oxford University Press, 1982.

22. Zandbergen, R.C.A., K.F. Wakker, and B.A.C. Ambrosius. *Application of satellite altimeter data to orbit error correction and gravity model adjustment*, Adv. Space Res., **10**, pp. 249-267, 1990.

23. Visser, P.N.A.M., *The Use of Satellites in Gravity Field Determination and Model Adjustment*, PhD thesis, Delft University of Technology, Sept., 1992.

24. Xu, P., *Monitoring Sea Level Rise*, Reports of the Faculty of Geodetic Engineering, Mathematical and Physical Geodesy, DUT, no. 90.1, Delft, 1990.

25. Schrama, E., and R. Ray. *A Preliminary Tidal Analysis of Topex/Poseidon Altimetry*, accepted for Journal of Geophysical Research Oceans, special issue on Topex/Poseidon, 1993.

26. Nerem, R.S., E.J.O. Schrama, C.J. Koblinsky, B.D. Beckley. *A Preliminary Evaluation of Ocean Topography from the Topex/Poseidon Mission*, accepted for Journal of Geophysical Research Oceans, special issue on Topex/Poseidon, 1993.

27. Gordon, A.L., and W.F. Haxby, *Agulhas eddies invade the South Atlantic: Evidence from GEOSAT altimeter and shipboard CTD survey*, J. Geophys. Res., **95**, pp. 3117-3125, 1990.

28. Naeije, M.C., K.F. Wakker, R. Scharroo, E. Wisse, P. Visser, and B.A.C. Ambrosius. *GEOSAT Ocean Currents; a computer animation of ocean variability as deduced from GEOSAT altimeter data*, DUT/SOM Video Ltd., February/March 1992, VHS E30 tape.

29. Feron, R.C.V., W.P.M. de Ruijter, and D. Oskam. *Ring Shedding in the Agulhas Current System*, Journal of Geophysical Research, **97**, no. C6, pp. 9467-9477, 1992.

30. Feron, R.C.V., *Comparing the UK Fine Resolution Antarctic Model (FRAM) with 3-years of Geosat data*, in Lecture Notes in Earth Sciences 50, Satellite Altimetry in Geodesy and Oceanography, ed. R. Rummel & F. Sansò, Springer, Berlin, 1993.

31. Cushman-Roisin, B., E.P. Chassignet, and B. Tang, *Westward motion of mesoscale eddies*, J. Phys. Oceanogr., **20**, pp. 758-768, 1990.

32. Feron, R.C.V., *The mean sea surface dynamic topography from satellite observations of horizontal eddy fluxes*, Submitted to Proceedings of the KNAW colloquium on the modelling of oceanic vortices, 1993.

33. Pedlosky, Y., *Geophysical Fluid Dynamics*, 2nd edition, Springer Verlag, New York, pp. 710, 1987.

34. Flather, R.A., *Results from a tide model of the North Atlantic Ocean*, in: Proceedings of the 10th International Symposium on Earth Tides, Madrid, 1981, p. 970, Consejo Superior Investigationes Cientificas, 1981.

35. Rummel, R., L.S. Sjöberg, and R.H. Rapp. *The Determination of Gravity Anomalies from Geoid Heights Using the Inverse Stokes Formula, Fourier Transforms, Least Squares Collocation*, Reports of the Department of Geodetic Science, Report no. 269, OSU, Columbus, Ohio, 1977.

36. Haxby, W.F. G.D. Karner, J.L. LaBreque, and J.K. Weissel. *Digital Images of Combined Oceanic and Continental Data Sets and Their Use in Tectonic Studies*, EOS 64 (52), pp. 995-1004, 1983.

37. Sandwell, D.T., *A Detailed View of the South Pacific Geoid from Satellite Altimetry*, Journal of Geophysical Research, **89**, no. B2, pp. 1089-1104, 1984.

38. Rummel, R., and R.H.N. Haagmans. *Gravity Gradients from Satellite Altimetry*, Marine Geodesy, **14**, pp. 1-12, 1990.

39. Craven, P., and G. Wahba, *Smoothing noisy data with spline functions*, Numerische Mathematik, **31**, pp. 377-403, 1979.

40. Khafid, *Filtering of Satellite Altimetry Data with Optimal Smoothing Cubic Splines to Compute Geoid Heights, along-track Geoid and Gravity Gradients in the Indonesian Waters and its Surroundings*, Afstudeerscriptie, Sectie FMR, Faculteit der Geodesie, TU Delft, 1993.

41. Welting, B., *Correlatie tussen het zwaartekrachtveld en de bathymetrie in de Noordatlantische Oceaan*, afstudeerscriptie, sectie FMR, Faculteit der Geodesie, TU Delft, 1992.

7 Gravity field

The general mathematical theory of the determination of the gravity field was studied to get a better understanding how the different measurement types relate to the gravity field. Specific tests have been carried out to evaluate the possible contribution to the knowledge of the gravity field that can be determined from satellite gradiometry. For direct application in practice, numerical improvements were made in the field of geoid determination.

7.1 Gravity field theory

For the determination of the earth's gravity field many types of observations are available nowadays: e.g., terrestrial gravimetry, airborne gravimetry, satellite to satellite tracking (SST) and (satellite) gradiometry. The mathematical connection between these observables, the gravity field and the shape of the earth is called the geodetic boundary value problem (GBVP). In its classical form the problem is defined as the determination of the gravity potential and the shape of the earth from the observations of the gravity vector and potential on the earth's surface. With the introduction of new measurement techniques other formulations of the GBVP were developed. The goal is to include all observations available, of different type, quality and density into one optimal solution of the earth's gravity field. Furthermore a possibility is required to evaluate the contribution to the knowledge of the gravity field of future measurement campaigns.

7.1.1 Theory

Studies in the field of geodetic boundary value problems are presented below for the real earth and an imaginary two-dimensional version.

General

The theory of the determination of the shape of the earth and its gravity field is based on solving a non-linear free boundary value problem from continuous boundary functions. Since a direct solution cannot be found, approximate solutions have to be used; if desired improved by means of an iteration procedure.

Usually the tools of potential theory are applied for the derivation of the solution. In Delft, however, solutions were sought along a new line. A GBVP, simplified in the coefficients of the boundary operator (the earth's surface and the equipotential surfaces are approximated by a sphere), is formulated as a system of observation equations, with the coefficients of a series expansion for the disturbing potential as unknowns, which are solved by a least-squares adjustment. If real (discrete) observations are introduced the system has to be solved numerically. A closed solution can be obtained for the limiting case: a complete, continuous coverage of the earth's boundary by observation functions. These solutions are identical to those obtained by the classical methods of potential theory for the problem formulated with the same degree of approximation, e.g., the well-known Stokes integral. Not only solutions were obtained for combinations of observables, where none was available up to now, e.g., the determination of the potential solely from the deflections of the vertical [1], but this new formulation also gives more insight into the GBVP by clearly separating the known and unknown parameters and connecting them by a matrix equation.

With this approach new types of observations can be easily incorporated. Also the *overdetermined* GBVP can be solved along the same lines with convolution integrals and by introducing relative weights between the incorporated types of observables. In this way a complete structure has been established providing the relationship between all kinds of observables and the solution for the gravity potential. Simple and exact analytical solutions could only be found for the modified GBVP (the spherical approximation) and only with continuous observations on the boundary, but the level of approximation is suitable for most applications. Usually an interpolation step is made before applying the integral operators, e.g. least-squares interpolation. A more accurate solution can be obtained by an iteration. Basically this is based on the series expansion for the inverse of a matrix; occasionally referred to as a Neumann series. It can be implemented as a direct iteration or by means of correction terms to the original solution.

The formulation of the GBVP as a system of linear observation equations makes error prediction straightforward. If a priori (co)variances for the observations are known, the inverse normal matrix directly yields the error estimates for the potential coefficients to be determined. Also for the (inverse) normal matrix analytical expressions are available.

Two-dimensional earth

The transition from a discrete GBVP (which we have with real data) to the continuous GBVP (for which in some cases a solution exists) gives, although not yet mathematically rigorous, a connection between the practical situation and the idealization. The GBVP is closely related to (smoothing) collocation, for which convergence of the solution to the GBVP solution was proven by Krarup [2].

The work on the theory of the GBVP was mainly concentrated on a study of the GBVP for an (hypothetical) two-dimensional earth [3]. It seemed attractive to try the same concept as demonstrated above on a two-dimensional earth. This two-dimensional earth is not a planar approximation of the curved boundary of the real earth, but a complete two-dimensional world with an one-dimensional boundary, as used in [4,5]. This hypothetical earth can be imagined as an infinitely thin slice of the real earth through its center and poles. The two-dimensional earth has a number of advantages over the three-dimensional one. The reduction of the dimension by one releases us from awkward things such as meridian convergence, azimuths and Legendre functions. Strong mathematical tools are available: conformal mapping, used by Gerontopoulos for his solutions to the two dimensional GBVP, the theory of complex numbers and Fourier series. The extensive literature on time series, with well-formulated theorems on sampling, discrete and continuous signals, averaging and noise modelling, can be applied to the GBVP. The formulae are simpler and more compact, because of the reduction of the number of parameters. This facilitates not only the interpretation of the formulae, but also the implementation of numerical tests.

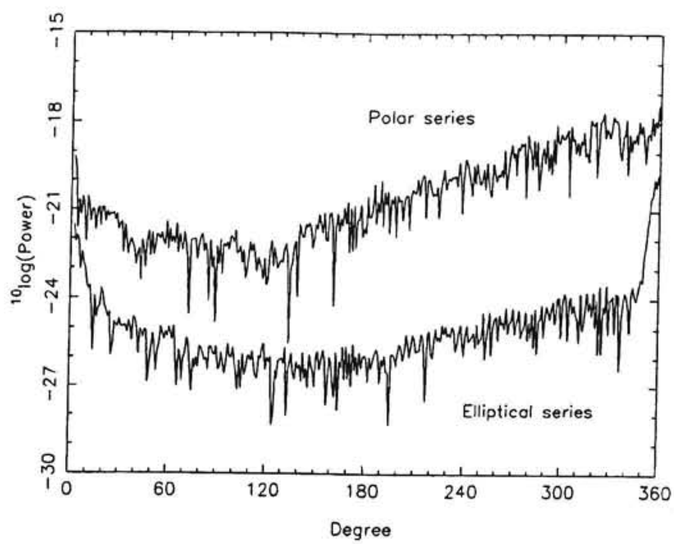

Figure 7.1 The error power spectra of the solved two dimensional potential coefficients with two types of series in a simulation run.

First the GBVP is formulated as for the three-dimensional earth, and its solutions were derived. For the improvement of the initial solution an iteration method was developed. The theory was validated by means of numerical simulations. A two-dimensional earth with a gravity field was synthesized and its GBVP solved by means of the various methods. It was demonstrated that iteration is a feasible way to get more accurate solutions. The convergence of the iteration mainly depends on the data quality and the level of approximation of the GBVP. For solutions of the potential up to high degree, convergence can be greatly improved by the use of elliptical harmonics; see Figure 7.1. Comparison of the error in the potential coefficients, obtained from the simulations, with simple analytical formulae for error prediction as proposed in [6], showed good agreement at the two.

7.1.2 Signal and noise prediction

For the judgement of the contribution of the various types of observation to the improvement of the knowledge of the earth's gravity field, error propagation is mandatory. Rigorous error prediction is often possible, but usually time-consuming and not required. Therefore approximate, more simple relations are employed.

Most quantities of interest for gravity field determination can be related with reasonable accuracy by linear operators. The measurable quantities are (at the level of spherical and constant radius approximation) linear functionals of the fundamental unknown, the earth's gravity (disturbance) potential. Their natural field representation is in terms of an infinite spherical harmonic series. With the spherical harmonics as system of eigenfunctions the eigenvalue representation of the linear operators is derived, and consequently the spectral connection among all (measurable) linear gravity functionals. Error prediction is performed most easily by covariance propagation.

If the covariance functions are homogeneous and isotropic (not dependent on position and the azimuth), they can be propagated by multiplying their spectral coefficients with the square of the eigenvalue of the corresponding operator. If for one quantity related to the gravity field a signal power spectrum model is available, e.g. Kaula's rule for the disturbing potential, the signal power spectrum for the other quantities can be obtained directly. By comparing signal and error power spectra of the measurements, predictions can be made of the resolution and accuracy of the gravity field as computed from the observed values.

The operators connecting the disturbing potential and its radial derivatives and the operators to get the disturbing potential at a different height, have the spherical harmonics as eigenfunctions and are fully determined by their eigenvalues. This leads to the scheme as shown in Figure 7.2. First ideas in these directions are given in [7]. Also quantities like gravity anomalies or geoid heights can be incorporated since they are a linear combination of T and $\partial T/\partial r$.

It was more difficult for the operators involving horizontal differentiation. Since they are generally azimuth dependent, the spherical harmonics are not their eigenfunctions so an eigenvalue representation is not directly feasible. An incorporation of deflections of the vertical into the scheme of Figure 7.2, which are the horizontal derivatives of the potential in the spherical approximation, was achieved by combining them into a vector, the surface gradient. If this combination is available in each point and both components carry the same weight in the adjustment, the solution of their GBVP is again a convolution integral. Also second order derivatives of the potential involving horizontal differentiation could only be included into the scheme if they are available in combinations.

More mathematically it can be explained as follows. The operators for radial differentiation are self-adjoint and isotropic. They have the spherical harmonics as their eigenfunctions. For tangent vector fields (tangent to the sphere) a similar structure exists. Their basefunctions are related to the spherical harmonics by applying the surface gradient operator to them. These vectorial spherical harmonics form a complete and orthonormal set of basefunctions for tangent vector fields. For the complete vector of first derivatives of the potential, a set of vectorial basefunctions is required with three elements. It consists of the scalar spherical harmonics for the radial part of the vector and zero's for the other two elements and a second set with a zero for the radial part and the vector spherical harmonics as the other two elements.

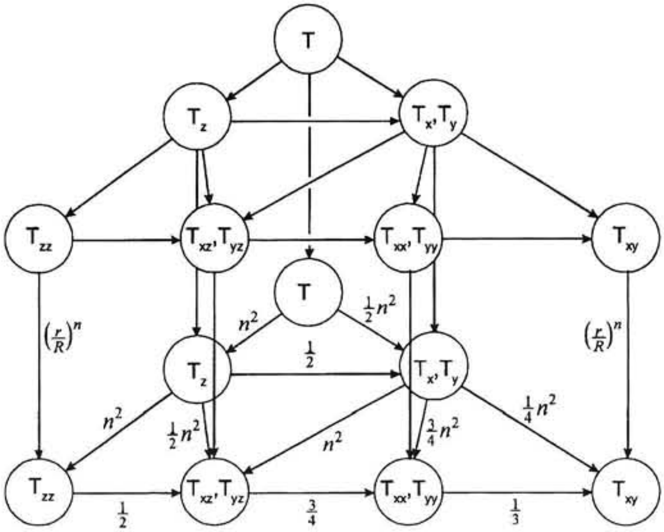

Figure 7.2 Approximate relations between the power spectra of the zero, first and second order derivatives of the gravity potential.

For the second derivates of the potential, the gradients of the gravity vector, the tensorial spherical harmonics form a complete and orthonormal system for second-order tensor fields on the sphere. Three sets of these harmonics (they are identical to the pure-spin harmonics known from physics) form a complete and orthonormal basis for second-order tensor functions on the sphere.

In practice the assumptions of isotropy and homogeneity of the (error)covariance function will never be met; inhomogeneities in the data quality and distribution are almost inevitable. The operator equations are also based on the assumption of continuous data distribution. If the data distribution is fairly regular and homogeneous of quality, these assumptions are not too far from reality and the scheme can be used for error prediction. But we do have to design the error models in such a way that they reflect the actual data quality as good as possible within the limits defined before. This was studied in more detail, and especially the results for satellite data were very promising. Comparison to more sophisticated error propagation yielded only small differences. However, irregular data distribution, such as caused by the polar caps with satellite missions, or the availability of land data on continents only, and effects like aliasing, cannot be represented properly by the existing models. It will have our attention in the next phase.

7.1.3 Computational aspects

Further progress has been made in the field of global spherical harmonic analysis and synthesis. By re-examining old german literature, Gauss [8,9] and Neumann [10,11], recent advances in global spherical harmonic analysis could be placed in a more historical perspective. More specific, the independent treatment of latitude and longitude information, which allows for very efficient algorithms, was discussed and applied already in this old literature. Furthermore a remedy was found for the loss of orthogonality of Legendre polynomials after discretization. One of the approaches is the use of Gauss-Legendre quadrature as known in numerical analysis. The solutions that were found make use of special quadrature weights, which can be computed even for high sampling rate along the meridians. e.g. latitude sampling $\Delta\theta = \pi/360$ or $\pi/720$. The adaptions of Neumann's methods, necessary for the computation, were found in the meteorological literature [12].

In conclusion, this research has led to a deeper understanding of global spherical harmonic analysis of functions on a sphere, which are given on a regular grid. The Neumann methods, and in general other quadrature methods as well, could be fit into a generalized framework of a weighted least squares approach towards spherical harmonic computation [13,14,15].

7.2 Gravity field determination

In preparation of the altimetric satellite missions TOPEX/Poseidon and ERS-1 a whole new generation of geopotential models was computed. Examples are the TEG-2 model of the University of Texas at Austin, GEM-T1 to GEM-T3 of NASA's Goddard Space Flight Center, JGM-1 and JGM-2 as the joint effort of these two groups, and GRIM4-S1 and GRIM4-C1 of the German/French DGFI/GRGS combination. Characteristic to the fields represented by these models is that all program parts were carefully evaluated and improved, more data from measurements to more satellites was included and a thorough error assessment took place. These models serve as current standard of satellite based gravitational field modelling. On the other hand, applications in solid earth physics, oceanography, navigation, geodesy and surveying still require more detailed and accurate information about the gravitational field of the earth. Indeed there exist concepts to further improve our current knowledge of the earth's gravitational field in terms of resolution and accuracy. New to these concepts is that they are based on a single dedicated gravity field satellite mission. The question thus arises whether such an expectation is well-founded or, more general, where does geopotential modelling by satellites go to?

With good approximation, a satellite orbiting the earth can be considered a harmonic oscillator. Its two eigen-modes are the zero and once-per-revolution frequency. Any structure of the earth's gravity field contributing to these eigen-modes causes relatively large perturbations on the satellite's orbit. For example, when expressing the gravity field in a series of spherical harmonics with corresponding potential coefficients, we observe that the main orbit perturbations are caused by certain clusters of potential coefficients, namely those that contribute to the above two resonance frequencies. Coefficients outside the resonance bands have a much smaller, e.g. short periodic, effect on the orbit [16]. Typically a satellite is tracked at most 10 to 15 % of a full revolution. This is sufficient to determine the zero and once-per-revolution frequency. Consequently the potential coefficients close to the resonance bands can be determined very well. However, tracking density and precision do not suffice to reproduce the short-periodic orbital motions related to the potential coefficients outside the resonance bands. For geopotential modelling the consequence is that only certain clusters of coefficients are well estimable. Of course, by using several satellites covering a wide range of altitudes, inclinations and eccentricities the range of estimable potential coefficients becomes wider, but in tendency the above rule remains valid.

As a remedy, in order to obtain from the estimation procedure also some results for the non-resonant coefficients, a priori information is introduced into the adjustment process of geopotential modelling. Often the a priori values of the potential coefficients are considered to be zero, while their variance is described by some signal degree-variance model. This variance is added to the normal matrix of the least-squares adjustment procedure. The result is that certain groups of coefficients (e.g. the non-resonant) are determined solely by a priori information, carrying little or no relevant satellite information, whereas others (e.g. the coefficients in the resonance bands) are determined partly from the a priori information and mainly by satellite information [17]. In conclusion the expectation is that along the traditional path of satellite orbit tracking and analysis no significant further improvement of the geopotential models can be achieved any more. The natural limit has almost been reached. Thus, how must one proceed in the future?

New microwave tracking concepts, such as DORIS and PRARE, are not only aiming at greater precision but also at a ground tracking coverage of up to 80 to 90 % of a full revolution. Then short wavelength features in the orbit tend to get visible. The traditional limitation sketched above gets overcome. This is even more the case for the method of space-borne GPS, where a low-flying satellite, carrying one or more GPS receivers, is tracked simultaneously by several high-flying GPS satellites (what is called SST: Satellite-to-Satellite Tracking). With this method we have continuous measurement coverage so the complete satellite orbit (full revolutions) can be determined. For maximum precision the GPS measurements are carried out in the differential mode, relative to some network of selected ground stations. With TOPEX/Poseidon (T/P) this method is actually tested for the first time. Unfortunately, the T/P satellite is not drag-free, hence the problem remains of separating gravitational from non-gravitational (air drag, solar radiation pressure, etc.) accelerations.

In the case of SST it is, in fact, the relative motion between high and low satellites in the direction of their line of sight which is measured. With satellite gravity gradiometry (SGG), however, instead of the orbit the tiny differential accelerations between adjacent test masses inside a spacecraft are the principle observables. From these acceleration differences some or all of the nine elements of the gravitational tensor $\partial^2 V/\partial x^i \partial x^j$ (of which only five are independent) are deduced. Typical for a differential accelerometry setup is the so-called common-mode rejection: linear disturbing accelerations due to e.g. air drag are to a large extent eliminated from the measurements by taking acceleration differences. Nevertheless, the existence of non-gravitational accelerations like rotations and residual air drag, puts high demands on the applied technology.

Both methods SST and SGG share the fact that (explicitly or implicitly) gravitational variations between the trajectories of two or more masses moving in space are analyzed. In the case of SST (space-borne GPS) these masses are separate satellites and the distances between them are relatively large. This makes SST especially suitable for determination of the long and medium wavelengths of the gravitational field. With SGG the masses are two or more small test-masses situated inside one satellite at a typical distance of about 50 to 100 cm. So, SGG is well suited for the determination of small wavelength features of the gravity field. Both techniques are thus complementary and the combination of the two on one satellite yields a very promising mission concept for global gravity field determination [18,19,20]. Until now, two missions have been proposed by ESA: ARISTOTELES and STEP, the latter in cooperation with NASA, none of them was realised.

Thus the general trend for gravity field determination from space is to track a satellite with very high sample rate and uninterrupted, ideally throughout its mission life time. In conjunction with a low altitude and an almost polar and circular orbit, all spherical harmonics up to a certain maximum degree become estimable, in principle. Higher spatial resolution can be attained by not only following the orbit of one satellite but by means of space-borne GPS and/or SGG.

7.2.1 Spherical harmonic analysis and synthesis

The resolution of the gravity field to be obtained from such a dedicated gravity field mission is expected to be much higher than the resolution of current geopotential models. Typically one can think of a maximum degree and order of 200-300 in terms of a spherical harmonic expansion of the gravitational potential. For example, a maximum degree of 200 implies a total number of some 40,000 potential coefficients. Numerical computations with such huge series are very time consuming and put high demands on the software as well as the hardware. For such computations one usually makes use of geopotential models up to high maximum degree, typically 180 or 360 like the OSU models from the Ohio State University, which are derived from combinations of data types like satellite orbit tracking, terrestrial gravity measurements, satellite altimetry and geophysical knowledge. Although these kind of models suffer from inhomogeneity in precision they are of particular importance for simulation studies.

In the past a considerable amount of effort was dedicated to the development of fast spherical harmonic synthesis and analysis software. For spherical harmonic synthesis (computation of potential functionals like gravity gradients from a priori given geopotential models) up to high degree and order, software, especially tailored for use on vector computers, was developed. In terms of calculation speed this vectorized software seemed to be the most efficient [21]. Other computational methods exist, each with its own software and hardware related problems, like underflow, stability and computational speed. A comparative study in this field was performed with several software packages developed at different European centres [22]. Spherical harmonic synthesis and analysis can be described in a rather dual manner and many of the problems related to synthesis play a role in analysis too. When using satellite observations, however, two at first sight rather different approaches for the analysis step are possible.

7.2.2 Timewise versus spacewise approach

It is remarkable to observe that dynamic satellite geodesy and physical geodesy, although strongly cross-fertilizing from each other, developed as two rather independent branches. No serious attempt for a unified theory of gravity field determination has been undertaken. The former addresses gravitational field estimation from the solution of the equations of motion for earth orbiting satellites, the latter solves the gravitational field and the shape of the earth in the form of a boundary value problem with the earth's surface as known or unknown boundary. Gradiometric measurements are ideally suited for a study of the similarities and differences of these two approaches since they are on the one hand performed inside an earth orbiting satellite but on the other hand are direct functionals of the gravitational potential.

Simply put, the main difference between the two approaches is that in physical geodesy observations are usually performed in a static measurement setup and are thus considered to be given as function of spatial position only whereas in dynamic satellite geodesy successive measurements performed in or to an earth orbiting satellite are considered a time series, i.e. being in the first place a function of time t. Appropriately the former is therefore called *spacewise approach* and the latter *timewise approach.* The main advantage of the spacewise approach (and really a disadvantage of the timewise approach) considers computation time. In the spacewise approach the millions of observations which are collected during a typical dedicated gravity field mission are usually comprised into a world-wide equi-angular grid.

Block averages are then used as derived observations in the actual analysis, decreasing the required computation time drastically. In the time-wise approach, however, each original observation has to be handled separately in the analysis. Other differences between the two approaches concern the geometry and the dynamical behaviour of the satellite orbit and the description of the instrument noise characteristics.

The spacewise approach, in fact, fully coincides with the techniques well established in the field of physical geodesy. In this interpretation satellite gradiometry can be analyzed with the tools discussed in Section 7.1 [23]. For the timewise approach, on the other hand, the intimate relation to satellite perturbation theory is evident, as will be discussed below. This close connection of the timewise approach with orbit perturbation analysis, as usually applied in dynamic satellite geodesy, becomes even more pronounced if we look at a measured tensor component from a slightly different angle. In differential accelerometry, as it has to be applied within the ARISTOTELES mission, an arbitrary tensor component is measured by prohibiting two neighbouring test masses from their free motion (fall) in orbit and by constraining them to a fixed levitated position inside the instrument by means of some feedback mechanism. The feedback signal suitably differentiated is translated into the gradient measure. It permits reconstruction - or is equivalent to the measurement - of the relative acceleration between adjacent test masses in free fall at known distance, as discussed in [24]. Hence the signal could be modelled by means of perturbation theory of two neighbouring space trajectories. As the two trajectories are highly similar, their absolute shape and location is of lesser importance. The gradiometric information is concealed in their relative differences [25].

This view leads to a nice connection with the fundamental physics project STEP. There, the relative motion between two test masses is used to test the famous equivalence principle of gravitational and inertial mass (see also below). Satellite gradiometry viewed upon in this way thus bears close connections to the general theory of relativity. Indeed it can be shown that in relativistic terms the elements of the gravity gradient tensor exactly describe the curvature of four-dimensional spacetime [24,26,27]. In fact, the relativistic model for satellite gradiometry is based upon the same view as above, namely the so-called equation of geodesic deviation, where the two adjacent test mass trajectories are considered as neighbouring geodesics in spacetime.

Spacewise approach

Consider first the satellite as a carrier of an instrument that delivers the gravitational tensor components Γ_{ij} at regular intervals. At each measurement epoch the spatial position of the instrument is expressed by the coordinate triple $\{\varphi, \lambda, r\}$ (geocentric spherical coordinates), representing the position of the satellite's center of mass, which is usually only known approximately. With each revolution of the spacecraft a new circle of densely spaced measurements is delivered. Depending on the choice of the orbit, in particular of the orbital inclination I and the precession rate of its node $\dot{\Omega}$, an almost arbitrarily dense coverage of the earth can be achieved. With $\Gamma_{ij}(\varphi , \lambda , r)$ - or approximated $\Gamma_{ij}(\varphi , \lambda)$ if the height variation of the satellite can be neglected or all observations are reduced to one sphere $\sigma(0 , r)$ - each tensor component represents a gravity related functional, given on a known (or unknown) boundary surface. The determination of the global gravity field in terms of spherical harmonics from such a functional is carried out by quadrature techniques or the solution of a geodetic boundary value problem (g.b.v.p.). For each gradiometric component, certain combinations of components and the full tensor, solutions of the g.b.v.p. have been computed. The approach is rather simple, but the results agree well with those from the timewise approach discussed below. A number of studies, in particular for error analysis, were based on this view. Its drawback is that the peculiarities of the actual satellite orbit, in particular resonances, and specific measurement error characteristics such as coloured noise, are not taken care of.

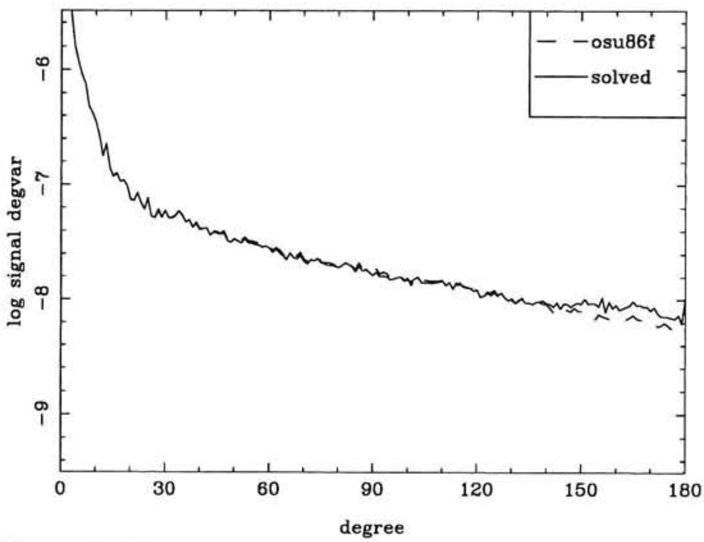

Figure 7.3 Degree variances of potential coefficients derived from 1 month simulated gradient data using the spacewise approach compared to the original signal degree variances from the OSU86F model.

A full analysis, aiming at the recovery of potential coefficients from satellite gradiometric observations, based on the spacewise approach will consist of an iterative solution procedure. In each iteration step potential coefficient correction estimates are computed and the nominal orbit is updated. In this way the gravity field is solved from the measurements as is the satellite's orbit [28]. For the first part of this procedure, the estimation of potential coefficients, a functioning analysis program has been developed. For testing purposes use was made of a large one month mission simulation of gradiometric measurements computed at the Space Research Center of the University of Texas at Austin. From this data set a full field of potential coefficients up to maximum degree and order 180 was estimated, see Figure 7.3. Although this test comprised only a first step of the iterative procedure, the results were promising and give confidence that the method could be applied to real mission data [27,21].

Timewise approach

Equally well, the measured sequence of tensor components may be viewed upon as a discrete time series, $\Gamma_{ij}(t)$, ideally spanning the entire mission length without interruption. In reality, though, data gaps may occur due to instrument failures, excessive drag variations and satellite orbit manoeuvres. In a six months mission, however, consisting of one or more repeat periods, a so dense coverage is obtained that the influence of such data gaps is likely to be overcome. In this approach the determination of spherical harmonic coefficients becomes possible only after connecting the spherical harmonic representation given in an earth fixed coordinate system with the time series provided along the inclined, slowly precessing orbital plane. Various ways are conceivable for this connection and for the parametrization of the time series. In any case, the relation to dynamic satellite geodesy is obvious and this approach is therefore particularly suited for studies of the influence of the choice of the orbit parameters on gravity field recovery and, as measurement sampling is actually a time process, for analysis of realistical instrument error models.

Measured gravity gradients, considered as a time series, can be connected to potential coefficients by means of a series expansion in so-called inclination functions [29]. Inclination functions, in fact, describe a rotation from an earth fixed to an orbit related coordinate system [30]. In [30] or [31] they are derived in a elegant way by means of a group theoretical approach which makes use of so-called representation coefficients (or Wigner coefficients). Inclination functions have three spectral indices and computation of them for a certain value of the inclination I up to high degree and order is a large computational task. Several methods to compute inclination functions are possible. They can e.g. be computed in a direct manner by means of stable recursion schemes based on the algorithm by Emeljanov & Kanter [32]. Software which makes use of this algorithm has been documented in [30]. In an indirect way they can be computed by using Fourier methods [33]. Both methods have been worked out in operational software. For potential functionals involving cross-track derivatives related inclination functions, so-called cross-track inclination functions, have to be used. They can be derived and computed in a similar manner as the ordinary inclination functions [34].

For a number of years considerable effort has been invested in the development of an error propagation model and computer software that allow a realistic study of the influence of the error behaviour of SGG and SST/GPS on global gravity field determination. Realistic in this context means that the model should be capable of properly reflecting the orbit characteristics (altitude, inclination), mission length and sampling rate and instrument characteristics, in particular coloured noise behaviour and band limitation. With the developed software package extensive simulations have been carried out in preparation of the ARISTOTELES and STEP experiments and for the general ESA studies CIGAR. Simultaneously, theoretical work has started to find systematic structures for a unified analysis of all satellite techniques that could be employed for gravity field recovery, so-to-say a second pocket-guide (see Section 7.3), this time for dynamic satellite geodesy. The timewise approach discussed here is particularly suitable for such a pocket-guide. In this approach, the analysis model can be set up in two ways [35].

First, the equations connecting successive measurements of a time series (as in our case gravity gradients or other potential functionals measured in an earth orbiting spacecraft) with potential coefficients can be used as observation equations for gravity field analysis. This approach can be called timewise *in the time domain* [27]. In essence, the observation equations are used in a least-squares adjustment procedure to estimate the unknown harmonic coefficients from the available measurements. In the framework of an error analysis the solution of the system of normal equations corresponds to the propagation of a given variance-covariance matrix of the observables into an a posteriori variance-covariance matrix of the unknown parameters. A typical expansion degree for analysis of gradiometric data is $L = 240$ or a total of $L^2 = 57600$ unknown field parameters. These are to be estimated from millions of observations to be collected in a six months mission. Even for modern mainframe computers such a problem can be solved in a reasonable time only when the normal matrix has a certain favourable structure. Under the assumptions of a circular repeat orbit and a constant data sampling it can be shown that, if we order the unknown parameters in a specific manner, the normal matrix attains a block diagonal structure [36]. This is due to the orthogonality properties of the trigonometric series expansion of the gradients in inclination functions. The block-diagonality reduces the computation time drastically [27,37].The size of the largest sub-block is "only" $(L/2+1) \times (L/2+1)$.

The same assumptions mentioned above allow us to view upon the time series also in another manner. In the theory of signal processing uninterrupted time series with constant sample rate may be considered a discrete Fourier series. By applying now FFT techniques to the time series we obtain a set of Fourier coefficients which, in a second stage, can be translated into a set of coefficients with two spectral indices, corresponding to the so-called lumped coefficients. These lumped coefficients, i.e. the Fourier spectrum of the observables, are now used as a kind of pseudo-observations. They are linearly related to the unknown spherical harmonic coefficients of the earth's gravity field [38]. In this view, the block-diagonality of the normal matrix becomes very obvious. This approach is called timewise *in the frequency domain*. In this formulation it is very easy to include other observation types from satellite geodesy, like space-borne GPS, in the same model. For the case of GPS it is assumed that in some pre-adjustment from the combination of observed carrier-phase and pseudo-range measurements orbit perturbations Δx, Δy, Δz can be determined relative to a given reference orbit. The connection between Δx, Δy, Δz

and the accelerations $\Delta\ddot{x}$, $\Delta\ddot{y}$, $\Delta\ddot{z}$, both given in a local orbit system, has been established from the solution of the Hill equations. The acceleration perturbations can directly be related to the gradient of the gravitational potential.

Each specific type of observable requires a specific relationship between the lumped coefficients and the harmonic coefficients. These ''transfer coefficients'' depend upon orbit characteristics, curvature of the gravity field and, in the case of GPS position estimates, on space-craft dynamics. The pocket-guide of dynamic satellite geodesy, mentioned earlier, would comprise the total set of observable specific relationships. One important part in this spectral formulation (Fourier vs. spherical harmonics) are the orbital mechanics. One choice would be to use the linear perturbation theory, developed by Kaula [29], based on Lagrange's Planetary Equations. Alternatively, as it is done in the error analysis software, Hill equations could be employed [38,39].

With the gradiometry and space-borne GPS propagation model the propagation can be analyzed of given a priori errors of all measurement types to the estimated gravity parameters. Input are the error spectra of the observable gradiometric or GPS time series. This choice allows modelling of band limitation and coloured noise and may be different for each observable. The actual error propagation takes place by inversion of the normal matrix. For certain, non-ideal, mission scenarios, one or more sub-blocks of the normal matrix may be ill-conditioned or even numerically singular, requiring some stabilization technique to be applied. In such case one usually adds certain a priori information (often some signal degree variance model like ''Kaula's rule'') to the normal matrix for preventing it from being singular. However, the consequence of such technique is that the estimates become biased. This aspect of gravity field determination has been investigated in general in terms of biased estimation and ridge regression [17] and for satellite gradiometry in particular [40,27].

Summarizing, the error propagation model, as it stands now, accepts as observables all possible gradiometric components and GPS. Our model can accept input error spectra on the level of position, velocity and acceleration. This is important if e.g. drag compensation or drag modelling needs to be studied. So far only GPS multipath effects got some special attention.

The main features of our error propagator are:
- the program accepts all six measurable gradiometer components (either in an earth-pointing or space-stable orientation) and orbit perturbations in x, y, and z on position, velocity and acceleration level (as e.g. derived by space-borne GPS); these quantities can be analyzed individually or in any combination;
- for each measurement type an appropriate spectral error model can be implemented; the model may contain band limitations and/or coloured noise;
- orbit altitude and inclination are input parameters; a circular orbit is assumed so far;
- the mission length is equal to the length of one or several ground-track repeat cycle(s); the sample rate of each observable can be chosen;

- the normal matrix can be combined with a degree variance model representing a priori information for exclusion of singularities;
- output are error variances and covariances of the set of spherical harmonic coefficients to be estimated; from these quantities an estimate of any potential functional error, e.g. the expected geoid height or gravity anomaly error, can be deduced.

With this model we are confident to produce experiment error analyses that are quite realistical, deviations being only of second order. Nevertheless, the simplicity of the procedure has its price. Such analyses cannot replace full end-to-end simulations [37]. In particular, the manner in which GPS is included is rather ''global''. For example, our procedure does not take into account the geometric constellation of the actually received GPS satellites, nor the distributions of ground sites or the actual combination of carrier-phase and pseudo-range observations. Thus for the actual analysis of real data a differential orbit determination technique should be developed, similar to what is applied in geopotential model computations from satellite tracking.

7.2.3 ARISTOTELES

So far, a dedicated gravity field mission carrying a satellite gradiometer has not flown yet. Several proposals, though, for such or similar missions have been presented, e.g. NASA's Geopotential Research Mission [41] and ESA's ARISTOTELES mission [42]. The latter was under study for several years. Its main characteristics are an on-board GPS-receiver, a planar gradiometer measuring only two gradient tensor components (second-order radial components V_{zz} and second-order cross-track component V_{yy}), non drag-free satellite resulting in a band limited and coloured noise measurement error spectrum at the 0.01 E/Hz^{½} level (1E = 10^{-9} s^{-2}), a 95° inclination and low (200 km) orbit, six months mission with 4 seconds sampling rate. In the context of the ARISTOTELES mission we participated in several projects concerning gravity field determination from SGG and SST/GPS. During the course of these projects the error analysis model and software described above were developed and improved. It was shown that the results from the spacewise and the timewise approaches coincide, at least for an ideal mission scenario (polar orbit, white measurement noise) [35] It appeared that polar gaps and limitations of the measurement bandwidth due to disturbing accelerations, strongly influence the quality of the results obtained from such missions. The existence of polar gaps makes the application of some stabilization technique inevitable. Band limitation, especially lower band limitation, causes the lower degrees of the gravity field spectrum to become inestimable and distorts the remaining part of the spectrum [35,43]. The long-wavelength problem thus requires the application of the complementary technique of space-borne GPS. Study of error sources in case of GPS was performed as far as it concerns multipath effects. It appeared, however, that for a mission like ARISTOTELES, multipath effects play no important role [44]. Furthermore, the influence of orbital altitude and mission duration, was made clear by means of error analysis studies [43].

Results are usually presented in terms of error degree variance spectra of the solved potential coefficients and global error r.m.s. values for gravity anomalies and geoid undulations. Thereby it is not to be forgotten that, depending on further applications, the results from the error propagation only represent the commission part of the error. The gravity field, in reality, is a continuum to be represented by an infinite number of harmonics. The part of this spectrum which cannot be solved from SGG or SST/GPS has to be regarded as omission error [43].

Parallel to the development of the ARISTOTELES gradiometer and satellite, a scientific study was performed for ESA by a consortium of several European scientific institutes. This study focused on gravity field determination methods and missions with, at first instance, emphasis on ARISTOTELES/SGG but turning into a general study for the combination SGG and SST/GPS [45,46,47]. Our main contribution in these projects concerned the theoretical background of global gravity field analysis from space, the development of the error analysis software for SGG and SST/GPS, analytical and numerical techniques involved in the error analysis model and extensive gravity field analysis simulations. The goals for a combined SGG/SST mission would be to improve our current knowledge of the earth's gravity field up to a resolution of at least 100 km half wavelength (corresponding to a maximum degree and order of 180 in a spherical harmonic series expansion) and an accuracy of less than 5 mgal in terms of gravity anomalies or less than 10 cm in terms of geoid undulations. The error simulations showed that with a mission like ARISTOTELES this would have been possible, at least for the SGG/SST combination. Resolution could even be improved up to degree and order 240. SGG alone would suffer too much from the band limitations of the gradiometer so the complementary technique space-borne GPS is really needed. The coloured noise error spectrum has only a small influence on the results. This in contrast to the polar gaps, which require addition of a priori information for stabilizing the solution. It appeared that small polar gaps (up to 93° inclination) do not distort the solution but only larger gaps do (like with ARISTOTELES). Additionally many different mission scenarios (in terms of satellite altitude, inclination, mission duration, band limitation) were studied, all based on our global error analysis approach.

7.2.4 STEP

STEP (Satellite Test of the Equivalence Principle) is a joint ESA/NASA mission in the discipline area of fundamental physics. Its scientific objectives are:
- to test the Equivalence Principle to one part in 10^{17}, six orders of magnitude better than has been achieved on the ground;
- to search for a new interaction between quantum-mechanical spin and ordinary matter, and
- to determine the constant of gravity G with a precision of one part in 10^6 and to test the validity of the inverse square law (ISL) with the same precision, both two order of magnitude better than has been achieved on the ground.

The extreme demands of the fundamental physics experiments on STEP in terms of drag-free environment, cryogenics for the use of superconducting electronics and precise accelerometry, also offer an opportunity for a unique geodesy experiment. STEP will consist of several superconducting accelerometers, two of which can be used as a very precise one-axis gradiometer, in this particular case measuring the second order cross-track gradient V_{yy}. With STEP's orbit rather low (550 km) and almost polar ($i = 97°$) the global gravity field can be mapped with considerable detail. The long wavelength features of the gravity field are extracted from the orbit which is determined with cm-level precision since the satellite is drag-free and continuously tracked in three dimensions using GPS. Laser reflectors mounted on the satellite remove ambiguities and convert this precision to accuracy.

The medium wavelengths (down to 130 km half wavelength) are derived from SGG using the two G/ISL accelerometers. They will provide the out-of-plane gravity gradient component with a precision of 10^{-4} E/Hz^{½}. This extremely high precision largely compensates for the natural attenuation effect with height. The combination of the two geodesy elements (gradiometry and GPS) on a drag-free satellite are unique and would result in a gravity field which comes close to that from ARISTOTELES, see Figure 7.4..

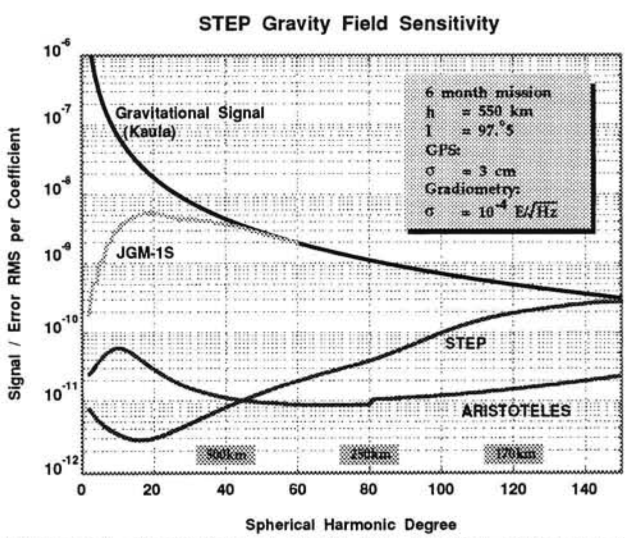

Figure 7.4 Comparison of gravity field recovery performance from STEP and Aristoteles in relation to current knowledge.

Delft participated in the STEP Phase A study [48]. Many mission scenarios have been investigated on their gravity field recovery capabilities [39], using the error analysis techniques described above. The baseline configuration (550 km altitude, 97°.5 inclination, six months mission, GPS tracking, out-of-plane single axis gradiometer with precision 10^{-4} E/Hz^{½}) would increase our knowledge of the gravity field enormously. The long wavelengths (up to degree 70) would gain 2-3 orders in precision, while the resolution would improve up to degree and order 150 approximately (half wavelength 130 km). Reduction of the satellite altitude would give the STEP-satellite even "ARISTOTELES"-capabilities. Furthermore, the STEP drag-free system has been evaluated, i.e. the effect of residual drag-free noise on the gravity field recovery.

7.3 Gravity and geoid

Study of the gravity field of the earth has been a major task of geodesy. The geoid is the equipotential surface of the earth at mean sea level. Its classical determination requires gravity to be available all over the earth. In recent years the geometric shape of the earth, continents and ocean surface, became measurable with an unprecedented precision, due to the enormous progress of space methods like GPS and altimetry.

In geodesy the geoid is the reference surface for height measurements. The classical method to determine the height above the geoid is levelling. This is a very time consuming and expensive method. However with modern space techniques like GPS positioning, it is possible to determine the topographic heights independently. A necessary condition is that the geoid must be available with a very high precision. In modern geodesy we use global reference systems which should be connected to the local systems by datumshift transformations. For the connection of the height datums in the different continents and for the connection of the horizontal datum points it is also necessary to know the gravity field or more precise the geoid.

7.3.1 Gravity measurements

Characteristic for the data collection in The Netherlands is the position near the sea. For geoid computation we need data up to a distance of at least 500 km around the country. The collection of sea gravity data is therefore a necessity. Dutch gravity measurements are divided in four steps: the absolute gravity measurements on four points, the relative gravity measurements (first order net) of about 40 points, the relative gravity measurement (second order net) with point distance of 2 km and the gravity measurements at sea.

A general overview of most of these gravity activities is given in [49] and are briefly described in the sections below. Next to this work, theoretical research was done on orthometric corrections which must be applied to levelling measurements [50]. The new results have great impact on practical computations.

Absolute gravity measurements

To determine the scale and absolute level of the Netherlands gravity net, it is necessary to determine three or four absolute gravity points. These measurements give also a reliable connection to the international gravity network. Secondly, repeated measurements give us an insight in the change of gravity in time. This is important in connection with the study of land subsidence and sea level change.

In the Netherlands such an instrument is not available, therefore the Institut für Erdmessung in Hannover was asked to execute these measurements. In 1991 three stations were measured: Delft, Kootwijk and Westerbork. The measurements in Kootwijk and Westerbork were very accurate, they have a precision of a few parts of 10^{-9} g. However, Delft was less accurate (3.10^{-8} g) due to micro seismics caused by the unstable ground [51]. Since three good stations was the minimum condition for determining the scale and stability of the network, it was decided to measure a forth station in 1993. This one is situated in Epen, South Limburg, in a newly built seismic station of the KNMI. It turned out that this station was extraordinary stable, one of the best stations in Europe. Also Kootwijk was measured again.

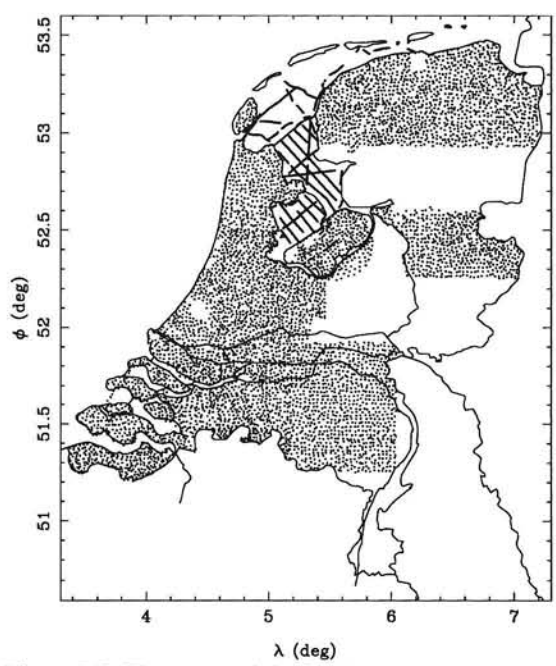

Figure 7.5 The status of the Dutch gravity network on December 1993

First order gravity net

Relative gravity measurements are carried out by extraordinary precise spring gravimeters. The extension of the spring is a measure for the gravity. Only gravity differences between points can be measured with this method, as the name relative gravity measurements indicates. In 1984 a Lacoste Romberg gravimeter was purchased and in the same year a new gravity net was measured. In 1985 a contract was agreed with the Survey department of Rijkswaterstaat (RWS) to set up a common gravity network. In 1987 and 1990 RWS measured a first order net which will be combined with the net of the DUT. The adjustment of the gravity networks is done by the DUT. In future the first order network will be remeasured with intervals of three to five years, in order to determine gravity changes in time [49].

Second order network

For precise geoid computation it is necessary to have a very dense gravity network of one point per 5 square km. In 1989 and 1990 some testnets were measured near Eindhoven and in South Limburg [52]. In 1991 RWS started with the big job to measure the whole country of the Netherlands. This will be finished in 1994. DUT is actively participating in adjustment of the measurements and quality control of several aspects of the project. This gravity network will not be the first second order network; see figure. Already in the fifties Royal Dutch/Shell measured a detailed gravity network, however with less accurate instruments.

Sea-gravimetry

In the footsteps of Vening Meinesz the DUT continued the sea gravity measurements after 1960. A modern sea gravimeter was purchased and used in several international projects. In recent years there has been cooperation in the following sea gravity expeditions [53,54,55]:

- 1985: *Snellius* expedition in Indonesia, with University of Amsterdam.
- 1986: *Navgrav* expedition on the North Sea.
- 1991: *Survey* western Mediterranean, with University of Amsterdam.
- 1992: *Wadgrav* survey on the IJsselmeer and Waddenzee.

The Navgrav and Wadgrav expeditions on the North Sea and IJsselmeer respectively were specially organized to complete the gravity database on land. This was necessary for the precise geoid computation. The Navgrav expedition covered the dutch part of the North Sea. The ship tracks had a spacing of 20 km. 20000 point values were registrated. The precision could be checked on 350 cross points, giving a precision of 1.1 mgal. The Wadgrav expedition is a similar expedition on the Waddenzee and the IJsselmeer.

7.3.2 Geoid computation

As mentioned before geoid computation is necessary for several purposes, both scientific and practical. To compute the geoid with a precision of one cm is a big problem. Accurate gravity measurements are needed all over the earth. For the long wavelength structure of the gravity field the gravity model OSU91 is used [56].

This is a model in terms of spherical harmonics up to degree 360, equivalent to a resolution of $1^{\circ}\times 1^{\circ}$ gravity values. In Europe the data is completed by a 10×10 km^2 dataset provided by the University of Hannover [57]. In the Netherlands the gravity field should be measured in most detail. The described gravity campaign will provide us with a point density of one point per 5 km^2. The sea gravity campaigns will complete the picture.

If the measurements are available it is still possible to use different methods of computation, each having its own advantages, disadvantages and approximations. Main topics of research are the comparison of the methods, improvement and renewal, estimation of all kinds of small error sources, and computation of the final precision. Theoretical and practical comparison of different methods like several numerical integration techniques and collocation are done [58]. One of those methods using point gravity values and a triangulation network [59] was developed ten years ago, but in 1992 further improved [60] with promising results. Although all methods start from the same continuous formula on the sphere too large errors show up in the different solutions, which need to be investigated more closely in the near future. A planar method based upon two dimensional FFT, which was widely used in geodesy for geoid computation from gravity data was given a complete new direction with an approximated spherical 2D FFT method [61]. Many approximations appeared to be unnecessary. This method was successfully applied for the geoid computation of the USA [62]. Later a final improvement of this method without any approximations was found at DUT based upon one dimensional FFT and numerical integration [63]. This method has a lot of international attention, and already led to an improved geoid for Canada and part of the USA [64]. The two dimensional FFT methods especially show large errors in mountainous areas. Further studies gave an inventory and estimation of many sources of errors in the geoid computation process [65] and an improved way to describe error propagation of gravity data to geoid heights [66]. With the publication of the geopotential field GEM-T1 in 1988, a complete variance/covariance matrix of the coefficients was made available for the first time. With this information the global characteristics of the error covariances of geoid heights exclusively derived from this model can be directly determined. In local geoid computations a geopotential model is used for the long wavelengths. The influence of neglected correlations for errors and geoid heights was studied. It was found that the neglect of the error covariances of this model can lead to errors up to 10 - 20 cm in the local geoid [67].

7.4 References

1. Rummel, R., and P.J.G. Teunissen, *Horizontal Type Boundary Value Problem, Least-Squares Collocation and Astronomical Levelling*, Geodaetisk Institut, Meddelelse, 58, Festschrift to T. Krarup, eds.: E. Kejlsø, K. Poder and C.C. Tscherning, 285-297, Denmark.

2. Krarup, T., *A Convergence Problem in Collocation Theory*, Boll. Geod. Scie. Aff., **3**, 225-241, 1981.

3. Gelderen, M. van, *The Geodetic Boundary Value Problem in Two Dimensions and its Iterative Solution*, Netherlands Geodetic Commission, New Series, **35**, 1992.

4. Sansò, F., *The Geodetic Boundary Value Problem in Gravity Space*, Memorie, **14**, 1a, 3-97, 1977.

5. Gerontopoulos, P., *Molodenskii's Problem in the Plane*, Mitteilungen der geodätischen Institut der TU Graz, **32**, 1978.

6. Meissl, P., *A Study of Covariance Functions Related to the Earth's Dist. Potential*, OSU-report, 151, 1971.

7. Rummel, R., P. Teunissen, M. van Gelderen, *Uniquely and Overdetermind Geodetic Boundary Value Problems by Least Squares*, Bull. Geod., 63, 1989.

8. Gauss, C.F., *Methodus Nova Itegralium Valores per Approximation Inveniendi*, in: Werke, Göttingen, Königliche Gesellschaft der Wissenschaften, C.F. Gauss, 163-196, 1814.

9. Gauss, C.F., *Allgemeine Theorie des Erdmagnetismus*, in Gauss and Weber: Resultate aus den Beobachtungen des Magnetischen Vereins im Jahre 1838, Göttingen und Leipzig, 121-193, 1838.

10. Neumann, F., *Über eine neue Eigenschaft der Laplaceschen Y(ñ) und ihre Anwendung zur analytischen Darstellung derjenigen Phänemene, welche Funktionen der geographischen Länge und Breite sind*, Schumachers Astron. Nachr., 313-325, (reprinted in Math. Ann., 567), 1838.

11. Neumann, F., *Vorlesungen über die Theorie des Potentials und der Kugelfunktionen, Leipzig*, Teubner, 135-154, 1887.

12. Ellsaesser, H.W., *Expansion of Hemispheric Meteorological Data in Antisymmetric Surface Spherical Harmonic (Laplace) Series*, J. Appl. Meteorology, 263-276, 1966.

13. Sneeuw, N.J., *Discrete Spherical Harmonic Analysis: Neumann's Approach*, in: Geodesy and Physica of the Earth, Symp. No. 112, Potsdam, Germany, Oct, 5-10, 1992 (eds.: H. Montag & Ch. Reigber), Springer, 233-236, 1993.

14. Sneeuw, N.J., *Global Spherical Harmonic Analysis by Least Squares and Numerical Quadrature Methods in Historical Perspective* (submitted for publication in Geophysical Journal International).

15. Bun, R.J.G., *Bolfunctieontwikkeling met de 2D-Fourier transformatie*, thesis, Delft University of Technology, 1993.

16. Reigber, C., *Gravity Field Recovery from Satellite Tracking Data*, in: Lecture Notes in Earth Sciences, **25**, Theory of Satellite Geodesy and Gravity Field Determination, F. Sansò, R. Rummel (Eds.), Springer-Verlag, Berlin, Heidelberg, New York, 1989.

17. Xu, P.L. and R. Rummel, *The Value of Minimum Norm Estimation of Geopotential Fields*, Geophysical Journal International, **111**, 170-178, 1992.

18. Rummel, R. and E.J.O. Schrama, *Two Complementary Systems On-board 'Aristoteles': Gradio and GPS*, ESA Journal, **15**, 135-139, 1991.

19. Visser, P.N.A.M., *The use of satellites in gravity field determination and model adjustment*, Dissertation, Delft University of Technology, Delft University Press, ISBMN 90-6275-802-9/CIP, 1992.

20. Visser, P.N.A.M., K.F. Wakker, B.A.C. Ambrosius, *Global gravity field recovery from the ARISTOTELES satellite mission*, 11 p., J. Geophys. Res., **99**, B2, 2841-2851, February 10, 1994.

21. Koop, R. and D. Stelpstra, *Potential Coefficient Recovery from the CSR Set of Simulated Satellite Gradiometry Observations*, Geophysical Research Letters, **18**, 10, 1897-1900, 1991.

22. Balmino, G., J. Barriot, R. Koop, B. Middel, N.C. Thong and M. Vermeer, *Simulation of Gravity Gradients: A Comparison Study*, Bulletin Géodésique, **65**, 218-229, 1991.

23. Rummel. R., M. van Gelderen, R. Koop, E. Schrama, F. Sansò, M. Brovelli, F. Miggliaccio and F. Sacerdote, *Spherical Harmonic Analysis of Satellite Gradiometry*, Netherlands Geodetic Commission, Publications on Geodesy, New Series, **39**, 1993.

24. Misner, C.W., K. Thorne and J.A. Wheeler, *Gravitation*, Freeman, New York, 1973.

25. Rummel, R., *Satellite Gradiometry*, in: Lecture Notes in Earth Sciences, **7**, Mathematical and Numerical Techniques in Physical Geodesy, H. Sünkel (Ed.), Springer-Verlag, Berlin, Heidelberg, New York, 1986.

26. Soffel, M.H., *Relativity in Astrometry, Celestial Mechanics and Geodesy*, Springer-Verlag, Berlin, Heidelberg, New York, 1989.

27. Koop, R., *Global Gravity Field Modelling using Satellite Gravity Gradiometry*, Netherlands Geodetic Commission, Publications on Geodesy, New Series, **38**, 1993.

28. Rummel, R. and O.L. Colombo, *Gravity Field Determination from Satellite Gradiometry*, Bulletin Géodésique, **59**, 233-246, 1985.

29. Kaula, W.M., *Theory of Satellite Geodesy*, Blaisdell, Waltham, Massachusetts, 1966.

30. Sneeuw, N.J., *Inclination Functions. Group Theoretical Background and a Recursive Algorithm*, Faculty of Geodetic Engineering / Dept. of Mathematical and Physical Geodesy, report **91.2**, Delft University of Technology, 1991.

31. Sneeuw, N.J., *Representation Coefficients and Their Use in Satellite Geodesy, Manuscripta Geodaetica*, **17**, 117-123, 1992a.

32. Emeljanov, N.V. and A.A. Kanter, *A Method to Compute Inclination Functions and their Derivatives*, Manuscripta Geodaetica, **14**, 77-83, 1989.

33. Schrama, E.J.O., *The Role of Orbit Errors in Processing of Satellite Altimeter Data*, Netherlands Geodetic Commission, Publications on Geodesy, New Series, **33**, 1989.

34. Sneeuw, N., *Non-singular Cross-track Derivatives of the Gravitational Potential using Rotated Spherical Harmonics*, in: From Mars to Greenland: Charting Gravity with Space and Airborne Instruments, O.L. Colombo (Ed.), IAG nr.110, Springer-Verlag, New York, 349-357, 1992b.

35. Koop, R., E.J.O. Schrama, R. Rummel and M. van Gelderen, *Gravity Field Recovery Performance*, Aristoteles Add-On Study, Part 1, Dornier W.P., 2410/1, 1989.

36. Colombo, O.L., *The Global Mapping of the Gravity Field with an Orbiting Full-Tensor Gradiometer: an Error Analysis*, presented at XIX Assembly of the IUGG, Vancouver, Canada, 1987.

37. Balmino, G. and J. Barriot, *Methods of Global Recovery of Harmonic Coefficients from SGG in the General Case*, Workpackage 520, Study on Precise Gravity Field Determination Methods and Mission Requirements, Final Report (Phase 2), ESA Contract No. 8153/88/F/FL, 1990.

38. Schrama, E.J.O., *Gravity Field Error Analysis: Application of GPS Receivers and Gradiometers on Low Orbiting Platforms*, NASA Technical Memorandum, 100769, 1990.

39. Sneeuw, N., R. Koop and E. Schrama, *Global gravity Field Error Analysis for the STEP Geodesy Co-experiment using GPS and Gradient Observations*, Pisa STEP Symposium, 1993.

40. Xu, P.L., *Determination of Surface Gravity Anomalies using Gradiometric Observables*, Geophysical Journal International, **110**, 321-332, 1992.

41. Keating, T., P. Taylor, W. Kahn and F. Lerch,, *Geopotential Research Mission*, science, engineering and program summary, NASA Technical Memorandum 86240, 1986.

42. ESA, *The Solid-Earth Mission ARISTOTELES*, Proceedings of an International Workshop, Anacaori, Italy, ESA SP-329, 1991.

43. Koop, R., R. Rummel and E.J.O. Schrama, *Commission and Omission Error*, ALENIA - ESA/NASA Cooperative Study, 1991.

44. Alenia, ARISTOTELES - Rider 1 Study, 1993.

45. CIGAR I, *Study on Precise Gravity Field Determination Methods and Mission Requirements*, Final Report Phase 1, ESA Contract 7521/87/F/FL, 1988.

46. CIGAR II, *Study on Precise Gravity Field Determination Methods and Mission Requirements*, Final Report Phase 2, ESA Contract 8153/88/F/FL, 1990.

47. CIGAR III, *Study of the Gravity Field Determination using Gradiometry and GPS*, Final Report Phase 1, ESA Contract 9877/92/F/FL, 1993.

48. Blaser, J.-P., M. Bye, G. Cavallo, T. Damour, C.W.F. Everitt, A. Hedin, R.W. Hellings, Y. Jafry, R. Laurance, M. Lee, A.M. Nobili, H.J. Paik, R. Reinhard, R. Rummel, M.C.W. Sandford, C. Speake, L. Spencer, P. Swanson, P.W. Worden Jr., *STEP: Satellite Test of the Equivalence Principle*, Report on the Phase A Study, ESA/NASA SCI (93) 4, 1993.

49. Min, E.J. de, *Themanummer zwaartekracht*, Geodesia, 2, 1993.
Strang van Hees, G.L., *Geoïde en zwaartekracht; coördinaatstelsels en hoogtesystemen*, Geodesia, 2, 1993.
Lorenz, G.K., and R.E. van Ree, *Absolute zwaartekrachtmetingen*, Geodesie, 2, 1993.
Min, E.J. de, and P. Plugers, *Relatieve zwaartelrachtmetingen*, Geodesia, 2, 1993.

50. Strang van Hees, G.L., *Practical Formulas for the Computation of the Orthometric*, Dynamic and Normal heights, Zeitschrift fur Vermessungswesen, **117**, 11, 727-734, 1992.

51. Ree, R.E. van, *Absolute zwaartekracht in Nederland*, Afstudeerscriptie Faculteit der Geodesie, Technische Universiteit Delft, 1991.

52. Nohlmans, R.A.M., *Gravity measurement, processing and evaluation, Test cases de Peel and South-Limburg*, Afstudeerscriptie Faculteit der Geodesie, Technische Universiteit, Delft, 1990.

53. Strang van Hees, G.L., *Gravity in the Banda Sea*, Snellius II Expedition, Indonesia, Bureau Gravimetrique International, Bulletin d'Information, **72**, 1993.

54. Strang van Hees, G.L., *Navgrav, Navigation and Gravimetric experiment at the Northsea*, Publication of the Netherlands Geodetic Commission, 32, 1989.

55. Woodside, J., D. Jongsma, M. Thommeret, G. Strang van Hees, T. Puntodewo, *Gravity and Magnetic field measurements in the eastern Banda Sea* Netherlands Journal of Sea Research, 24, 185-203, 1989.

56. Rapp, R., Y.M. Wang and N.K. Pavlis, *The Ohio State 1991 geopotential and sea surface topography harmonic coefficient models* Report 410, Dept. of Geodetic Science and Surveying, The Ohio State University, Columbus, 1991.

57. Torge, W., G. Weber, and H.-G. Wenzel, *6' x 10' free air gravity anomalies of Europe including Marine Areas*, Universität Hannover, 1983.

58. Min, E.J. de, *A comparison of three geoid computation methods* Proc. of Session G3 - EGS XVIII General Assembly, Wiesbaden, Germany, May 3-7, 1993.

59. Rummel, R., *Gravity parameter estimation from large data sets using stabilized integral formulas and a numerical integration based on discrete point data*, Report 339, Dept. of Geodetic Science and Surveying, Columbus, The Ohio State University, 1982.

60. Burger, M., *Geoïdebepaling*, afstudeerscriptie TU Delft, 89, 1993.

61. Strang van Hees, G.L., *Stokes formula using Fast Fourier Techniques*, Manuscripta Geodaetica, **15**, 4, 1990.

62. Milbert, D.G., *Geoid90; a high-resolution geoid for the United States*, EOS, Trans., AGU, **72**, 49, 1991.

63. Haagmans, R. E. de Min, M. van Gelderen, *Fast evaluation of convolution integrals on the sphere using 1D-FFT, and a comparison with existing methods for Stokes' integral*, Manuscripta Geodaetica, **18**, 5, 1993.

64. Sideris, M.G., *A New, High-Resolution Geoid for Canada and Part of the U.S. by the 1D-FFT Method*, Presented at the IAG General Meeting, Beijng, P.R. China, 1993.

65. Min, E.J. de, *On the Computation of the Geoid and its Errors, with special Attention to the Inner Zone*, afstudeerscriptie TU Delft, 1990.

66. Strang van Hees, G.L., *Precision of the geoid, computed from terrestrial gravity measuremeents*, Manuscripta Geodaetica, 1986.

67. Haagmans, R.H.N., M. van Gelderen, *Error Variances-Covariances of GEM-T1: Their Characteristics and Implications in Geoid Computation*, J. of Geoph. Res., **96**, B12, 20,011-20,022, 1991.

8 Outlook

The project Earth Oriented Space Research at Delft University of Technology covers a major part of the space-geodetic component of the multi-disciplinary issue of global change. Crustal motions, the gravity field, ocean currents and mean sea level are all interrelated features of an incredibly complex and dynamic system in which the solid earth interacts with the oceans and atmosphere. As such, a research project like this one necessarily is a long-term effort and the team at DUT is aware of its responsibility to continue to develop and deploy its expertise in space-geodesy in the study of global change. In the summer of 1993, the team therefore issued a new research plan for the project Earth Oriented Space Research at Delft University of Technology, covering the period 1994 - 1997 [Wakker, K.F., P.J.G. Teunissen, and E. Vermaat, *Earth Oriented Space Research at Delft University of Technology*, Research plan 1994 - 1997, Faculty of Geodetic Engineering and Faculty of Aerospace Engineering, Delft University of Technology, Delft, July 1993].

The space-geodetic techniques, including the modeling aspects, seem to continue to improve by an order of magnitude over each decade. Global station positions are now being determined with sub-centimeter accuracy and satellite orbits can be reconstructed at the few centimeter level. Even the orbits of "flying monster" satellites, not at all optimized for precise orbit determination, e.g. the low-flying ERS-1 and the satellites of the high-altitude GPS constellation, can be modeled with unprecedented precision. Still, the precision of the measurement systems is at least one order of magnitude higher than the accuracy of the current models. This means that there is a continuous drive for further improvement of the results.

A key problem in the application of space-geodetic techniques is the modeling of the gravity field of the earth. Over the last decade, dramatic improvements have been achieved in this area, primarily through the analysis of the tracking data of a large variety of satellites. However, further developments are now limited by the lack of suitable measurement information. Therefore, a new class of satellites is required which will be able to sense the higher-frequency variations of the gravity field by flying into lower orbits. They will provide in-situ observations using new measurement devices such as gravity gradiometers and space-borne GPS receivers.

For this purpose, several missions have been studied and proposed (e.g. GRM, ARISTOTELES, STEP and GP-B), but none of them has been approved until now. Besides, the orbital characteristics of all but one of these missions are sub-optimal, because gravity field research is not the primary goal of those missions. So, there is still a great interest to fly a dedicated gravity mission. Therefore, it may be useful to study the possibilities to design a new slightly less ambitious mission which might be executed by a small cheap satellite, carrying only a geodetic precision GPS receiver as payload, and flying in a low, decaying orbit.

An important research area which will benefit from an improved gravity field is the oceanography. Such improvement will allow a better separation of the dynamic sea surface topography from the geoid, which is crucial for a better understanding of the ocean circulation system. This research area has also received a significant boost from the successful ERS-1 and TOPEX/Poseidon missions, which have provided an enormous amount of invaluable radar altimeter measurements. It is of extreme importance that the time-series of measurements compiled by these missions be continued in the future, so that long-term variations in the ocean circulation system and in mean sea-level can be detected. Therefore, there is a large interest in the upcoming ERS-2 and ENVISAT missions, which will hopefully provide these measurements.

Another measurement technique which has been decisive for the recent advances in space geodesy is SLR. The global SLR record now dates back some twenty years. Extremely precise reference system definition on a global scale has resulted, with unique contributions to the monitoring of the rotation of the earth over these years and providing a stable reference for global tectonic plate motion models and for constraining regional networks for crustal deformation studies in plate boundary regions. Especially the orbits of high satellites (e.g LAGEOS-1 and -2) have proven to provide a unique long-term stable framework for these applications. It is considered of utmost importance, that the joint groups continue to support the maintenance of the historical records based on the SLR technique, at state-of-the-art level, by exploiting its expertise and capabilities in this area.

A further motivation to continue the SLR effort is the increasingly important role of GPS in high-precision positioning. It calls for a new strategy of deploying the transportable SLR systems, optimally answering to the complementary role of SLR as compared to the significantly increased capability of GPS. It is of major importance that this new strategy will preserve the history of the epoch measurements, which have been obtained in the previous years, e.g. in the WEGENER/MEDLAS project in the Mediterranean. Similarly, this strategy should encompass the measurements of fiducial sites elsewhere, satisfying the programs for the study of post-glacial uplift and mean sea level change. In all areas, emphasis needs to be placed on the vertical component of position, for which SLR is particularly suited.

The GPS Global Positioning System, which has already been mentioned twice above, has evolved into a major measurement technique over the last decade, and will certainly find increased application in the foreseeable future. The trend is towards continuously operating permanent networks at local regional and global scales. The International GPS Service for geodynamics (IGS) has set a standard for the global network and is seeking densification at regional scales. An example of this could be the dedicated GPS network for WEGENER (WEGNET), which is currently being studied. Through overlap with IGS, it would provide access to the global reference frame established by this service, for small-scale local or national measurement campaigns. Also, such continuous monitoring regional networks will provide "real-time" information on the deformations in those networks. The joint groups at DUT can provide significant contributions to these developments. Apart from their commitments to the WEGENER project, since 1994, they are already involved in a GPS research project in South-East Asia, sponsored by the EU. Also, there are serious plans to provide assistance in the establishment of a new IGS site in Indonesia.

Another important application of GPS is for low-earth satellite tracking. The first experimental geodetic-precision receiver was successfully flown in 1992 onboard the TOPEX/Poseidon satellite. It demonstrated that this tracking concept has enormous advantages, since it provides 3-dimensional coverage, which makes the orbit determination almost independent of dynamical modeling. Conversely, this also means that the dynamical models, in particular the gravity field, can be improved using the GPS tracking data from low-orbit satellites. This principle has also already been demonstrated on basis of the TOPEX/Poseidon data, and forms the background of missions like ARISTOTELES and the proposed dedicated GPS-based gravity field mission mentioned earlier. It is expected that there will be a large increase in this application of GPS. The joint groups at DUT are very interested in these developments and have all the capabilities to participate in the data analysis.

The need for strengthening the capability for geophysical interpretation of the research results has been of concern for some time now and it motivated us to embed our research to a large extent in international programs, e.g. the WEGENER, Crustal Dynamics, ERS-1 and TOPEX/Poseidon projects. Through that cooperation, expertise has been accumulated within the team, regarding the geophysical and oceanographic significance of space-geodetic results. In addition, in the last years in particular, the contacts with the "Instituut voor Aardwetenschappen" at the University of Utrecht have been reinforced. The Delft and Utrecht groups have recognized the clear interrelation which exists between their respective research, with common interest in particular in the tectonics in the Mediterranean region. We are aware of the unique perspective of combining knowledge on tectonic motions, gravity field and geophysical processes in the earth's crust. In view of this recognition, both groups are working towards intensifying and formalizing the cooperation, possibly with the perspective of joint participation in a Research School on Earth Sciences.

Publications

The table below gives an overview of the relevant publications of the Faculty of Aerospace Engineering and the Faculty of Geodetic Engineering in the period 1990-1993. Additional investigation results, presented at meetings and conferences but not documented in Proceedings, are not included here.

Ambrosius, B.A.C., H. Leenman, R. Noomen and K.F. Wakker, *Precise orbit computations of LAGEOS for WEGENER-MEDLAS*, Adv. Space Res., **10**(3/4), 205-220, 1990.

Ambrosius, B.A.C., R. Noomen, H. Leenman, K.F. Wakker and R.J. de Muynck, *Quick-look data analysis: An overview*, Proc. of the Fourth International Conference on the WEGENER/MEDLAS Project, Scheveningen, The Netherlands, June 1989, Delft University of Technology, Delft, The Netherlands, 349-370, February 1990.

Ambrosius, B.A.C., P.N.A.M. Visser and K.F. Wakker, *On the use of GPS for the ARISTOTELES mission*, in: Dornier/ESA ARISTOTELES Additional Study Final Report, Delft University of Technology, Delft, The Netherlands, March 1990.

Ambrosius, B.A.C., R. Noomen and K.F. Wakker, *First results of WEGENER/MEDLAS data analysis*, in: Vyskocil, P., Ch. Reigber and P.A. Cross (eds.), Global and Regional Geodynamics, International Association of Geodesy Symposia, **101**, Edinburgh, UK, July 1989, 105-113, 1990.

Ambrosius, B.A.C., J.A. Bax, B.H.W. van Gelder, D.L.F. van Loon, R. Noomen, A.J.M. Verheijen, E. Vermaat and K.F. Wakker, *Positioning of the Tromsø station by satellite laser ranging; Campaign 1990 data aquisition and analysis*, Report LR-668 / MFG-91.5, Delft University Press, Delft, The Netherlands, ISBN 91-6275-745-6/CIP, November 1991.

Ambrosius, B.A.C., R. Noomen, B. Overgaauw and K.F. Wakker, *Crustal motions in Greece determined from GPS and SLR observations*, in: Mertikas, S.P. (ed.), Proc. of the International Workshop on Global Positioning Systems in Geosciences, Chania, Crete, June 8-10, 1992, Technical University of Crete, Greece, 183-207, 1993.

Ambrosius, B.A.C., *Mediterranean Sea, Environment and Geosciences*, in: Mertikas, S.P. (ed.), Proc. of the International Workshop on Global Positioning Systems in Geosciences, Chania, Crete, June 8-10, 1992, Technical University of Crete, Greece, 413-415, 1993.

Ambrosius, B.A.C., D.C. Kuijper, H. Leenman, G.J. Mets, R. Noomen and K.F. Wakker, *Earth rotation parameters derived from SLR data on LAGEOS-1*, in: IERS 1994 Technical Note on the SEARCH'92 Campaign, International Earth Rotation Service, Paris, France, December 1993 (to be published).

Balmino, G., J. Barriot, R. Koop, B. Middel, N.C. Thong and M. Vermeer, *Simulation of gravity gradients: a comparison study*, Bull. Géod., **65**, 218-229, 1991.

Beutler, G., J. Kouba and T.A. Springer, *Position paper on combining the orbits of IGS processing centers*, in: Kouba, J. (ed.), Proc. of the 1993 IGS Analysis Center Workshop, Ottawa, Canada, 19-56, October, 1993.

Blaser, J.-P., M. Bye, G. Cavallo, T. Damour, C.W.F. Everitt, A. Hedin, R.W. Hellings, Y. Jafry, R. Laurance, M. Lee, A.M. Nobili, H.J. Paik, R. Reinhard, R. Rummel, M.C.W. Sanford, C. Speake, L. Spencer, P. Swanson and P.W. Worden jr., *STEP-Satellite test of the equivalence principle*, Report on the phase A study SCI (94) 4, Report to NASA/ESA, Noordwijk, The Netherlands, 1993.

Day, G.A., O.B. Andersen, K. Engsager, E.G. Finnstrom, J. Hospers, T. Liebe, J. Makris, S. Plaumann, G. Strang van Hees and S.A. Walter, *North Sea gravity map*, in: Blundell, D.J., and A.D. Gibbs (eds.), Tectonic evolution of the North Sea rifts, Oxford Science Publications, Oxford, UK, 64-70, 1990.

Feron, R.C.V., M.C. Naeije and D. Oskam, *Quality of ocean variability results from satellite altimetry*, Marine Geodesy, **15**, 1-18, 1992.

Feron, R.C.V., W.P.M. de Ruijter and D. Oskam, *Ring shedding in the Agulhas current system*, J. of Geophys. Res., **97**(C6), 9467-9477, 1992.

Francis, C.R., A. Caporali, L. Cavaleri, A. Cenci, P. Ciotto, L. Ciraolo, W. Gurtner, F.H. Massmann, D. del Rosso, R. Scharroo, P. Spalla and E. Vermaat, *The calibration of the ERS-1 radar altimeter - The Venice calibration campaign*, ESA Report ER-RP-ESA-RA-0257, Issue 2.0, ESA/ESTEC, Noordwijk, The Netherlands, March 1, 1993.

Gelder, B.H.W. van, *Global positioning system: state of the state*, in: Polydorides, N.D. (ed.): Data acquisition for spatial information systems, vol. 7 of the series on computers in planning, URSA-NET, 36-42, 1990.

Gelder, B.H.W. van, and E. Vermaat, *Interpolating the WEGENER/MEDLAS Network by GPS*, in: Proc. of the Fourth International Conference on the WEGENER/MEDLAS Project, Scheveningen, The Netherlands, June 1989, Delft University of Technology, Delft, The Netherlands, 409-420, February 1990.

Gelderen, M. van, and R.H.N. Haagmans, *The GEM-T1 variance-covariance matrix, its characteristics and application in geoid computations*, in: Rapp, R.H., and F. Sansò, (eds.), Proc. of IAG Symposium 106 on Determination of the geoid, Present and future, Milan, Italy, June 1990, Springer-Verlag, New York, USA, 410-421, 1991.

Gelderen, M. van, *The geodetic boundary value problem in two dimensions and its iterative solution*, Ph.D. Thesis, Delft University of Technology, Delft, The Netherlands, 143 p., 1991.

Gurtner, W., G. Beutler, E. Brockmann, S. Fankhauser, M. Rothacher, T.A. Springer, S. Botton, L. Mervart, A. Wiget and U. Wild, *Automated data flow and processing at the 'Center for Orbit Determination in Europe' (CODE) during the 1992 IGS campaign*, in: Montag, H., and Ch. Reigber (eds.), Geodesy and Physics of the Earth, Proc. of IAG Symposium 112, Potsdam, FRG, October 1992, Springer-Verlag, Berlin, FRG, 20-23, 1993.

Haagmans, R.H.N., *The disturbing potential and its first and second derivatives from SEASAT altimeter data*, Rapport aan: Ministerie van Defensie, DWOO, Den Haag, Delft University of Technology, Delft, The Netherlands, 1990.

Haagmans, R., *Satellite altimetry: the ocean surface as a link between oceanography, geophysics and geodesy*, Geodetical Info Magazine, **5**(11), 29-34, 1991.

Haagmans, R.H.N., and M. van Gelderen, *Error variances-covariances of GEM-T1: their characteristics and implications in geoid computation*, J. of Geophys. Res., **96**(B12), 20,011-20,022, 1991.

Haagmans, R., E. de Min and M. van Gelderen, *Evaluation of Stokes' and other integrals using 1D-FFT and a comparison with existing methods*, in: Proc. of First Continental Workshop on the Geoid in Europe, Prague, Czechia, 348-363, 1992.

Haagmans, R., E. de Min and M. van Gelderen, *Fast evaluation of convolution integrals on the sphere using 1D FFT, and a comparison with existing methods for Stokes' integral*, Manuscripta Geodaetica, **18**, 227-241, 1993.

Haagmans, R., M.C. Naeije and R. Feron, *TOPEX/Poseidon and ERS-1; New dimensions in satellite altimetry (part 1)*, Geodetical Info Magazine (GIM), **7**(11), 46-51, November, 1993.

Haagmans, R., M.C. Naeije and R. Feron, *TOPEX/Poseidon and ERS-1; New dimensions in satellite altimetry (part 2)*, Geodetical Info Magazine (GIM), **7**(12), 69-71, December 1993.

Heck, B., and R. Rummel, *Strategies for Solving the Vertical Data Problem Using Terrestrial and Satellite Geodetic Data*, in: Sünkel, H., and T. Baker (eds.): Sea Surface Topography and the Geoid, Springer-Verlag, New York, USA, 116-128, 1990.

Hesper, E.T., B.A.C. Ambrosius and K.F. Wakker, *GPS performance on LANDSAT-5 in a satellite transmitter and ground receiver reference frame*, in: CIGAR III final study report, ESA, Paris, France, April 20, 1993.

Jong, C.D. de, *GPS - satellite orbits and atmospheric effects*, Report MFG-91.1, Faculty of Geodetic Engineering, Delft University of Technology, Delft, The Netherlands, 1991.

Koop, R., and D. Stelpstra, *Potential coefficient recovery from the CSR set of simulated satellite gradiometry observations*, Geophys. Res. Lett., **18**(10), 1897-1900, 1991

Koop, R., R. Rummel and E.J.O. Schrama, *Alenia - ESA/NASA Cooperative Study: Commission and Omission Error*, Delft University of Technology, Delft, The Netherlands, July 1991.

Koop, R., R. Rummel and E.J.O. Schrama, *Combination of GPS and SGG: Error modelling and effects on global recovery*, WP121, in: CIGAR.CISI.3: Study of the gravity field determination using gradiometry and GPS, Phase 1, Final Report, ESA contract 9877/92/F/FL, 1992.

Koop, R.J.J., *Global gravity field modelling using satellite gravity gradiometry*, Netherlands Geodetic Commission, New Series, 38, 1993.

Kootwijk Observatorium, *Position on Kootwijk - The role of the observatory for satellite geodesy at Kootwijk in the nineties*, Delft University of Technology, Delft, The Netherlands, 1991.

Kooij, M.W.A. van der, M.C. Naeije, D. Oskam and K.F. Wakker, *Preparations for the ERS-1 and TOPEX/Poseidon satellite altimetry missions*, final report BCRS project OP-3.5, BCRS-90-28, ISBN 90 5411 017, January 1992.

Kuijper, D.C., B.A.C. Ambrosius, R. Noomen and K.F. Wakker, *Analysis of SPOT-2 DORIS Data*, 43rd Congress of the International Astronautical Federation, IAF-92-0054, Washington, USA, August 28 - September 5, 1992.

Min, E.J. de, *A comparison of three geoid computation methods*, Proc. of Session G3 - European Geophysical Society, XVIII General Assembly, Wiesbaden, FRG, April 1993, Kort-og Matrikelstyrelsen, Copenhagen, Denmark, 65-70, 1993.

Naeije, M.C., K.F. Wakker, R. Scharroo and B.A.C. Ambrosius, *Observation of mesoscale ocean currents from GEOSAT altimeter data*, ISPR Journal of Photogrammetry and Remote Sensing, **47**, 347-368, November 1992.

Naeije, M.C., E. Wisse, R. Scharroo and K.F. Wakker, *Ocean dynamics from the ERS-1 35-day repeat mission*, in: Proc. of the 2nd ERS-1 Symposium: 'Space at the service of our environment', Hamburg, FRG, October 1993, ESA SP-361, 501-506, 1993.

Nerem, R.S., E.J.O. Schrama, C.J. Koblinsky and B.D. Beckley, *A preliminary evaluation of ocean topography from the TOPEX/Poseidon mission*, J. of Geophys. Res. (Oceans), TOPEX/Poseidon Special Issue, p. 24, November 1993 (to be published).

Noomen, R., B.A.C. Ambrosius and K.F. Wakker, *Results from 1986 and 1987 LAGEOS full-rate data analysis for WEGENER/MEDLAS*, Proc. of the Fourth International Conference on the WEGENER/MEDLAS Project, Scheveningen, The Netherlands, June 1989, Delft University of Technology, Delft, The Netherlands, 179-194, February 1990.

Noomen, R., B.A.C. Ambrosius and K.F. Wakker, *Earth rotation and station coordinates from four years of LAGEOS observations, DUT 90L01*, in: IERS Technical Note 5, International Earth Rotation Service, Paris, France, 61-65, June 1990.

Noomen, R., B.A.C. Ambrosius and K.F. Wakker, *Earth rotation and station coordinates computed from SLR observations on LAGEOS, DUT 91L01*, in: IERS Technical Note 8, International Earth Rotation Service, Paris, France, 117-122, October 1991.

Noomen, R., B.A.C. Ambrosius, H. Leenman, G.J. Mets and K.F. Wakker, *Earth orientation and station coordinates computed from SLR observations on LAGEOS, DUT 92L01*, in: Charlot, P. (ed.), IERS Technical Note 11, International Earth Rotation Service, Paris, France, 89-94, June 1992.

Noomen, R., B.A.C. Ambrosius, D.C. Kuijper, H. Leenman, G.J. Mets and K.F. Wakker, *Earth orientation and station coordinates from SLR observations on LAGEOS-1*, in: Charlot, P. (ed.), IERS Technical Note 14, International Earth Rotation Service, Paris, France, L-13/17, September 1993.

Noomen, R., B.A.C. Ambrosius and K.F. Wakker, *Crustal motions in the Mediterranean region determined from laser ranging to LAGEOS*, in: Smith, D.E., and D.L. Turcotte (eds.), Contributions of Space Geodesy to Geodynamics: Crustal Dynamics, Geodynamics Series, **23**, ISBN 0-87590-523-4, AGU, Washington, USA, 331-346, December 1993.

Oskam, D., *Sea surface variability in the North Sea as derived from Seasat altimetry*, Geophysical Journal International, **100**, 1-7, 1990.

Overgaauw, B., B.A.C. Ambrosius and K.F. Wakker, *Results of the analysis of the EUREF-89 GPS data from the SLR/VLBI sites*, in: Gubler, E., K. Poder and H. Hornik (eds.), Report No. 1 of the Subcommission for the European Reference Frame (EUREF), Verlag der Bayerischen Academie der Wissenschaften, Munich, FRG, 179-196, ISBN 3-7696-9795-2, December 1992.

Overgaauw, B., *Accurate height determination in The Netherlands using the Global Positioning System*, final report, contract MD 499, Delft University of Technology, Delft, The Netherlands, November 1993.

Overgaauw, B., B.A.C. Ambrosius and K.F. Wakker, *Analysis of the EUREF-89 GPS data from the SLR/VLBI sites*, Bull. Géod., **68**, 19-28, 1994.

Rothacher, M., G. Beutler, E. Brockmann, S. Fankhauser, W. Gurtner, T.A. Springer, S. Botton, L. Mervart, A. Wiget and U. Wild, *Results of the 'Center for Orbit Determination in Europe' (CODE) during the 1992 IGS campaign*, in: Montag, H., and Ch. Reigber (eds.), Geodesy and Physics of the Earth, Proc. of IAG Symposium 112, Potsdam, FRG, October 1992, Springer-Verlag, Berlin, FRG, 24-27, 1993.

Rummel, R., R. Koop and E.J.O. Schrama, *CISI Ingenierie: Study on Precise Gravity Field Determination Methods and Mission Requirements*, final report of phase 2, ESA Contract no. 8153/88/F/FL, Toulouse, France, 1990.

Rummel, R., and R.G. Hipkin, *Gravity, gradiometry and gravimetry*, Springer-Verlag, New York, USA, ISBN 3540972676, 1990.

Rummel, R., *The gravity field measured from space*, Proc. of the geodetic day in honor of Antonio Marussi, Academia Nationale dei Lincei, atti. dei convegni lincei 91, Rome, Italy, 115-124, 1991.

Rummel, R., *Solid Earth from space*, Report of the Earth observation user consultation meeting, ESA SP-1143, 1991.

Rummel, R., *On the principle of Aristoteles*, in: Proc. of the Workshop on Solid-Earth Mission Aristoteles, Anacapri, Italy, September 1991, ESA SP-239, ESA, Noordwijk, The Netherlands, 11-15, 1991.

Rummel, R., and E.J.O. Schrama, *Two complementary systems on-board 'Aristoteles': gradio and GPS*, ESA Journal, **15**, 135-139, 1991.

Rummel, R., and R.H.N. Haagmans, *Gravity gradients from satellite altimetry*, Marine Geodesy, **14**, 1-12, 1991.

Rummel, R., and P.J.G. Teunissen, *Measuring Sea Level Rise - What can Geodesy do about it?*, in: KNAW-ARA Symposium Zeespiegel fluctuaties in heden en verleden, meten en mechanismen, Amsterdam, The Netherlands, 1992.

Rummel, R., and M. van Gelderen, *Spectral analysis of the full gravity tensor*, Geophys. J. Int., **111**, 159-169, 1992.

Rummel, R., M. van Gelderen, R. Koop, E. Schrama, F. Sansò, M. Brovelli, F. Miggliaccio and F. Sacerdote, *Spherical harmonic analysis of satellite geodesy*, Netherlands Geodetic Comission, 39, ISN 0165 1706, Delft, The Netherlands, 1993.

Rummel, R., and F. Sansò (eds.), *Satellite altimetry in geodesy and oceanography*, Springer-Verlag, Berlin, FRG, ISBN 3-540-56818-2, 1993.

Rummel, R., *On the principles and prospects of gravity field determination by satellite methods*, in: Montag, H., and Ch. Reigber (eds.), Geodesy and Physics of the Earth, Proc. of IAG Symposium 112, Potsdam, FRG, October 1992, Springer-Verlag, Berlin, FRG, 67-70, 1993.

Scharroo, R., K.F. Wakker, R. Noomen, B.A.C. Ambrosius and H. Leenman, *On the along-track acceleration of LAGEOS*, Proc. of the Fourth International Conference on the WEGENER/MEDLAS Project, Scheveningen, The Netherlands, June 1989, Delft University of Technology, Delft, The Netherlands, 87-103, February 1990.

Scharroo, R., K.F. Wakker, B.A.C. Ambrosius and R. Noomen, *On the along-track acceleration of the LAGEOS satellite*, J. of Geophys. Res., **96**(B1), 729-740, January 1991.

Scharroo, R., K.F. Wakker, B. Overgaauw and B.A.C. Ambrosius, *Some aspects of the ERS-1 radar altimeter calibration*, paper IAF-91-367 presented at the 42nd Congress of the International Astronautical Federation, Montreal, Canada, October 1991.

Scharroo, R., K.F. Wakker, B.A.C. Ambrosius, R. Noomen, W.J. van Gaalen and G.J. Mets, *ERS-1 precise orbit determination*, Adv. Astr. Sci., **84**, part I, 293-307, 1993.

Scharroo, R., K.F. Wakker, B.A.C. Ambrosius, R. Noomen, W.J. van Gaalen and G.J. Mets, *ERS-1 precise orbit determination*, ESA SP-359, ESA, Paris, France, 477-482, March 1993.

Scharroo, R., K.F. Wakker and G.J. Mets, *The orbit determination accuracy of the ERS-1 mission*, in: Proc. of the 2nd ERS-1 Symposium: 'Space at the service of our environment', Hamburg, FRG, October 1993, ESA SP-361, 735-740, 1993.

Schrama, E.J.O., D. Oskam and R. Rummel, *Geodätische Aspekte bei der Verarbeitung von Satellitenaltimetriedaten*, Zeitschrift für Vermessungswesen, **115**(1), 13-23, 1990.

Schrama, E.J.O., *Gravity field error analysis: applications of global positioning system receivers and gradiometers on low orbiting platforms*, J. of Geophys. Res., **96**(B12), 20,041-20,051, November 10, 1991.

Schrama, E.J.O., *Some remarks on several definitions of geographically correlated orbit errors: consequences for satellity altimetry*, Manuscripta Geodaetica, **17**, 282-294, 1992.

Schrama, E.J.O., *Frozen orbits and their application in satellite altimetry*, in: Rummel, R., and F. Sansò (eds.), Lecture Notes in Earth Sciences, 50, Satellite Altimetry and Oceanography, Springer-Verlag, Berlin, FRG, ISBN 3-540-56818-2, 443-452, 1993.

Schrama, E.J.O., and R.D. Ray, *A preliminary tidal analysis of TOPEX/Poseidon altimetry*, J. of Geophys. Res. (Oceans), TOPEX/Poseidon Special Issue, pp. 18, October 1993 (to be published).

Schuyer, M.S., P.N.A.M. Visser and K.F. Wakker, *The role of the on-board GPS receiver in the ARISTOTELES satellite mission*, in: Mertikas, S.P. (ed.), Proc. of the International Workshop on Global Positioning Systems in Geosciences, Chania, Crete, June 8-10, 1992, Technical University of Crete, Greece, 347-356, 1993.

Shum, C.K., B.D. Tapley, B.J. Kozel, P.N.A.M. Visser, J. Ries and J. Seago, *Precise orbit analysis and global verification results from ERS-1 altimetry*, in: Proc. of the 2nd ERS-1 Symposium: 'Space at the service of our environment', Hamburg, FRG, October 1993, ESA SP-361, 747-750, 1993.

Smith, A.J.E., E.T. Hesper, D.C. Kuijper, G.J. Mets, B.A.C. Ambrosius and K.F. Wakker, *TOPEX/Poseidon data analysis study*, mid-term report, ESOC contract study 3-7619/92/D/IM, Delft University of Technology, Delft, The Netherlands, November 1993.

Sneeuw, N.J., *Inclination functions, Group theoretical background and a recursive algorithm*, Report MFG-91.2, Faculty of Geodetic Engineering, Delft University of Technology, Delft, The Netherlands, 1991.

Sneeuw, N.J., *Representation coefficients and their use in satellite geodesy*, Manuscripta Geodaetica, **17**, 117-123, 1992.

Sneeuw, N., *Non-singular cross-track derivatives of the gravitational potential using rotated spherical harmonics*, in: Colombo, O.L., (ed.), From Mars to Greenland: Charting gravity with space and airborne instruments, IAG Symposium 110, Vienna, 1991, Springer-Verlag, New York, USA, 349-357, 1992.

Sneeuw, N., R. Koop and E. Schrama, *Global gravity field error analysis for the STEP geodesy co-experiment using GPS and gradient observations*, Proc. of STEP Symposium, Pisa, Italy, April 1993 (to be published).

Sneeuw, N., *Discrete spherical harmonic analysis: Neumann's approach*, in: Montag, H., and Ch. Reigber (eds.): Geodesy and Physics of the Earth, Proc. of IAG Symposium 112, Potsdam, FRG, October 1992, Springer-Verlag, Berlin, FRG, 233-236, 1993.

Soler, T., and B.H.W. van Gelder, *Research note on covariances of eigenvalues and eigenvectors of second-rank symmetric tensors*, Geophys. J. Int., **105**, 537-546, 1991.

Springer, T.A., and G. Beutler, *Towards an official IGS orbit by combining the results of all IGS processing centers*, Proc. of 1993 IGS Workshop, Bern, Switzerland, 242-250, March 26, 1993.

Springer, T.A., *GIPSY-OASIS II and GPS related research at DUT/SSR&T*, GIPSY-OASIS II Newsletter, **1**(2), 4-6, Fall, 1993.

Springer, T.A., B.A.C. Ambrosius and R. Noomen, *Results from the WEGENER/GPS-92 campaign*, Geophys. Res. Lett., 1993 (to be published).

Strang van Hees, G.L., *Stokes formula using Fast Fourier techniques*, Manuscripta Geodaetica, **5**(4), 235-239, 1990

Strang van Hees, G.L., *Practical formulas for the computation of the orthometric, dynamic and normal heights*, Zeitschrift für Vermessungswesen, **117**(11), 727-734, 1992.

Strang van Hees, G.L., *Globale en Lokale geodetische systemen*, Nederlandse Commissie voor Geodesie, 30, 1-56, 1993.

Strang van Hees, G.L., *Some elementary relations between mass distributions inside the earth and the geoid and gravity field*, in: Montag, H., and Ch. Reigber (eds.), Geodesy and Physics of the Earth, Proc. of IAG Symposium 112, Potsdam, FRG, October 1992, Springer-Verlag, Berlin, FRG, 287-290, 1993.

Strang van Hees, G.L., *Gravity in the Banda Sea*, Snellius II Expedition, Indonesia, Bureau Gravimetrique International, Bulletin d'Information, **72**, 1993.

Vermaat, E., J.W. Offierski, K.H. Otten, W. Beek, C. van Es, and P. Sperber, *Transputer based control system for MTLRS*, In: Proceedings of the Eighth International Workshop on Laser Ranging Instrumentation, Annapolis, May 1992, NASA Conference Publication 3214, Goddard Space Flight Center, Greenbelt, 12/40-12/48, 1993.

Vermaat, E., K.F. Wakker and B.A.C. Ambrosius, *Earth Oriented Space Research at Delft University of Technology, Research Plan 1994-1997*, Research proposal to SRON, Delft University of Technology, Delft, The Netherlands, June 1993.

Visser, P.N.A.M., B.A.C. Ambrosius and K.F. Wakker, *Recovery of mean 1 deg by 1 deg gravity anomalies and geoid heights in a local area from GPS tracking of ARISTOTELES*, in: final CISI/ESA CIGAR Phase II Study Report, work package 420, CISI, ESA CR(P)-3057, March 1990.

Visser, P.N.A.M., K.F. Wakker and B.A.C. Ambrosius, *Determination of the regional geoid from simulated GPS measurements acquired by the ARISTOTELES solid earth satellite*, in: Rapp, R.H., and F. Sanso (eds.), Proc. of IAG Symposium 106, Springer-Verlag, 173-182, 1991.

Visser, P.N.A.M., *On the use of satellites in gravity field determination and adjustment*, Ph.D. Thesis, Delft University of Technology, Delft, The Netherlands, September 10, 1992.

Visser, P.N.A.M., and C.K. Shum, *Orbit analysis for the TOPEX altimeter calibration*, Technical Memorandum CSR-TM-93-08, Contract No. JPL 958122, Center for Space Research, University of Texas at Austin, USA, October 1993.

Visser, P.N.A.M., K.F. Wakker and B.A.C. Ambrosius, *Global gravity field recovery from the ARISTOTELES satellite mission*, J. of Geophys. Res., **99**(B2), 2841-2851, Feb. 10, 1994.

Visser, P.N.A.M., *ERS-1 precise orbit determination using TOPEX/ERS-1 dual satellite altimeter crossover differences*, Technical Memorandum CSR-TM-93-07, Contract No. NASA Grant NAGW 2132, Center for Space Research, University of Texas at Austin, USA, October 1993.

Visser, P.N.A.M., C.K. Shum, B.D. Tapley, J.C. Ries and G.L.H. Kruizinga, *Accuracy assessment of the TOPEX altimeter bias estimation*, Technical Memorandum CSR-TM-93-09, Contract No. JPL 958122, Center for Space Research, University of Texas at Austin, USA, December 1993.

Visser, P.N.A.M., K.F. Wakker and B.A.C. Ambrosius, *Dynamic sea surface topography from GEOSAT altimetry*, Marine Geodesy, **16**, 215-239, 1993.

Wakker, K.F., R.C.A. Zandbergen, M.C. Naeije and B.A.C. Ambrosius, *GEOSAT altimeter data analysis for the oceans around South Africa*, J. of Geophys. Res., **95**(C3), 2991-3006, March 1990.

Wakker, K.F., *Report by the Subcommittee on Intercomparison and Merging of Geodetic Data*, TOPEX/Poseidon Science Working Team, Report LR-638, Faculty of Aerospace Engineering, Delft University of Technology, Delft, The Netherlands, May 1990.

Wakker, K.F., B.A.C. Ambrosius and H. Leenman, *Satellite orbit determination and gravity field recovery from satellite-to-satellite tracking*, Report LR-605, Faculty of Aerospace Engineering, Delft University of Technology, Delft, The Netherlands, July 1990.

Wakker, K.F., M.C. Naeije, R. Scharroo and B.A.C. Ambrosius, *Extraction of mesoscale ocean currents information from GEOSAT altimeter data*, ESA SP-312, 221-226, December 1990.

Wakker, K.F., M.C. Naeije, R. Scharroo and B.A.C. Ambrosius, *Detection of mesoscale currents from GEOSAT altimeter data*, in: IGARSS'91 Remote Sensing: Global Monitoring for Earth Management, IEEE 91CH2971-0, 465-469, June 1991.

Wakker, K.F., *Earth oriented space research at Delft University of Technology*, contribution to: Geodetic Work in The Netherlands, Report prepared for the General Assembly of the International Association of Geodesy, Vienna, August 1991, Netherlands Geodetic Commission, Delft, The Netherlands, August 1991.

Wakker, K.F., R.C.A. Zandbergen and B.A.C. Ambrosius, *SEASAT precise orbit computation and altimeter data processing*, International Journal of Remote Sensing, **12**(8), 1649-1669, August 1991.

Wakker, K.F., R. Scharroo and B.A.C. Ambrosius, *Some results of the ERS-1 altimeter calibration*, ESA SP-326, ESA, 73-79, 1992.

Wakker, K.F., *Weekly report of the Delft University Quick-Look Data Analysis Center (QLDAC)*, Delft University of Technology, Delft, The Netherlands, No. 1-52, 1990-1993.

Wakker, K.F., E. Wisse, M.C. Naeije, R. Scharroo, P.N.A.M. Visser and B.A.C. Ambrosius, *ERS-1 radar altimetry over the North Atlantic*, ESA SP-359, ESA, Paris, France, 439-444, March 1993.

Wakker, K.F., M.C. Naeije, E. Wisse, R. Scharroo, P.N.A.M. Visser and B.A.C. Ambrosius, *GEOSAT and ERS-1 radar altimetry over the North Atlantic*, Adv. Space Res., **13**(11), ISSN 0273-1177, (11)305-(11)314, November 1993.

Wiejak, W., E.J.O. Schrama and R. Rummel, *Spectral representation of the satellite-to-satellite tracking observables*, Adv. Space. Res., **11**(6), 197-224, 1991.

Wisse, E., R. Scharroo, M.C. Naeije and K.F. Wakker, *Mean sea surface over the North Sea*, AVISO Altimetry Newsletter, **2**, 10, May 1993.

Wisse, E., R. Scharroo, M.C. Naeije and K.F. Wakker, *Mean sea surface computation from ERS-1 data*, in: Proc. of the 2nd ERS-1 Symposium: 'Space at the service of our environment', Hamburg, FRG, October 1993, ESA SP-361, 1053-1058, 1993.

Wisse, E., M.C. Naeije, R. Scharroo and K.F. Wakker, *Processing of ERS-1 and TOPEX/Poseidon altimeter measurements*, interim contract report of the Netherlands Remote Sensing Board project 1.2/OP-01, NRSP-2 report 93-11, ISBN 90-5411-092-9, December 1993.

Xu, P., *The second order design of geodetic networks using multiobjective optimization theory*, Boll. di Geod. e Scienze Affini, **3**, 185-194, 1990.

Xu, P., *Monitoring Sea Level Rise*, Report MFG-90.1, Faculty of Geodetic Engineering, Delft University of Technology, Delft, The Netherlands, 1990.

Delft University Press